Severity and Progression of White Matter Changes in Frontotemporal Dementia Subtypes Using Diffusion Tensor Imaging

Author:
Lam, Bonnie

Publication Date:
2014

DOI:
https://doi.org/10.26190/unsworks/17135

License:
https://creativecommons.org/licenses/by-nc-nd/3.0/au/
Link to license to see what you are allowed to do with this resource.

Severity and Progression of White Matter Changes in Frontotemporal Dementia Subtypes Using Diffusion Tensor Imaging

Bonnie Yin Ka Lam

A thesis in fulfilment of the requirements for the degree of
Doctor of Philosophy

School of Medical Sciences
Faculty of Medicine
May 2014

Originality statement

'I hereby declare that this submission is my own work and to the best of my knowledge it contains no materials previously published or written by another person, or substantial proportions of material which have been accepted for the award of any other degree or diploma at UNSW or any other educational institution, except where due acknowledgement is made in the thesis. Any contribution made to the research by others, with whom I have worked at UNSW or elsewhere, is explicitly acknowledged in the thesis. I also declare that the intellectual content of this thesis is the product of my own work, except to the extent that assistance from others in the project's design and conception or in style, presentation and linguistic expression is acknowledged.'

Signed …………   ……………………………………………

Date   ……………22nd May, 2014…………………………………………………

Copyright statement

THE UNIVERSITY OF NEW SOUTH WALES
Thesis/Dissertation Sheet

Surname or Family name: **Lam**

First name: **Bonnie**   Other name/s: **Yin Ka**

Abbreviation for degree as given in the University calendar: **PhD**

School: **Medical Sciences**   Faculty: **Medicine**

Title: **Severity and progression of white matter changes in frontotemporal dementia subtypes using diffusion tensor imaging**

Abstract 350 words maximum: (PLEASE TYPE)

The three main subtypes of frontotemporal dementia (FTD): behavioural-variant FTD (bvFTD), primary progressive aphasia-nonfluent variant (nfv-PPA) and semantic variant (sv-PPA) are characterised by progressive brain atrophy in the frontotemporal regions. The brain white matter also undergoes marked pathological alterations but is less studied. This thesis aimed to study i) the patterns of white matter changes in the three FTD subtypes, ii) the progression of white matter changes in the same FTD subtypes, and iii) the white matter changes in bvFTD with or without the *C9orf72* gene expansions.

Chapter 3 revealed distinctive patterns of white matter changes in each FTD subtype. White matter alterations were observed in orbitofrontal and anterior temporal tracts in bvFTD, bilateral (left>right) frontotemporal tracts in nfv-PPA and circumscribed left temporal lobe in sv-PPA. These white matter changes greatly overlapped with grey matter changes in bvFTD and nfv-PPA but not in sv-PPA. The white matter abnormalities varied depending on the diffusion tensor imaging (DTI) measurements used, with mean diffusivity being the most sensitive metric for all FTD subtypes.

Chapter 4 showed the 12-month longitudinal assessment of white matter changes in the same participants. White matter alterations appeared in regions shown at baseline but with additional changes extending beyond the original regions affected in all FTD subtypes. White matter abnormalities extended far beyond sites of grey matter atrophy in the same time period. Fractional anisotropy and radial diffusivity were most sensitive in detecting white matter abnormalities in this longitudinal assessment.

Chapter 5 compared bvFTD cases with or without *C9orf72* expansion carriers. *C9orf72* expansion carriers did not exhibit the typical frontotemporal white matter changes as shown in non-carriers. Stereotypical behaviour was less prevalent in *C9orf72* expansion carriers than non-carriers and the left cingulum and anterior thalamic radiation were predictive of stereotypical behavioural scores. Semantic knowledge was less affected in *C9orf72* expansion carriers and the left uncinate fasciculus was predictive of changes in semantic knowledge. These predictions significantly differentiated *C9orf72* expansion carriers from non-carriers.

Investigations using DTI presented in this thesis improved the understanding of white matter changes in FTD and contributed to the characterisation of the different FTD subtypes.

FOR OFFICE USE ONLY   Date of completion of requirements for Award:

THIS SHEET IS TO BE GLUED TO THE INSIDE FRONT COVER OF THE THESIS

Acknowledgements

I would like to give a special thank you to A/Prof. Olivier Piguet and Prof. Glenda Halliday for their invaluable advices and guidance throughout my PhD. They have not only showed me professionalism in a research career but also moral support and care of being a supervisor. They also provided me with sufficient resources and opportunities to widen my research exposure.

Many thanks to the Frontier team who has provide the sharing of resources and experiences. Their willingness to help one another in Frontier had helped my research projects in a great way. I also have to thank my dear friends at the Neuroscience Research Australia who had made my days, occasional late evenings and weekends at the workplace much more enjoyable.

I would like to send my gratitude to the patients, carers and control participants that were involved in my projects. Their contribution and support in medical research are invaluable and are highly appreciated.

Special thanks to my dear family, especially my parents and my two sisters. Thank you for their support, patience and encouragement throughout the highs and lows during these few years of my PhD.

Also special thanks to Jacky, who has supported, encouraged and had so much faith in me that has made me survived this journey.

Last but not least, thanks be to the Almighty Father who has provided me with this opportunity to study more about neuroscience and the capability to proceed successfully. Thank you for all the joys and graces that allow me to carry on each and every day with a smile on my face.

Abstract

The three main subtypes of frontotemporal dementia (FTD): behavioural-variant FTD (bvFTD), primary progressive aphasia-nonfluent variant (nfv-PPA) and semantic variant (sv-PPA) are characterised by progressive brain atrophy in the frontotemporal regions. The brain white matter also undergoes marked pathological alterations but is less studied. This thesis aimed to study **i)** the patterns of white matter changes in the three FTD subtypes, **ii)** the progression of white matter changes in the same FTD subtypes, and **iii)** the white matter changes in bvFTD with or without the *C9orf72* gene expansions.

Chapter 3 revealed distinctive patterns of white matter changes in each FTD subtype. White matter alterations were observed in orbitofrontal and anterior temporal tracts in bvFTD, bilateral (left>right) frontotemporal tracts in nfv-PPA and circumscribed left temporal lobe in sv-PPA. These white matter changes greatly overlapped with grey matter changes in bvFTD and nfv-PPA but not in sv-PPA. The white matter abnormalities varied depending on the diffusion tensor imaging (DTI) measurements used, with mean diffusivity being the most sensitive metric for all FTD subtypes.

Chapter 4 showed the 12-month longitudinal assessment of white matter changes in the same participants. White matter alterations appeared in regions shown at baseline but with additional changes extending beyond the original regions affected in all FTD subtypes. White matter abnormalities extended far

beyond sites of grey matter atrophy in the same time period. Fractional anisotropy and radial diffusivity were most sensitive in detecting white matter abnormalities in this longitudinal assessment.

Chapter 5 compared bvFTD cases with or without *C9orf72* expansion carriers. *C9orf72* expansion carriers did not exhibit the typical frontotemporal white matter changes as shown in non-carriers. Stereotypical behaviour was less prevalent in *C9orf72* expansion carriers than non-carriers and the left cingulum and anterior thalamic radiation were predictive of stereotypical behavioural scores. Semantic knowledge was less affected in *C9orf72* expansion carriers and the left uncinate fasciculus was predictive of changes in semantic knowledge. These predictions significantly differentiated *C9orf72* expansion carriers from non-carriers.

Investigations using DTI presented in this thesis improved the understanding of white matter changes in FTD and contributed to the characterisation of the different FTD subtypes.

Publications and presentations

Publication:

For Chapters 3 & 4:

Lam BYK, Halliday GM, Irish M, Hodges JR & Piguet O. (2014) Longitudinal white matter changes in frontotemporal dementia subtypes. *Human Brain Mapping* 35: 3547-57.

Published abstracts:

Lam BYK, Halliday GM, Hodges JR & Piguet O. (2012) Longitudinal white matter changes in frontotemporal Dementia Subtypes [Abstract]. The 8th International Conference on Frontotemporal Dementias. *Dementia and Geriatric Cognitive Disorders 34 Supp. 1,* 1-289.

Lam BYK, Halliday GM, Hodges JR & Piguet O. (2013) Longitudinal white matter changes in frontotemporal Dementia Subtypes [Abstract]. Society for Neuroscience Conference, San Diego, United States 2013. *Program No. 44.14/J9* Online.

Conference presentations:

Lam BYK, Halliday GM, Hodges JR & Piguet O. (2010 July) White matter changes in the language variants of frontotemporal dementia. *The Brain Sciences Symposium,* Sydney, Australia.

Lam BYK, Halliday GM, Hodges JR & Piguet O. (2012 July) Disease progression of white matter in frontotemporal dementia. *Aging and Neurodegeneration Theme Meeting,* Sydney, Australia.

Lam BYK, Halliday GM, Hodges JR & Piguet O. (2013 Nov) Progressive white matter changes and grey matter atrophy in frontotemporal dementia subtypes. *Tow Research Awards,* Sydney, Australia.

List of abbreviations

ACE-R	Addenbrooke's Cognitive Examination-Revised
AxialD	Axial diffusivity
bvFTD	Behavioural-variant frontotemporal dementia
C9neg	bvFTD without the C9orf72 gene expansions
C9orf72	Chromosome 9 open reading frame 72
C9pos	bvFTD with the C9orf72 gene expansions
CBI	Cambridge Behavioural Inventory
DTI	Diffusion tensor imaging
EPI	Echo-planar imaging
FA	Fractional anisotropy
FMRIB	Functional MRI of the Brain
FSL	Functional MRI of the Brain Software Library
FTD	Frontotemporal dementia
FTLD	Frontotemporal lobar degeneration
FTLD-FUS	FTLD-fused in sarcoma inclusions
FTLD-tau	FTLD-tau inclusions
FTLD-TDP	FTLD-TAR-DNA binding protein 43 inclusions
FUS	Fused in sarcoma
ILF	Inferior longitudinal fasciculus
JHU atlas	John Hopkins University atlas
lv-PPA	Logopenic variant primary progressive aphasia
MAPT	Microtubule associated protein tau

MD	Mean diffusivity
MND	Motor neuron disease
MNI	Montreal Neurological Institute
MRI	Magnetic resonance imaging
nfv-PPA	Nonfluent variant primary progressive aphasia
PPA	Primary progressive aphasia
RadialD	Radial diffusivity
RF	Radio frequency
SLF	Superior longitudinal fasciculus
sv-PPA	Semantic variant primary progressive aphasia
SYDBAT	Sydney Language Battery
TBSS	Tract-based spatial statistics
TDP-43	TAR-DNA binding protein 43
VBM	Voxel-based morphometry

List of symbols

b	b-value
D	Apparent diffusion coefficient/diffusion coefficient
G	Gradient strength
r^2	Square of mean displacement of particles during a diffusion time
S	Signal
So	Signal without diffusion weighting
t	Time
V_1	Primary eigenvector
V_2	Secondary eigenvector
V_3	Tertiary eigenvector
Δ	Distance between two gradients
δ	Duration of the gradients
λ_1	Primary eigenvalue
λ_2	Secondary eigenvalue
λ_3	Tertiary eigenvalue

Table of contents

List of figures

List of tables

Chapter 1: General introduction

Chapter One

1 GENERAL INTRODUCTION

Frontotemporal dementia (FTD), also referred to pathologically as frontotemporal lobar degeneration (FTLD), is a progressive neurodegenerative brain disorder. It is the second most common younger onset dementia after Alzheimer's Disease (Ratnavalli et al 2002). Prevalence of FTD is 4-15 per 100,000 with median age of onset at about 52.8-58 years old (Ratnavalli et al 2002, Rosso et al 2003).

FTD is a heterogeneous clinical disease making diagnosis difficult. Clinical presentations are diverse with the most prominent features being personality changes and progressive aphasia. Early studies referred to patients presenting with these symptoms as having Pick's disease, after Arnold Pick, an Austrian neurologist, who first described this clinical condition (Pick 1892).

The clinical classification of FTD is divided into three subtypes, namely, behavioural-variant FTD, and two subtypes of primary progressive aphasia (PPA), the nonfluent and semantic subtypes (Neary et al 1998, Rascovsky et al 2011) (Gorno-Tempini et al 2011). Insidious onset and gradual progression are common features of all subtypes of FTD but their clinical presentation differ which include variable underlying brain pathology, associated genetic predisposition, as well as patterns of grey matter atrophy and white matter degeneration. As the disease progresses, symptoms and regional pattern of atrophy across different subtypes tend to overlap.

Neuroimaging is therefore a useful tool to identify the regional pattern of atrophy in the different FTD subtypes supporting diagnostic decisions. Studies investigating grey matter changes and patterns of cortical atrophy in FTD have

been well documented. In contrast, alterations in brain white matter are much less studied in FTD.

The central objective of this thesis is to investigate the patterns of white matter change in FTD subtypes, to investigate the white matter change with disease progression. Further, to establish the white matter differences between sporadic FTD and a FTD group with a uniform pathologic subtype and genetic abnormality; and to investigate the white matter relations to clinical changes between these two groups.

1.1 Clinical presentations of Frontotemporal dementia

1.1.1 Behavioural-variant FTD

The behavioural-variant of FTD (bvFTD) is characterised by changes in personality, social behaviour and loss of insight. The recent revision of the international consensus criteria for bvFTD has provided guidelines to aid the diagnosis of the disease. At least three of the following six features must be present for the diagnosis of bvFTD (Rascovsky et al 2011): **1)** Early behavioural disinhibition in which patients produce socially inappropriate behaviour, loss of manners and impulsive, rash or careless actions; **2)** apathy or inertia, which often coexists with disinhibition, in which patients show reduced motivation, a loss of interest in previous hobbies and become socially isolated; **3)** loss of sympathy or empathy in which diminished response to social interest and the need and feelings of other people; **4)** early preservative, stereotyped or ritualistic behaviour; **5)** changes in eating behaviour such as impaired satiety, preferences towards sweet food and irregular patterns of food intake; **6)**

neuropsychological changes such as deficits in executive tasks but relative sparing in episodic memory and visuospatial skills. Symptom profiles differ from patient to patient but symptoms tend to increase in severity and frequency as disease progress (Diehl-Schmid et al 2006).

1.1.2   Primary progressive aphasia

1.1.2.1   Nonfluent variant primary progressive aphasia

The core features of nonfluent variant primary progressive aphasia (nfv-PPA) are: **1)** agrammatism in language production and **2)** effortful, halting speech with speech sound errors and distortions (also called apraxia of speech). This leads to hesitant and poor articulated sound based speech output (e.g., pronouncing "sitter" for "sister"). As indicated in the clinical diagnostic criteria (Gorno-Tempini et al 2011), at least two of the following three features must be present for the diagnosis for nfv-PPA: **i)** impaired comprehension of syntactically complex sentences, **ii)** spared single-word comprehension, and **iii)** spared object knowledge. (Gorno-Tempini et al 2004, Grossman et al 1996, Hodges & Patterson 1996).

1.1.2.2   Semantic variant primary progressive aphasia

The semantic variant primary progressive aphasia (sv-PPA) is the second PPA subtype. Unlike nfv-PPA, the core features include: **1)** progressive, fluent and empty spontaneous speech with impaired confrontation naming; **2)** as well as impaired single-word comprehension. At least three of the following three features must be present for the diagnosis for sv-PPA: **i)** impaired object knowledge, especially with items that are less frequently used; **ii)** surface

dyslexia or dysgraphia; **iii)** spared single-word repetition; and **iv)** spared speech production (grammar and motor speech). Emotion processing and facial emotion recognition are also affected in sv-PPA (Kumfor et al 2011). On the other hand, other features such as perceptual matching and drawing reproduction, and also the ability to read aloud and write to dictate orthographically regular words are well preserved in sv-PPA. Patients belonging to this FTD subtype also have relatively preserved insight and cognition (Gorno-Tempini et al 2004, Hodges et al 1992, Neary et al 1998). The progressive deterioration of receptive vocabulary may not be detected easily because the deficit affects only less common words initially and normal conversation does not necessarily require understanding of every single word (Hodges et al 1992).

1.1.2.3   Logopenic variant primary progressive aphasia

The PPA nomenclature includes a third subtype called the logopenic variant primary progressive aphasia (lv-PPA). This subtype has a clinical presentation resembling that of nfv-PPA with a slow rate of speech and deficits in single-word retrieval of spontaneous speech, naming and sentence repetition. Other features include phonological errors in spontaneous speech and naming but spared single-word comprehension, motor speech and agrammatism (Gorno-Tempini et al 2004, Gorno-Tempini et al 2011).

Unlike nfv-PPA and sv-PPA, which are part of the FTD pathological spectrum, lv-PPA is associated with an atypical pattern of Alzheimer's pathology. This thesis will only focus on nfv-PPA and sv-PPA and will not discuss lv-PPA further because of the different pathology involved.

1.1.3   Neurological diseases associates with FTD

A number of coexisting neurological conditions are observed in patients with FTD. In particular, motor neuron disease (MND) and extrapyramidal motor disorders such as corticobasal syndrome and progressive supranuclear palsy syndrome are not uncommon.

MND presents a neurodegenerative disease with gradual loss of abilities to execute everyday activities and demonstrates muscle weaknesses, fasciculation, spasticity, dysphagia and dysarthria (Brooks et al 2000). MND was long considered a pure motor disorder until recent evidence revealed cognitive and behavioural changes similar to those seen in patients with bvFTD. FTD-MND subjects exhibit executive dysfunction, apathy and disinhibition and cognitive impairment (Lillo et al 2011, Murphy et al 2007, Ringholz et al 2005).

Corticobasal syndrome presents as a syndrome of asymmetric rigidity and apraxia while progressive supranuclear palsy syndrome is characterised by slow and restricted saccades, with downgaze palsy, axial-dominant parkinsonism and profound retropulsion (Litvan et al 1996, Rebeiz et al 1968). Patients with these extrapyramidal disorders showed behavioural changes reminiscent of bvFTD or nfv-PPA (Josephs et al 2006b, Kertesz et al 2000, Kertesz et al 2005).

1.2 FTLD Neuropathology

The first microscopic abnormalities in the brain of FTD patients were described by Alois Alzheimer (Alzheimer 1911). Alzheimer and Altman described argyrophilic neuronal inclusions (Pick's bodies) and swollen cells (Pick cells) in the frontal and temporal regions where atrophy was observed. Hence, this became the pathology for Pick's disease. This classification has evolved with time and several different histopathologic conditions were identified to be categorised under the umbrella term of FTLD (Mackenzie et al 2010a).

The general histopathological patterns of FTLD revealed atrophy found in frontotemporal regions and are caused by increasing neuronal loss, astrocytosis, and microvacuolation, and also increasing glial apoptosis (Kril & Halliday 2011, Kril & Halliday 2004).

Subtypes of FTLD are broadly classified on the basis of the major protein constituents of cellular inclusions and can be divided into either FTLD with TAR DNA-binding protein 43 (TDP-43) inclusions (FTLD-TDP) or FTLD with tau deposition (FTLD-tau) with the remaining minority having mainly FTLD with the fused in sarcoma (FUS) inclusions (FTLD-FUS) (Mackenzie et al 2010a).

1.2.1 FTLD-TDP

FTLD-TDP is the most common pathological subtype of FTLD and is found in about 50% of cases. TDP-43 is a widely expressed nuclear protein and a highly conserved 414 amino acids of 43kDa (Mackenzie et al 2010b). It is responsible for a variety of different biological processes binding DNA and RNA, and as a transcription repressor and an activator in exon skipping (Ayala et al 2005). The pathological changes associated with FTLD-TDP consist of abnormally

7

hyperphosphorylated and ubiquitinated TDP-43 that leads to a reduction of normal nuclear TDP-43 and presence of cytoplasmic and nuclear inclusions (Cairns et al 2007, Neumann et al 2009a, Neumann et al 2007). FTLD-TDP is further divided into four sub-classifications (types A, B, C and D) depending on the distribution and type of inclusions (dystrophic neutrites, neuronal cytoplasmic inclusions or neuronal intranuclear inclusions) (Mackenzie et al 2011b).

Certain genes are associated with FTLD-TDP. Mutations in the TDP-43 gene give rise to MND while expansions in the non-coding region of *chromosome 9 open reading frame 72* gene is the most common genetic abnormality for both MND and FTLD-TDP (Pesiridis et al 2009, Sha et al 2012). Less common mutations are found in the *progranulin* gene which is found on chromosome 17, with rare mutations in the *valosin-containing protein* found on chromosome 9 also causing FTLD-TDP.

1.2.2   FTLD-tau

FTLD-tau, the second most common FTLD pathology, is found in about 40% of cases (Mackenzie et al 2010a, Spillantini & Goedert 1998). Tau is a microtubule associated phosphoprotein that is responsible for microtubule assembly and stabilisation. FTLD-tau is further divided into four sub-classifications (Pick bodies, astrocytic plaques, tufted astrocytes and globular glial tau) into Pick's disease, corticobasal degeneration, progressive supranuclear palsy and globular glial tau (Ahmed et al 2011, Dickson et al 2011).

Mutation of the *microtubule associated protein tau* gene found on chromosome 17 is associated with FTLD-tau and leads to neurodegeneration through the

following mechanisms: decreased ability to bind to microtubules; causing impaired microtubule assembly, stability and disruption of axonal transport; and increased affinity to self-aggregate into neurotoxic filamentous and insoluble inclusions.

1.2.3   FTLD-FUS

A small proportion of cases are FTLD-FUS (Mackenzie et al 2010a). FUS is a common protein in the brain that binds to DNA and regulates transcription and is also involved in messenger RNA processing (Neumann et al 2009b). Subtypes of FTLD-FUS include the atypical FTLD-U, neuronal intermediate filament inclusion disease and basophilic inclusion body disease (Mackenzie et al 2011a). Mutation in the *FUS* gene give rise to MND but not FTLD-FUS by interfering with messenger RNA transport affecting nerve cells that control muscle movement (Neumann et al 2009b).

1.3 Genetics of FTD

Genetic inheritance is found in up to 40% of FTD patients, with about 10% showing autosomal dominant inheritance patterns. bvFTD has the highest degree of heritability while sv-PPA appear to be the least heritable (Goldman et al 2005, Rohrer et al 2009a). In the familial cases of FTD, the most common genetic abnormalities are found in the *chromosome 9 open reading frame 72 (C9orf72)*, *progranulin* and *microtubule associated protein tau (MAPT)* genes (Majounie et al 2012, Seelaar et al 2008). Other disease-causing genes include *valosin-containing protein* and *chromatic-modifying protein 2B*.

1.3.1 Chromosome 9 open reading frame 72

Little is known about the function of the *chromosome 9 open reading frame 72 (C9orf72)* gene. Recent findings suggest the *C9orf72* gene regulates endosomal trafficking which includes endocytosis and autophagy (Farg et al 2014). The genetic abnormality in the *C9orf72* gene involves the expansion of GGGGCC hexanucleotide repeats in the non-coding region of chromosome 9. The hexanucleotide expansion may generate abnormal amounts of toxic RNA species that interfere with normal cellular activity by sequestering normal RNA and proteins involved in transcription regulation (Renton et al 2011). This recently identified gene is also responsible for the majority of familial cases with MND, suggesting a pathogenic link between MND and FTD (DeJesus-Hernandez et al 2011, Renton et al 2011).

1.3.2   Progranulin

Progranulin RNA in the brain is highly expressed in the hippocampal pyramidal cells and the Purkinje cells in the cerebellar cortex. Its functions include regulation of sexual differentiation in the brain, promotion of neuronal survival and stimulation of neuritic outgrowth (Suzuki et al 2009, Van Damme et al 2008). Mutations in the *progranulin* gene are loss of function mutations which decrease the progranulin protein and its anti-inflammatory and neuronal protective effects (Bossù et al 2011). *Progranulin* mutations are found in nfv-PPA (Snowden et al 2006) or bvFTD with associated corticobasal degeneration (Le Ber et al 2008).

1.3.3   Microtubule associated protein tau

The *microtubule associated protein tau (MAPT)* gene codes six isoforms of *tau* by the alternative splicing of exons 2, 3 & 10. Of these, three isoforms present with 3 microtubule binding amino acid repeats and three with 4 repeats (Goedert et al 1989). Two types of mutations are found: **i)** missense mutations in exons 9-13 which affect microtubule stabilisation, and hence, impact the normal function of the tau protein; and **ii)** intronic mutations that affect splicing at exon 10 at the mRNA level, leading to a change in ratio in the 3 repeat and 4 repeat tau isoforms (Goedert et al 1988). *MAPT* mutations cause accumulation of hyper-phosphorylated tau protein in neurons and/or glia cells, causing the disease through a toxic gain of function. *MAPT* mutations are found in bvFTD or nfv-PPA with association to corticobasal degeneration or progressive supranuclear palsy (Bird et al 1999, Bugiani et al 1999, Hutton et al 1998, Munoz et al 2007).

1.3.4   Other genes and linkages

Additional rare gene mutations identified include the *valosin-containing protein* and *chromatic-modifying protein 2B. Valosin-containing protein* mutations are linked to an autosomal dominant FTD syndrome with associated Paget's disease of the bone and inclusion body myositis (Watts et al 2004). The *chromatic-modifying protein 2B* gene mutation was found in a single Danish family with FTD phenotype (Gydesen et al 2002, Skibinski et al 2005). Although rare, the *TARDP* gene mutation, which gives rise to MND, has also been identified in bvFTD (Borroni et al 2009).

1.4   Clinico-patho-genetic relations

FTD is a heterogeneous disease with complex clinic-patho-genetic relations. In brief, the relations between genetics and pathology as described above are that *MAPT* mutations are associated with FTLD-tau while abnormalities in the *C9orf72, GRN,* and *VCP* genes are associated with FTLD-TDP. Relations between pathology and clinical presentation are mixed (Chare et al 2014). Patients with bvFTD tend to show approximately equal numbers of both FTLD-tau and FTLD-TDP (Hodges et al 2004). A majority of PPA-nfv patients show FTLD-tau (Hodges et al 2004). In contrast, PPA-sv patients tend to exhibit almost exclusively in FTLD-TDP (Davies et al 2005, Hodges et al 2004, Rohrer et al 2011) (see Figure 1.1).

Figure has been removed due to Copyright restrictions.

Figure 1.1 The clinical, pathological and genetic heterogeneity of FTD.

This diagram highlights the complex clinico-patho-genetic relations between the clinical syndromes within the FTD spectrum (on the right), the different pathological causes (in the centre) and the genetic causes (on the left) (Rohrer & Rosen 2013).

Note: In this thesis, FTD-ALS is referred to as FTD-MND.

1.5   Neuroimaging in FTD

The development of non-invasive neuroimaging, in particular magnetic
resonance imaging (MRI), greatly enhanced the ability to perform studies for
the visualisation of structure and function *in vivo*. The brain consists of two
major components: the grey and white matter. Grey matter atrophy is studied
with structural MRI using T1-images while changes in white matter integrity is
studied with the aid of diffusion tensor imaging which is a growing application
in the field of MRI using diffusion-weighted images.

The following sections provide an overview of grey and white matter changes in
FTD with the use of these powerful neuroimaging tools.

1.5.1   Grey matter changes in FTD

As expected by their clinical differences, each FTD subtype exhibits a distinctive
pattern of brain changes. In general, bvFTD is characterised by a bilateral
orbito-frontal and anterior temporal atrophy. In contrast, in nfv-PPA, the
atrophy is relatively focal and circumscribed to the left fronto-insular region.
Finally, sv-PPA is associated with an asymmetric pattern of atrophy involving
the anterior temporal region, generally more pronounced on the left than the
right (Figure 1.2)(Vitali et al 2008). With disease progression, brain atrophy
tends to become more widespread and diffuse, making differentiation across the
syndromes more difficult. A brief summary of the early imaging features of FTD
subtypes and the changes with disease progression will be provided
subsequently.

Figure has been removed due to Copyright restrictions.

Figure 1.2 Regions of brain atrophy in bvFTD, nfv-PPA and sv-PPA shown on coronal T1-weighted MRI.

Coronal T1-weighted MRI from patients with different clinical presentations of FTD. Note the bilateral grey matter loss in the inferior frontal gyrus (arrow), superior frontal gyrus (dashed arrow), the insula (dotted arrow), and the anterior cingulate (arrowhead) in the patient with bvFTD; the prominent atrophy in the left perisylvian region (arrow) in the patient with nfv-PPA; and the atrophy of the left temporal lobe (arrow) in the patient with sv-PPA (Vitali et al 2008).

1.5.1.1   Grey matter atrophy in bvFTD

In bvFTD, the pattern of atrophy is found bilaterally. In the frontal lobes, atrophy in the mesial frontal and orbitofrontal regions is apparent. The temporal lobes are also affected, as well as the anterior insula and subcortical structures including the thalamus (Schroeter et al 2008, Schroeter et al 2007, Seeley et al 2008). The pattern of atrophy varies according to disease severity. For example, when separating bvFTD patients according to their clinical dementia rating, different patterns of atrophy emerge. In the mild group, atrophy is present in the frontal lobes (rostromedial frontal, frontal pole, dorsolateral frontal and orbitofrontal), as well as the anterior insula, hippocampus, ventral striatum and dorsomedial thalamus. Patterns of atrophy

are bilateral but right dominant. In the severe group, atrophy becomes more extensive in the same areas, especially in the frontal lobes but also extends to posterior regions, including the posterior insula, temporal and parietal lobes (Seeley et al 2008).

1.5.1.2   Grey matter atrophy in nfv-PPA

In nfv-PPA, brain atrophy is focal and lateralised. It involves the left posterior fronto-insular region, which includes the inferior frontal gyrus, insula, pre-motor and supplementary motor areas (Gorno-Tempini et al 2004, Grossman et al 1996, Whitwell et al 2010). In contrast, other brain regions appear relatively free of significant atrophy.

As disease progresses, subsequent atrophy is found in the frontal, temporal and anterior parietal lobes, as well as the caudate nucleus and thalamus (Gorno-Tempini et al 2006, Rogalski et al 2011, Rohrer et al 2009b). In a study where nfv-PPA cases were separated according to the severity of their anomia, the authors reported cortical thinning in the left inferior frontal lobe, insula and premotor cortex in the mild group while the severe group showed cortical thinning in middle and superior frontal, superior and lateral temporal and the anterior parietal cortices (Rohrer et al 2009b).

1.5.1.3   Grey matter atrophy in sv-PPA

The sv-PPA is the most homogenous subtype within the FTD spectrum. In sv-PPA, brain atrophy is particularly pronounced in the anterior and inferior temporal lobe, specifically in the temporal pole, perirhinal cortex, anterior fusiform gyrus, hippocampus and the amygdala (Davies et al 2009, Davies et al

2004, Hodges & Patterson 2007). This atrophy tends to be asymmetric, generally more severe on the left than on the right. Early on, the clinical characteristics exhibited by sv-PPA patients are relatively more subtle than those with other FTD subtypes, leading to a longer delay of detection and disease diagnosis after first symptoms occur. In a study where sv-PPA cases were separated into groups based on the severity of anomia, results again showed these previously left-dominant changes extend to the homologous regions in the right temporal lobe. The mild group showed cortical thinning in the left anterior and inferior temporal lobes, with a minor area of thinning on the right anterior temporal lobe. On the other hand, the severe group demonstrated changes in the posterior and superior parts of the left temporal lobe. Additional changes were also found in the left frontal lobe, insula and anterior cingulate cortex. Involvement in the homologous regions of the right temporal lobe was also more extensive in this group (Brambati et al 2009, Rohrer et al 2009b).

1.5.2   White matter integrity in FTD

Patterns of grey matter atrophy *in vivo* have been well documented in all FTD subtypes (Boccardi et al 2005, Gorno-Tempini et al 2004, Hodges & Patterson 2007, Kipps et al 2007, Rosen et al 2002, Seeley et al 2008). In contrast, changes affecting the white matter integrity in FTD have received comparatively little attention.

Early studies tried to investigate white matter changes with signal intensity in T2- and proton density-weighted images. Visual inspection of increase signal intensity in the frontal and/or temporal lobes successfully distinguished FTD

from Alzheimer's disease (Kitagaki et al 1997). Another pioneering study attempted to compare white matter atrophy to grey matter atrophy using volumetric change on T1-, T2- and proton density-weighted images. White matter atrophy was found to largely parallel the patterns of grey matter atrophy in FTD (Chao et al 2007).

The need arose for a quantitative study providing direct measurement of the severity of damage to the white matter tract instead of signal intensity or volumetric measurements. This is made possible with the development of diffusion tensor imaging (DTI) that reflects microscopic structural changes in the white matter tissue (Le Bihan et al 2001). The development of this technique transformed the description of white matter integrity in FTD from vague description of changes in a broad region down to clearly defined tracts-of-interest.

The study of white matter using DTI is relatively novel in FTD. Existing studies have largely focused on measuring white matter integrity in the regions- or tracts-of-interest or in defining patterns of white matter change while less reported is white matter change with respect to disease severity. Findings regarding white matter changes in FTD subtypes are summarised below.

1.5.2.1   White matter changes in bvFTD

In bvFTD, alterations have been found bilaterally in the frontal white matter; including the superior longitudinal fasciculus, anterior cingulum and the genu of the corpus callosum; and in the temporal white matter, involving the uncinate fasciculus, inferior longitudinal fasciculus and inferior fronto-occipital

fasciculus (Agosta et al 2011, Avants et al 2010, Borroni et al 2007, Matsuo et al 2008, Whitwell et al 2010, Zhang et al 2009, Zhang et al 2013).

1.5.2.2 White matter changes in nfv-PPA

In nfv-PPA, white matter integrity is disrupted in the dorsal language pathway, in particular the left subcomponent of the superior longitudinal fasciculus (arcuate fasciculus) (Agosta et al 2012, Grossman et al 2013, Mahoney et al 2013, Schwindt et al 2013, Whitwell et al 2010, Zhang et al 2013). Bilateral but left predominant white matter alterations in other tracts such as the inferior fronto-occipital fasciculus and uncinate fasciculus, as well as the genu of the corpus callosum have also been reported (Agosta et al 2011, Schwindt et al 2013).

1.5.2.3 White matter changes in sv-PPA

The sv-PPA showed asymmetric left predominant white matter abnormalities in the inferior longitudinal fasciculus and uncinate fasciculus (Acosta-Cabronero et al 2011, Agosta et al 2010, Agosta et al 2011, Borroni et al 2007, Galantucci et al 2011, Mahoney et al 2013, Schwindt et al 2013, Whitwell et al 2010, Zhang et al 2013). Some reported subcomponents of the superior longitudinal fasciculus being affected (Acosta-Cabronero et al 2011, Agosta et al 2010, Galantucci et al 2011, Schwindt et al 2013, Whitwell et al 2010) and other tracts reported with white matter alterations included the inferior fronto-occipital fasciculus and genu of the corpus callosum (Agosta et al 2010, Borroni et al 2007, Schwindt et al 2013).

1.6   Measuring white matter integrity

About 50-60% of the human body is composed of water (Watson et al 1980).

Diffusion tensor imaging captures the movement of water molecules to reveal

the local diffusion profile and architecture of the highly organised white matter.

In order to further answer questions about patterns of white matter change in

the brain of FTD and how these changes evolve with disease progression, it is

necessary to understand the working principles of diffusion tensor imaging,

including data acquisition, the interpretation of diffusion measurements and the

implications of white matter changes reflected from such technique.
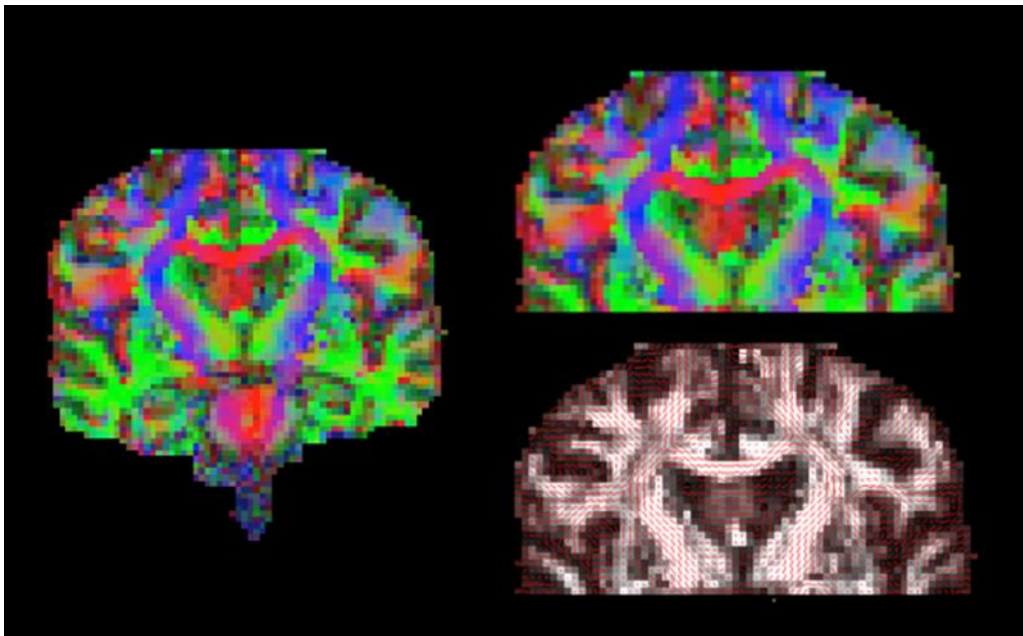
Figure 1.3 Example of a diffusion tensor imaging colour map.
The colour maps (left and top right) illustrated as red, green and blue
corresponded to the x-, y- and z- directions respectively. The image in the
bottom right is composed of small red lines that indicate preferred diffusion
direction at each voxel.

1.6.1   What is diffusion?

Diffusion is the process by which matter is transported from one part of a system to another as a result of random molecular motion. The irregular movement of particles caused by the bombardment of other particles is called the Brownian motion after Robert Brown, a botanist, who first observed the perceptual motion of pollen grains suspended in water under a microscope (Brown 1828). When a particle is placed in an environment with a high concentration medium, the collision among particles is frequent, and hence, displacement of particles will be fast. Particles tend to move from a high concentration medium to a low concentration medium until equilibrium of concentration is reached. This movement is called diffusion.

1.6.2   How is diffusion measured?

Albert Einstein described the thermally driven time-distance relationship of the random motion of particles with reference to the Gaussian displacement distribution concept and derived the following equation (Einstein 1905):

$$r^2 = 6Dt$$

Formula 1.1*: r² = **the square of mean displacement of particles during a diffusion time; D = diffusion coefficient; t = time.**

With this equation, the mean displacement of a particle with no diffusion restrictions can be calculated.

1.6.3 Diffusion in the brain white matter and apparent diffusion coefficient

There are two types of diffusion: isotropic and anisotropic. When there are few or no constraints by any physical boundaries, water movement is random and uniform in every direction. This is termed isotropic diffusion. The random motion of water molecules, however, is influenced by a variety of factors such as restrictions due to cell membranes, cytoskeleton and macromolecules (Tanner & Stejskal 1968). This will create a preferred direction for water molecules to travel and such diffusion is referred to as anisotropic diffusion (Rosenbloom et al 2003).

Figure has been removed due to Copyright restrictions.

Figure 1.4 Isotropic and anisotropic diffusion.
A) Water molecules in the brain are constantly moving (i.e., in Brownian motion). When motion is unconstrained, as in the large fluid-filled spaces deep in the brain (i.e., the ventricles, as illustrated in the MRI on the left), diffusion is isotropic, which means that motion occurs equally and randomly in all directions. B) When motion is constrained, as in white matter tracts (illustrated on the right), diffusion is anisotropic, meaning that motion is oriented more in one direction than another (e.g., along the y-axis rather than along the x-axis) (Rosenbloom et al 2003).

White matter is highly organised tissue comprised of bundles of axons. As such, diffusion of water that is perpendicular to the direction of the axonal bundle will be more restricted than water travelling parallel to the bundle. Diffusion in the healthy brain white matter, therefore, is anisotropic. Apparent diffusion coefficient, as compared to diffusion coefficient, describes the "apparent" molecular motion of water molecules in a constrained environment where cell membranes, cytoskeleton and macromolecules interfere. It is often used interchangeably with diffusion coefficient, D, as mentioned in Formula 1.1.

1.7 Diffusion-weighted image and its acquisition

Images from the same biological material with different contrast mechanisms can be constructed using different MRI sequences. T1, T2, proton density-weighted and diffusion-weighed images are examples of the output using different MRI sequences. The focus of this thesis is on diffusion tensor imaging which consists of diffusion-weighted images, and thus, is further elaborated.

1.7.1 Diffusion-weighted images

A magnetic resonance image acquired with diffusion weighting is called a diffusion-weighted image. This type of image is acquired by sensitising diffusion motion with the use of strong gradients. Multiple diffusion-weighted image of various diffusion directions (at least diffusion-weighted images along 6 non-collinear directions) together with one base image (image acquired without diffusion weighting: b-value = 0 s/mm²) form a fundamental set of diffusion tensor imaging data.

1.7.2   Acquisition of diffusion-weighted images

T1, T2 and proton density-weighted images are acquired with conventional spin-echo pulse sequences, the most basic sequence in MRI (Stejskal & Tanner 1965). For diffusion-weighted images, however, the spin-echo pulse sequence with a single-shot, echo-planar imaging (EPI) readout is more commonly used (Nagy et al 2007).

The EPI sequence consists of a 90 degree excitation radio frequency (RF) pulse, and a 180 degree rephasing pulse, followed by an echo. The first gradient pulse dephases the magnetisation across all voxels, followed by a rephasing of magnetisation of the second pulse. The change in magnetic field gives rise to different effects to the spins.

The principle of measuring diffusion is the moving spins which will be translated as magnetic resonance signal attenuation (signal loss). For non-diffusive stationary molecules, the pulses induced by both the 90 and 180 degree gradient pulses are designed to cancel each other out, leading to the absence of signal attenuation. On the other hand, when diffusion movement is along the direction of the applied gradient, the bulk motion of phase shifts by different amount for each gradient pulse leads to a net phase shift. This phase shift is proportional to the displacement, the area of diffusion gradient pulse (G), the duration of gradient applied (δ), and the distance between the gradient pulses (Δ) (Nagy et al 2007) . The greater the phase shift, the greater loss of signal, and hence, reflecting a higher rate of diffusion.

EPI is the most efficient type of MRI imaging sequence and is less sensitive to motion compared to standard spin-echo sequences. It is, however, considerably more sensitive to artefacts due to eddy currents and susceptibility.

Figure has been removed due to Copyright restrictions.

Figure 1.5 Schematic of a diffusion-weighted EPI pulse sequence.
A spin echo is used to achieve diffusion-weighting from the gradient pulse pairs (coloured). The imaging gradients are shown in grey. Diffusion-weighting gradients can be applied in any arbitrary direction using combinations of G_x (red), G_y (green) and G_z (blue).
Abbreviations: RF-radio frequency; G-gradient strength in x-, y- or z-directions; TE-time to echo (time from insertion of radio frequency to signal appearing); δ-duration of gradients; Δ-distance between two gradients (Nagy et al 2007).

The relationship between the radio frequency signal (signal attenuation) and the gradient pulse is determined by the apparent diffusion coefficient (as described above) and the b-value (which summarises the influence of applied gradient including gradient amplitude and timing) according to the following equation (Stejskal & Tanner 1965, Torrey 1956).

$$S = Soe^{-bD}$$

Formula 1.2: *S = Signal; S_o = signal without diffusion weighting; b = b-value; D = apparent diffusion coefficient*

where $b \ = \ \delta^2 \ (\varDelta - 1 \ \delta)G^2$

Formula 1.3: δ = the duration of the gradients; Δ = the distance between the two gradients; G = gradient strength.

Signals can be measured at different b-values, by varying the gradient magnitude. Diffusion-weighted maps are usually acquired with one set at a lower b-value (e.g., b = 0 s/mm²) image and another at a higher b-value (e.g., b = 1000 s/mm²) in order to provide useful information of diffusion.

1.8   The diffusion tensor model and diffusion tensor imaging

In the Gaussian model of diffusion in an anisotropic and restricted environment (e.g., axonal bundle), diffusion-weighted image is not sufficient to describe the anisotropy of water diffusion and to estimate the principal diffusion direction. DTI, which is a tensor instead of a scalar measurement, is therefore used to compute a diffusion tensor which can be described in a 3 x 3 matrix (Formula 1.4), and consists of six independent elements: *Dxx, Dyy, Dzz, Dxy, Dxz, Dyz.*

This provides an explanation for a basic set of DTI to be composed of at least six diffusion-weighted images of non-collinear directions.

$$D = \begin{bmatrix} Dxx & Dxy & Dxz \\ Dyx & Dyy & Dyz \\ Dzx & Dzy & Dzz \end{bmatrix}$$

Formula 1.4: Diffusion tensor characterised by a 3 x 3 matrix.

1.9   DTI parameters

In diffusion tensor imaging, changes of water molecule diffusion influenced by their immediate environment and motility can be expressed as variations in diffusion metrics in terms of varying direction and magnitude. The diffusion tensor composes of three mutually orthogonal eigenvectors (V_1, V_2 & V_3) and three real eigenvalues (λ_1, λ_2 & λ_3), describing the diffusion ellipsoid in its x-, y- and z-plane. Understanding alterations in diffusion and anisotropy allows interpretation of white matter changes.

1.9.1   Axial and radial diffusivities

The main eigenvalue, λ_1, is parallel to the principal axis that reflects diffusivity along the fibre length and is termed axial diffusivity (AxialD). On the other hand, the two perpendicular diffusion coefficients λ_2 and λ_3 are termed radial diffusivity (RadialD) when they are averaged.

$$RadialD = \frac{(\lambda_2 + \lambda_3)}{2}$$

Formula 1.5: RadialD = Radial diffusivity; λ = eigenvalue of the tensor matrix.

Changes in these diffusivities reflect certain pathological changes. In brief, AxialD is associated with axonal damage while RadialD is related to myelin loss (Pierpaoli et al 2001, Song et al 2003, Song et al 2002, Sun et al 2006). In a mouse model of demyelination and remyelination, the decrease in AxialD was found to associate strongly with axonal damage (Sun et al 2006). The exact mechanism underlying the AxialD change in unclear but the build-up of cellular debris from the breakdown of axonal structure, the disordering of microtubule arrangement and the aggregation of filaments which all could restrict the freedom of water movement in directions parallel to the white matter fibre (Arfanakis et al 2002, Beaulieu et al 1996). On the other hand, an increase in RadialD was observed in *shiverer* mutant mice compared to control mice in a study of demyelination. The increase in RadialD in this scenario reflects greater freedom of water movement in directions perpendicular to the white matter fibre due to the lack of myelin, suggesting that RadialD is associated with myelin loss (Song et al 2002).

1.9.2 Mean diffusivity

The mean diffusivity (MD) is the average of the three eigenvalues (λ_1, λ_2 & λ_3) and is independent of any tissue directionality.

$$MD = \frac{(\lambda_1 + \lambda_2 + \lambda_3)}{3}$$

Formula 1.6: MD = Mean diffusivity; λ = eigenvalue of the tensor matrix.

1.9.3   Fractional anisotropy

Fractional anisotropy (FA) measures the fraction of the magnitude of the diffusion tensor that attributes to anisotropic diffusion and is illustrated as a point scale ranging from 0 to 1 (Basser & Pierpaoli 1996). Healthy brain white matter fibres are highly organised. In this instance, water molecules in healthy white matter tend to diffuse with a higher degree of anisotropy, and hence, having an FA value closer to 1. In contrast, the brain white matter with neurodegenerative diseases may experience structural damage to axons and myelin resulting in a loss of directional barriers to water diffusion. This results in a reduction in the degree of anisotropy, giving an FA value closer to 0. FA is a scalar quantity derived from the diffusion tensor and the equation is as below:

$$FA = \sqrt{\frac{1}{2}} \frac{\sqrt{(\lambda_1 - \lambda_2)^2 + (\lambda_2 - \lambda_3)^2 + (\lambda_3 - \lambda_1)^2}}{\sqrt{\lambda_1^2 + \lambda_2^2 + \lambda_3^2}}$$

Formula 1.7: FA = fractional anisotropy; λ = eigenvalue of the tensor matrix.

The DTI parameters described above creates a geometric model, the diffusion ellipsoid, to assess the model of anisotropy. The shape of the diffusion ellipsoid represents directionality and magnitude of diffusion (Winston 2012).

Figure has been removed due to Copyright restrictions.

Figure 1.6 Diffusion sphere and ellipsoid.
With isotropic diffusion, diffusion is equal in all directions and is represented in a sphere (left) while anisotropic diffusion is represented as an ellipsoid (right) (Winston 2012).

1.10 Image acquisition issues and limits of DTI

Artefacts consist of deviations in an image containing erroneous information. Variables such as noise and eddy currents could potentially cause artefacts in the acquisition of DTI and are discussed below.

1.10.1 Signal to noise ratio

Signal to noise ratio is the ratio of the amplitude of the magnetic resonance signal to the average amplitude of the background noise. Noise is the undesired signal resulting from the magnetic resonance system, the environment and the subject. It can impact DTI measurement in two main ways. First, if the recorded signal to noise ratio became too low, the highest eigenvalue λ_1 will be overestimated while the lowest eigenvalue λ_3 will be underestimated and will

lead to an inaccurate FA value which is often overestimated. Second, noise may cause eigenvalues to be negative when estimated using least square test but achieving a negative eigenvalue is not physically possible. Therefore, positive definite constraints may be applied when estimating the tensor and the acquisition of diffusion tensor images may also be repeated for averaging to increase the signal to noise ratio.

1.10.2 Eddy currents

Eddy currents are induced by the conductor (MRI magnets) in a changing magnetic field. In conventional MRI, the diffusion gradients are usually applied briefly and eddy currents that are induced by rising and falling edges of the pulse would tend to self-cancel. In diffusion tensor imaging, however, the gradients are applied for a longer period of time in order to achieve the desired b-value with limited gradient power. Hence, eddy currents induced are greater and do not self-cancel. When the spin echo pulse-gradient with EPI readout is employed in DTI, the bandwidth in the phase-encoded direction is small, and thus, more errors occur in achieving the desired gradient. It is, therefore, essential to correct for eddy currents in diffusion tensor imaging.

1.11 DTI application

DTI can be applied in many ways, for example, to assess white matter in development and degeneration and to learn more about tissue pathology. One of the most successful examples in the early 1990s was the discovery of water diffusion change at the very early stage of an ischemic event in a cat brain (Warach S et al 1992). It can also be used for the localisation of tumour in

relation to white matter tracts (infiltration, deflection, etc.) and the reconstruction of a tract for surgical planning. Information of the white matter using DTI can be obtained by whole-brain measurement or tractography.

1.11.1   Whole-brain measurement

DTI can provide information about anatomical connectivity using a whole-brain voxelwise analysis by measuring anisotropic diffusion in white matter tracts. FA is frequently used as a parameter for probing white matter properties such as restriction, hindrance, tortuosity and multiple compartments (Le Bihan 1995). The directional information of the fibre tract can be visualised on a colour-coded FA map in which left-right, anterior-posterior and inferior-superior directions are represented by the red, green and blue colour channels respectively.

1.11.2   Tractography

Tractography is the visualisation of white matter tracts based on DTI measurements (Le Bihan et al 2001, Mori et al 2002). The main diffusion axis, V1, represents the primary diffusion direction of underlying white matter axonal fibres. Hence, by following the direction of V1 by each consecutive voxel, the microscopic fibre pathways can be traced non-invasively. Tractography allows visualisation of the white matter trajectory in a three-dimensional space and segmentation of specific brain regions.

Whole-brain analysis is an exploratory approach and determines where the white matter changes are in the brain. This method allows an overview of

patterns of white matter changes and allows multiple group comparisons (Smith et al 2006). Tractography, however, is adopted when known changes of white matter integrity is found in a particular region or tract. This method has high specificity but can only measure individual persons (Behrens et al 2007).

The aim of this thesis is to define the patterns of white matter changes across the whole brain in subtypes of FTD, therefore, whole-brain analysis will be conducted in the context of the thesis.
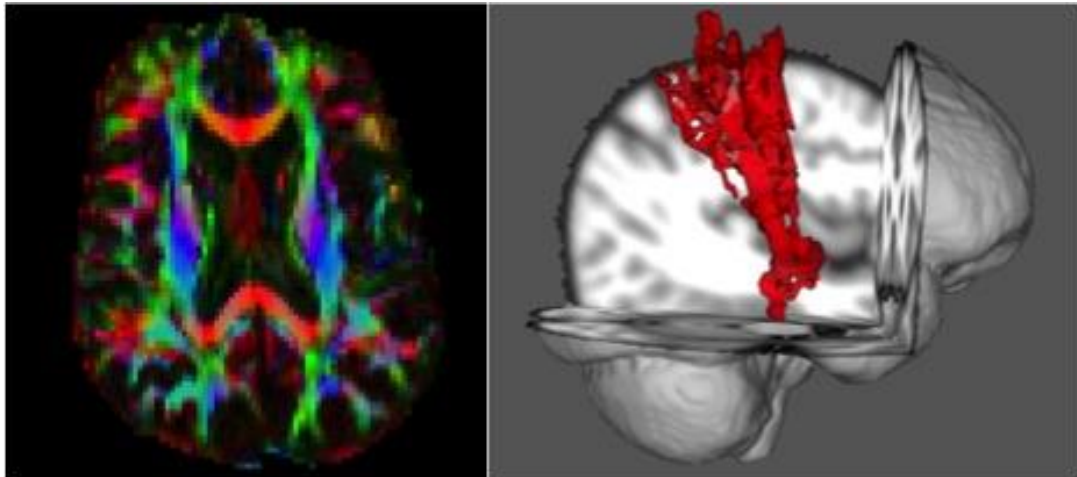
Figure 1.7 Whole-brain DTI colour map (left) and tractography (right).

The colour-coded FA map (left) shows diffusion properties of the whole-brain in left-right (illustrated in red), anterior-posterior (illustrated in green) and inferior-superior directions (illustrated in blue).
The tractography figure (right) shows reconstructions of the corticospinal tract (red). The tract is superimposed onto the T1-weighted image of the subject.

1.11.3   Imaging software packages

A number of imaging software packages are freely available online. Functional Magnetic Resonance Imaging of the Brain Software Library (FSL) (Smith et al 2004) consists of a program specifically for white matter analysis which is called the tract-based spatial statistics (TBSS) (Smith et al 2006). This program is specialised for the analysis of diffusion data and allows comparison of diffusion measures such as fractional anisotropy between groups (Smith et al 2006), and hence, has a higher sensitivity to group differences in diffusion measures when compared to other software packages such as Statistical Parametric Mapping in which a voxel-based-morphometric style of analysis is adopted (Frackowiak et al 1997). In addition, FSL also offers a well-developed diffusion toolbox that allows pre-processing of white matter and the option of performing probabilistic tractography of the white matter data.

Moreover, the FSL suite comprised of a large range of tools to in variable imaging modalities. Other than diffusion MRI, other analysis tools are also available for structural and functional MRI such that the data collected can be utilised with different imaging modalities and is supported by the same software package (Jenkinson et al 2012).The above advantages led to the selection of using FSL as the main tool of analysis in this thesis.

1.11.4   Beyond the diffusion tensor model

Since the development of D, alternative diffusion model with improved resolution or alternative quantitative measure to interpret white matter changes have been introduced. For example, the high angular resolution diffusion imaging can be used to resolve crossing fibres by estimating diffusion or fibre

orientation distribution functions, which is particularly useful for performing tractography (Tuch et al 2002). The alternative tool to measure white matter integrity includes apparent fibre density (Raffelt et al 2012) which aims to improve fibre detection in a multiple fibre voxel. While these models generate more specific diffusion measures, they perform best if acquired with a high resolution MRI scanner (> 3 Tesla) and with multiple diffusion directions (>40 directions).

Although there are different models, the diffusion tensor model and its derived metrics, fractional anisotropy, mean, axial and radial diffusivities, are used because the aim of this thesis emphasised on whole-brain measurement of white matter changes rather than the generation of tractography in high resolution. Taking into account the resources available (3 Tesla MRI scanner and 32 diffusion directions), diffusion tensor model with the use of fibre specific measurements in tract-based spatial statistics to solve crossing fibres will allow accurate and robust measurements of white matter integrity (Jbabdi et al 2010).

1.12 Research questions

DTI provides an optimal measurement of white matter integrity of the brain. Yet this imaging technique is relatively novel compared to conventional MRI, resulting in a limited number of studies measuring white matter changes in FTD. A summary of the current findings in measuring white matter changes in FTD is provided below (Table 1.1), followed by the research questions, aims and hypotheses of this thesis.

Early FTD studies on white matter reported changes that were either for the whole FTD or PPA spectrum, thus, the representation of white matter change in each subgroup might have been obscured (Borroni et al 2007, Matsuo et al 2008, Zhang et al 2009). Other studies have focused on a specified region of interest or a selected tract for tractography measurement and showed evidence of white matter degeneration in fibres connecting the fronto-temporal network in FTD with clear subdivision into bvFTD and PPA subtypes (Agosta et al 2010, Galantucci et al 2011, Whitwell et al 2010, Zhang et al 2013). The patterns of white matter degeneration in each FTD subtype and comparisons with grey matter atrophy were more clearly identified at a whole-brain voxelwise level of analysis (Acosta-Cabronero et al 2011, Agosta et al 2011, Mahoney et al 2013, Schwindt et al 2013, Zhang et al 2013). Importantly, recent studies showed that changes in the white matter are not confined to regions underlying the site of grey matter pathology but also extend beyond the regions in all major subtypes of FTD (Agosta et al 2011, Mahoney et al 2013, Schwindt et al 2013).

Despite the growing literature on white matter changes in FTD, a few issues remain unresolved. Firstly, white matter integrity in FTD subtypes over time has not been hitherto reported. As such, the differential rates of white matter changes over time are unknown. Also, the coupling between regional white matter changes and grey matter atrophy over time remains unknown. In addition, the severity and locations of changes appears to vary depending on the DTI metrics employed. For example, investigations of changes in FA, a global measure of tissue integrity, may be insensitive to specific changes in other

metrics such as AxialD or RadialD. This point is relevant as different DTI metrics may reflect different neuropathological processes in the tissues (Beaulieu 2002, Song et al 2002) and highlights the importance of investigating different DTI metrics concurrently in order to obtain an accurate picture of white matter integrity.

Importantly, studies of white matter integrity in pathologically homogeneous FTD cases are currently limited. Individuals who harbour the *C9orf72* gene expansions represent an ideal cohort for the study of clinical and imaging association in disease severity and progression in FTD as they demonstrated a slower disease progression (Boeve et al 2012, Khan et al 2012).

Only two studies thus far have examined white matter tracts changes in *C9orf72* carriers at a whole-brain level using diffusion tensor imaging (Mahoney et al 2012b, Mahoney et al 2014). One investigated white matter integrity in patients with or without the *C9orf72* gene expansions as part of a comprehensive study which measured grey matter atrophy and cortical thickness (Mahoney et al 2012b). Only one study to date compared white matter alterations of *C9orf72* expansion carriers and non-carriers in the same clinical phenotype (Mahoney et al 2014). This study showed different patterns of brain changes in bvFTD with or without the *C9orf72* gene expansions, despite the fact that all patients meet the same clinical diagnostic criteria. The relation between clinical symptoms and white matter degeneration in bvFTD patients with or without the *C9orf72* gene expansions has not been studied.

1.13 Aims and hypotheses

The first aim of this thesis is to establish the patterns of white matter changes in FTD subtypes compared to controls using DTI measurement. The second aim is to establish the patterns of longitudinal white matter changes in FTD subtypes over a 12-month time interval. Finally, patterns of white matter changes in association with changes in clinical symptoms in a pathologically homogenous FTD group with *C9orf72* gene expansions will be examined.

This thesis aims to address the key questions in neuroimaging of FTD and the study will be conducted in 3 parts:

1) Measure patterns of white matter change in FTD subtypes (bvFTD, nfv-PPA, sv-PPA) as compared to controls at baseline; compare white matter integrity measured with different DTI metrics; and overlay white matter changes to grey matter atrophy (Chapter 3).

   Hypothesis 1: White matter changes are specific to each subtype of FTD. Individuals at the initial visit exhibit changes in white matter tracts connecting the frontotemporal regions.

2) Conduct longitudinal investigation on white matter changes for each FTD subtype at 12-month follow up; compare white matter integrity measured with different DTI metrics; and study the relation of grey-white matter progression over the same time period (Chapter 4).

   Hypothesis 2: All types of FTD start with relatively circumscribed regions of white matter change. As disease progresses, white matter abnormalities progress to involve additional brain regions. White matter losses are hypothesised to map or exceed regions of grey matter atrophy.

The different sensitivity of the DTI metrics may be stage-specific and may help indicate the different stages of the disease.

3) Determine the distinctive pattern of white matter change and associated clinical deficits in the *C9orf72* expansion cases compared to those without the expansions (Chapter 5).

Hypothesis 3: Less white matter abnormalities and reduced clinical abnormalities will be identified in the *C9orf72* expansion group.

Table 1.1 Literature review on white matter studies in frontotemporal dementia.

Paper	Subjects (n)	Method	Software	Statistical method	MRI Scanner strength; DTI direction
Borroni et al., 2007	bvFTD(28), PPA(8) and control(23)	Fibre tracking (tractography)	BrainVisa 1.6 Software & SPM2	2-sample t-test	1.5T scanner; 6 directions
Matsuo et al., 2008	bvFTD(14), PPA(6)and control(17)	Tractography	PRIDE	Mann-Whitney U test	1.5T scanner; 15 directions
Zhang et al., 2009	FTD(18), AD(18) and control(19)	Tractography guided ROI	Volume-one and dTV software & SPM2	MANOVA; followed by univariate post-hoc test	4T scanner; 6 directions
Whitwell et al., 2010	bvFTD(16), sv-PPA(4) and nfv-PPA(7)	ROI	DTI Studio	ANCOVA	3T scanner; 21 directions
Agosta et al., 2010	sv-PPA(5) and control(8)	Tractography; ROI (Left ILF/SLF/UF & CC)	In-house software	Linear mixed effects model	3T scanner; 55 directions
Galantuci et al., 2011	nfv-PPA(9), sv-PPA(9) and control(9)	Probablistic tractography (ILF/UF/SLF)	PROBTRACKX	ANCOVA	3T scanner; 64 directions
Agosta et al., 2011	bvFTD(13), sv-PPA(7), nfv-PPA(9) and lv-PPA(4)	Whole-brain	TBSS & VBM	Non-parametric permutation test	3T scanner; 32 directions
Schwindt et al., 2011	sv-PPA(9) and control(16)	Whole-brain	TBSS	Non-parametric permutation test	3T scanner; 23 directions
Acosta-Cabronero et al., 2011	sv-PPA(10) and controls(21)	Whole-brain	TBSS & tractography	Non-parametric permutation test	3T scanner; 63 directions
Mahoney et al., 2012	nfv-PPA(13), lv-PPA(10) and sv-PPA(10)	Whole-brain	CAMINO, TBSS & SPM8 & DARTEL	Non-parametric permutation test	3T scanner; 64 directions
Zhang et al.,2013	bvFTD(13), sv-PPA(6) and nfv-PPA(6)	ROI	SPM8	Wilcoxon rank-sum test	4T scanner; 6 directions

Abbreviations: ROI = region-of-interest; ILF = inferior longitudinal fasciculus; SLF =superior longitudinal fasciculus; UF = uncinate fasciculus; CC = corpus callosum; MANOVA = multivariate analysis of variance; ANCOVA = analysis of covariance.

Chapter 2: General methodology

2 GENERAL METHODOLOGY

2.1 Participants

2.1.1 Case selection

Participants diagnosed with bvFTD, nfv-PPA or sv-PPA were recruited from the Frontier research clinic at Neuroscience Research Australia, Sydney, Australia into this study. All patients were seen by an experienced neurologist and underwent the same examination procedure: comprising neurological examination, cognitive and behavioural assessment, structural brain imaging and informal questionnaire. Diagnosis was established by consensus among the neurologist, neuropsychologist and occupational therapist. All patients met current clinical diagnostic criteria for FTD (Gorno-Tempini et al 2011, Rascovsky et al 2011). Participants were the largest sample size available and no specific age range was set for inclusion.

In addition, age- and sex-matched healthy controls were recruited from the Neuroscience Research Australia brain donor program and from local community clubs.

2.1.2 Genetic screening

Genetic screening and analysis were conducted by experienced scientists in the genetic laboratory after informed consent. Genomic DNA was extracted from either peripheral blood lymphocytes or frozen brain tissues in accordance with standard DNA extraction procedures. All participants included in the thesis are non-carriers of any genetic mutation, except for the *C9orf72* positive subgroup

used in Chapter 5. For screening of the *C9orf72* gene, the proband DNA collected was amplified and screened for the hexanucleotide repeat expansion in *C9orf72* by repeat-primed polymerase chain reaction (Renton et al 2011). *C9orf72* gene expansions were only considered pathogenic when more than 30 GGGGCC hexanucleotide repeats were observed.

2.1.3   Ethics

Ethical approval for this study was obtained from the Southern Eastern Sydney and Illawarra Area Health Service and the University of New South Wales ethics committees. All participants, or their person responsible, provided informed consent in accordance with the Declaration of Helsinki.

Information on neurological examination, cognitive and neuropsychological tests, blood test (for protein analysis and genetic mutation screening) and imaging were only available with authorised access in the Frontier patient database, Filemaker.

2.2   General cognitive screening

Participants were first assessed with the clinical dementia rating scale and Addenbrooke's Cognitive Examination-Revised as a general measure of global cognitive functioning. Cognitive assessments were collected by research assistants in the Frontier research clinic at Neuroscience Research Australia.

2.2.1   Clinical dementia rating scale

The clinical dementia rating scale quantifies the severity of symptoms of dementia across six domains of cognitive and functional performance: memory,

orientation, judgement and problem solving, community affairs, home and hobbies, and personal care. The composite score ranges from 0-3 with zero reflecting no evidence of dementia while higher scores indicate greater severity of dementia (Morris 1997). Controls are required to obtain a clinical dementia rating score of 0.

2.2.2 Addenbrooke's Cognitive Examination-Revised

The Addenbrooke's Cognitive Examination-Revised (ACE-R) is a general cognitive screening test which tests for the following five domains: attention/orientation, memory, fluency, language, and visuospatial skills. It has a maximum score of 100 with higher scores reflecting better performance. A cut-off score of 88/100 is used to distinguish healthy controls and dementia patients with 94% sensitivity and 89% specificity (Mioshi et al 2006).

2.3 General cognitive assessment

In addition, several neuropsychological tests were used to the integrity of the main cognitive domains (memory, visuospatial skills, executive function, language and behaviour). These tests were utilized for the purpose of diagnosis and for the comparison of clinical characteristics of the *C9orf72* expansion carriers and non-carriers.

2.3.1 Attention, working memory and episodic memory

Digit span, which was originally a subtest of the Wechsler Adult Intelligence Scale-III (Wechsler 1997), was administered to assess verbal short term memory/working memory. In digit span-forward, a sequence of numbers is

read out to the participant and the participant is required to repeat the sequence in the same order; in digit span-backward, the participant is required to repeat the given numbers in reverse order. Working memory was assessed by calculating the maximum backward span-the longest string of numbers correctly answered (maximum length = 8).

The Rey-Osterrieth Complex Figure is a test commonly used to measure visual episodic memory (Meyers & Meyers 1995). Initially participants are required to copy a geometric figure provided, and then 3 minutes later, reproduce the drawing from memory alone (immediate recall). Scoring is based on accuracy of the drawing at recall, with a maximum score of 36.

Doors and People is another test of visuoperceptual episodic memory (Baddeley et al 1994). Only the Doors test (part A) was used in this thesis as an index of visual recognition (Appendix 2.3.1).

2.3.2 Visuospatial skills

The delayed recall task of the Rey-Osterrieth Complex Figure is used to assess visuospatial skills (Meyers & Meyers 1995). Scoring is based on accuracy of the copy, with a maximum score of 36.

2.3.3 Executive functions

The Trail Making Test is used as an index of executive functions, visual search, scanning, speed of processing and mental flexibility (Reitan & Wolfson 1985). It consists of two parts, A and B. Part A requires the participant to draw a line sequentially connecting 25 encircled numbers distributed on page while part B requires the participant to connect circles which alternate between numbers and

letters (i.e.,1-A-2-B-3-C, etc). The test is scored by recording the amount of time that is taken to complete each task, where shorter time indicates better performance. To measure executive function, the time difference between Part A and Part B is calculated.

2.3.4 Language

Language integrity was measured with the Sydney Language Battery (SYDBAT) (Savage et al 2013). SYDBAT assesses single-word processing and comprises four subtests: i) picture naming, ii) word comprehension (word-picture matching), iii) semantic association (picture-picture matching) and iv) word repetition (Appendix 2.3.4). The same 30 items are used across the four subsets and include items of decreasing word frequency. The maximum score on each subtest is 30.

2.3.5 Behaviour

Assessment of behaviour was performed using the Cambridge Behavioural Inventory (CBI)-revised (Wear et al 2008). The CBI-revised was developed to measure changes in behaviour associated with dementia. Two versions were completed: one filled in by the participant and the other by a family member. Briefly, it assesses behaviour changes across various aspects: memory and orientation, everyday skills, self-care, abnormal behaviour, mood, beliefs, eating habits, sleep, stereotypical and motor behaviours and motivational level. Frequency and level of disturbance are rated for each item to measure the degree of behavioural disturbance. This instrument is sensitive in distinguishing

FTD from Alzheimer's disease and other dementia syndromes. (e.g.,

Huntington's disease and Parkinson's disease).

2.4 Imaging procedures

All participants underwent brain magnetic resonance imaging which included

diffusion-weighted and T1-weighted images. Participants included in the study

described in Chapter 4 also underwent a 12-month follow-up visit and clinical,

neuropsychological testing and MRI scans that were identical to the baseline

visit.

2.4.1 Image acquisition

Whole-brain diffusion-weighted and T1 images were obtained from a 3-Tesla

scanner (Philips Achieva 3.0T TX) with a standard 8-channel head coil. For the

diffusion-weighted sequence, two sets of whole-brain echo-planar images were

acquired with 32 non-collinear gradient directions (repetition time/echo

time/inversion time: 8400/68/90 ms; b-value = 1000 s/mm^2; 55 slices,

horizontal slice thickness 2.5 mm, end resolution: 2.5 x 2.5 x 2.5 mm^3; field of

view: 240 x 240 mm, 96 x 96 matrix). Two sets of 3D T1-weighted images were

also acquired in the coronal plane (echo time/repetition time: 2.6/5.8ms, 200

slices, slice thickness 1 mm, in-plane resolution: 1 X 1 mm^2, in-plane matrix: 256

x 256).

2.5 Exclusion criteria

Participants were only included if initial diagnosis was purely bvFTD, nfv-PPA

and sv-PPA such that participants who also exhibit other clinical syndromes

were excluded from the study. Given the focus on FTD and FTLD pathologies, patients with lv-PPA with Alzheimer's pathology predominantly were also excluded from this study.

Participants were excluded if they exhibited any of the following criteria: prior history of mental illness, history of other neurological disorders, significant head injury with loss of consciousness longer than 5 minutes, neurological movement disorders, evidence of cerebrovascular disease on imaging, alcohol and other drug abuse, use of psychotropic medication or any drugs with central nervous system side effects, and limited English proficiency.

Visual inspection of images was conducted to eliminate images with a large degree of head movement which led to a decrease in image quality (causing blurriness) and making imaging registration and analysis difficult. Images with obvious white matter hyper-intensities were excluded to eliminate participants with the possibility of small vessel disease. As MRI uses high-field magnets in a confined environment, individuals with ferromagnetic implants or a prior history of claustrophobia were also excluded.

2.6 Image processing and analysis

After image acquisition, processing and analysis of imaging data were performed using Functional MRI of the Brain Software Library (FSL v 4.1.9)(Smith et al 2004), a freely available software tool. Within the FSL suite, tract-base spatial statistics and voxel-based morphometry are both whole-brain voxelwise analysis tools to be used for white and grey matter analysis respectively. FreeSurfer version 4.2, another grey matter analysis tool, was used

to measure cortical thickness of the brain (Fischl & Dale 2000). An overview of the imaging processing and analysis conducted is provided below.

2.7 Tract-base spatial statistics

DTI data were processed with Tract-based spatial statistics (TBSS v 1.1) (Smith et al 2006), part FSL v 4.1.9 (Smith et al 2004).

2.7.1 TBSS pre-processing steps

The image pre-processing involved the following steps: Firstly, the two DTI sequences were combined and averaged to improve signal-to-noise ratio before being corrected for eddy current distortions and head movements using affine registration to the non-diffusion volumes (b = 0 s/mm^2). Then, the Brain Extraction Tool was applied to both the b0 images and the diffusion-weighted images (Smith 2002). Each brain was visually checked to ensure the accurate removal of all non-brain tissues during the skull-stripping process. Finally, a tensor model was fitted into the diffusion images using Functional MRI of the Brain (FMRIB) diffusion toolbox, and the primary, secondary and tertiary tensor eigenvalues (λ_1, λ_2 & λ_3) were generated (Smith et al 2004). The four DTI metrics obtained were: i) *AxialD,* which is the diffusion coefficient along the main axis; ii) *RadialD,* the averaged diffusion coefficient along the perpendicular axes; iii) *MD*, the averaged diffusion coefficient along all axes; and iv) *FA*, which is the ratio of the above metrics, generating a value between 0 to 1 to show the overall magnitude and orientation of water diffusion in tissue.

2.7.2   TBSS processing steps

DTI data were then processed using the following methodology, which can be summarised in four steps-Firstly, the FA map from each individual was transformed to the FMRIB58 fractional anisotropy template obtained from the FSL software using nonlinear registration. All aligned FA images were affine-registered into the Montreal Neurological Institute standard space (MNI-152) (Andersson et al 2007a, Andersson et al 2007b). Secondly, the averaged FA data were thinned to create a skeleton of white matter that signified the centres of each white matter tract (i.e., lines of maximum FA) common to the group. Thirdly, each individual FA data point was projected on the mean FA skeleton to correct residual misalignment and to line up the centres of individual tracts. As white matter voxels could be contaminated by signals from the neighbouring grey matter or corticospinal fluid, a threshold of 0.2 was set to the mean FA skeleton to minimise such potential partial volume effects. Lastly, AxialD, RadialD and MD data were also mapped onto the skeleton using projection vectors from the FA-to-skeleton transformation for each individual (Smith et al 2006).

2.7.3   White matter atlases

Two DTI white matter atlases were provided by the John Hopkins University (JHU), one for white matter tractography and the other as white matter labels (Mori et al 2008, Oishi et al 2008). The 20 tracts on the tractography atlas were created by averaging results of tractrography of 28 normal subjects. The ICBM-DTI-WM labels atlas consisted of 51 white matter tract labels and was created by

hand segmentation of a standard-space average of diffusion tensor maps from 81 subjects.

2.7.4   Regions-of-interest masks

Based on the JHU atlases, eleven regions-of-interest masks were created and thresholded in FSL. The specific regions-of-interest included the forceps major and minor, cingulum (anterior and posterior), superior longitudinal fasciculus (superior-inferior and temporal), inferior longitudinal fasciculus, inferior-fronto-occipital fasciculus, uncintate fasciculus, corticospinal tract and the anterior thalamic radiation.

The masks created were then overlaid onto TBSS results to obtain DTI measurements (FA, MD, AxialD and RadialD) of each participant within that region for quantification.

The masks can be divided into 3 groups according to the fibre connections to the different brain regions:

Commissural fibres

Forceps major

The forceps major are fibres that connect the occipital lobes and cross the midline via the splenium of corpus callosum (Orrison 2008). The change in forceps major integrity is correlated with memory function (Duering et al 2011). This tract is not the most common to be studied in FTD measuring white matter integrity but was shown to be mildly affected (Matsuo et al 2008).
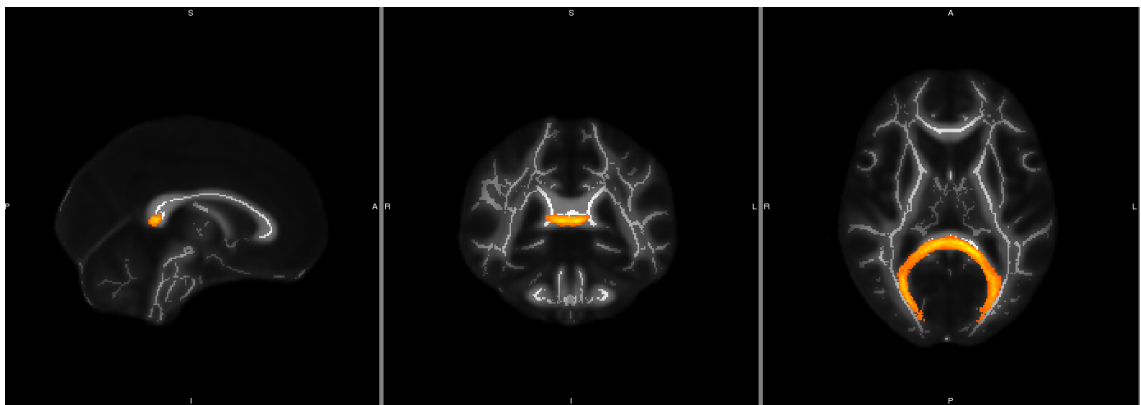
Figure 2.1 Mask of the forceps major in sagittal (left), coronal (middle) and axial (right) planes.

Forceps minor

The forceps minor are fibres that connect the frontal lobes and cross the midline via the genu of corpus callosum (Orrison 2008). The change in forceps minor integrity is correlated with processing speed (Duering et al 2011). This tract is significantly affected in FTD (Agosta et al 2010,

Agosta et al 2011, Schwindt et al 2013, Whitwell et al 2010, Zhang et al 2009).
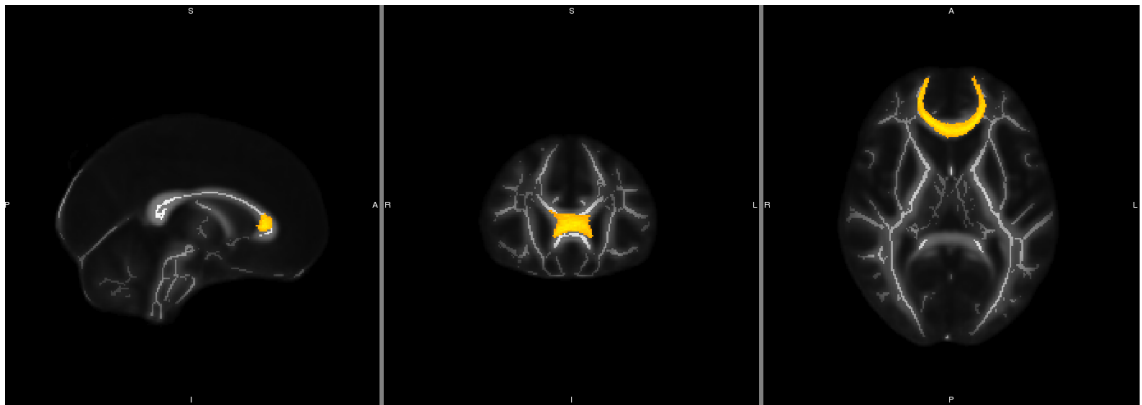
Figure 2.2 Mask of the forceps minor in sagittal (left), coronal (middle) and axial (right) planes.

Association fibres

Cingulum (anterior and posterior)

The cingulum bundles encircle the corpus callosum and connect the cingulate gyrus and the entorhinal cortex of the brain.

The cingulum can be divided into anterior and posterior portions. The anterior cingulum has connections from the anterior cingulate cortex to the orbitofrontal cortex, mesial temporal and striatal structures. These regions are central for emotion regulation (Philips & Robberecht 2011). Lesions of the anterior cingulum itself is also associated with apathy (Kim et al 2011). The posterior cingulum, on the other hand, is related to executive functioning, attention and memory (Delano-Wood et al 2012, Schermuly et al 2010). Both portions are shown to be affected in FTD (Agosta et al 2011, Whitwell et al 2010, Zhang et al 2009).
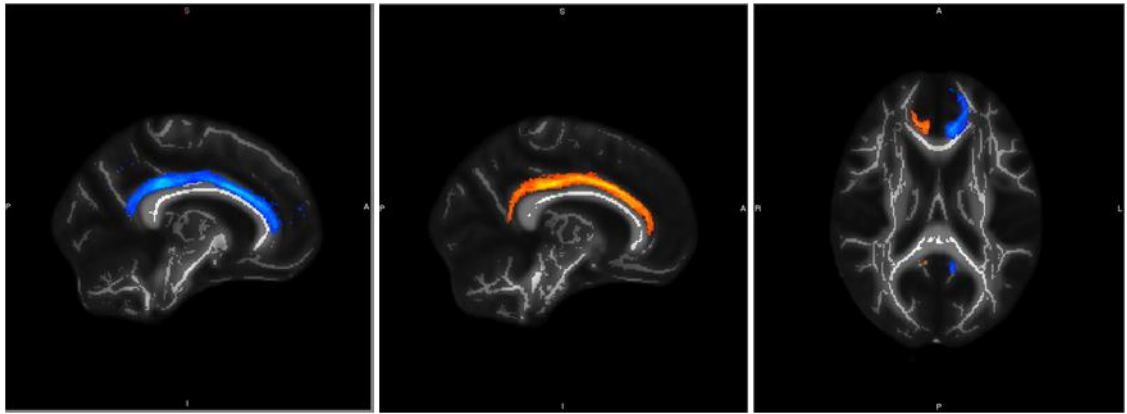
Figure 2.3 Mask of the anterior cingulum: left (in blue) and right (in orange).
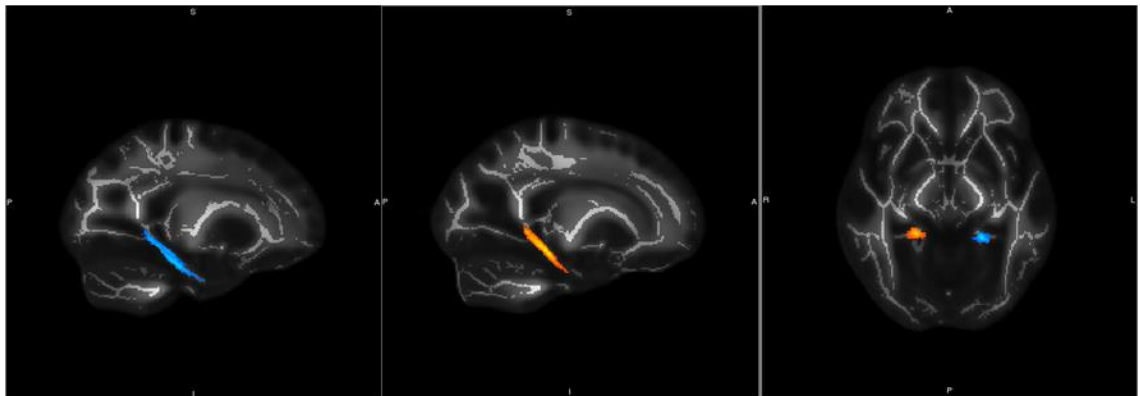
Figure 2.4 Mask of the posterior cingulum: left (in blue) and right (in orange).

Note: The anterior and posterior cingulum bundles are referred to as cingulum (cingulate gyrus) and cingulum (hippocampus) respectively in the JHU atlas.

Superior longitudinal fasciculus

> The superior longitudinal fasciculus is a long association fibre interrelating the cortex of the frontal, temporal, parietal and occipital lobes of the brain (Orrison 2008). The mask of the superior longitudinal

fasciculus, which includes the arcuate fasciculus, is subdivided into superior-inferior and temporal components as described in the JHU atlas (Mori et al 2008). The superior longitudinal fasciculus plays a major role in visual and oculomotor aspects of spatial function (Mountcastle et al 1975), phonological processing (Duffau et al 2003) and language functions (Bernal & Ardila 2009). This tract is severely affected in FTD (Agosta et al 2011, Galantucci et al 2011, Matsuo et al 2008, Schwindt et al 2013, Whitwell et al 2010).
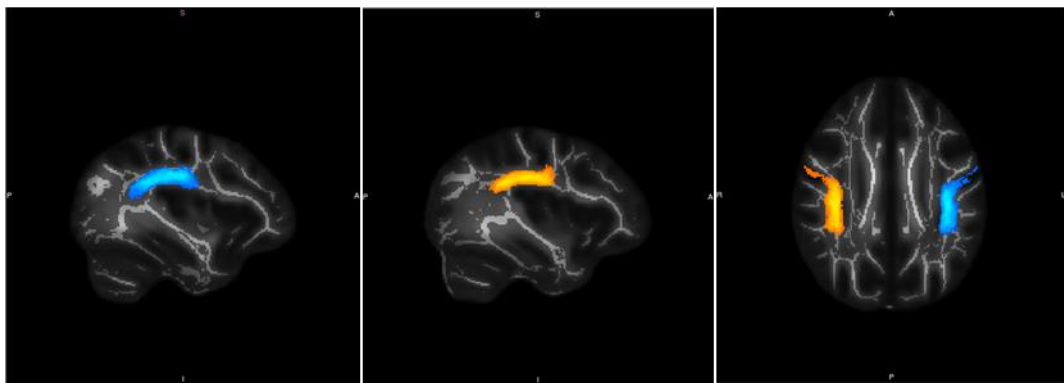
Figure 2.5 Mask of the superior longitudinal fasciculus-superior-inferior: left (in blue) and right (in orange).
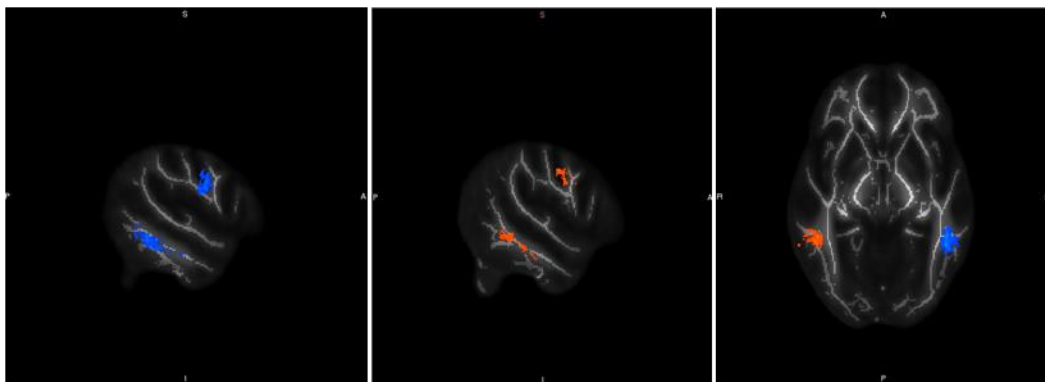
Figure 2.6 Mask of the superior longitudinal fasciculus-temporal: left (in blue) and right (in orange).

Inferior longitudinal fasciculus

The inferior longitudinal fasciculus connects the temporal and occipital lobes and runs laterally and inferiorly above the optic radiation fibres (Orrison 2008). Although it is known that inferior longitudinal fasciculus is responsible for part of the larger functional network, its functionality is still poorly understood, primary due to technical difficulty in measurement. Nonetheless, recent findings suggest that the inferior longitudinal fasciculus is associated with visual-perception and object recognition (Ortibus et al 2012). This tract is severely affected in FTD (Agosta et al 2011, Galantucci et al 2011, Mahoney et al 2013, Matsuo et al 2008, Schwindt et al 2013, Whitwell et al 2010).
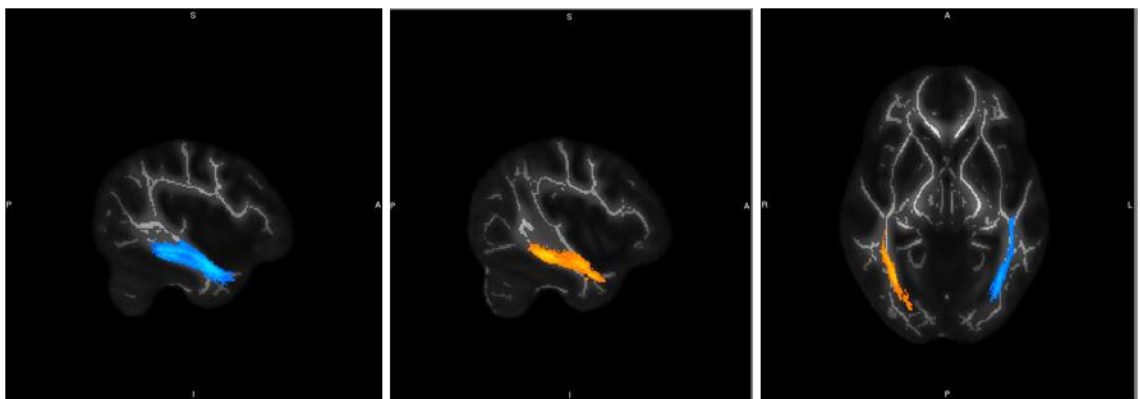
Figure 2.7 Mask of the inferior longitudinal fasciculus: left (in blue) and right (in orange).

Inferior-fronto-occipital fasciculus

The inferior-fronto-occipital fasciculus connects the orbitofrontal to posterior temporal areas and occipital lobes (Orrison 2008). It runs medially and above the optic radiation fibres and overlaps the inferior

longitudinal fasciculus along part of their pathways. This tract has clear

roles in semantic language processing, as demonstrated by semantic

paraphasias when it is stimulated (Mandonnet et al 2007). This tract is

also severely affected in FTD (Borroni et al 2007, Schwindt et al 2013).
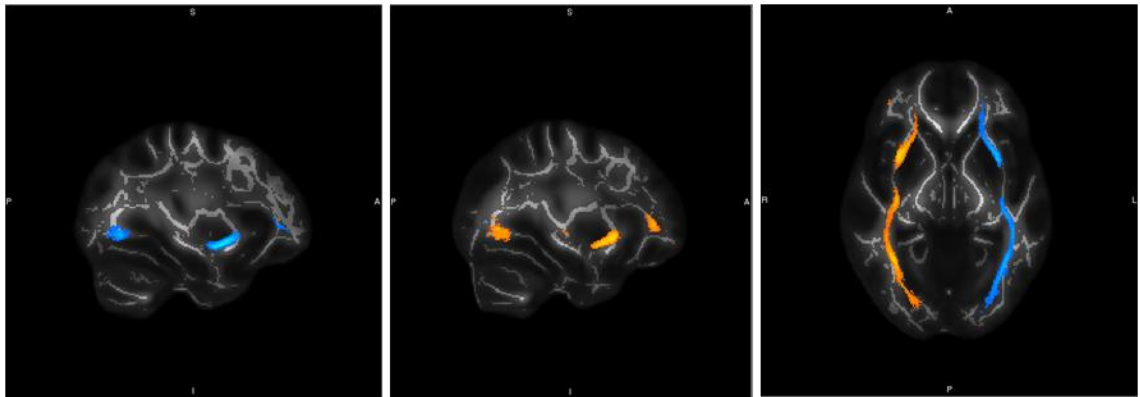
Figure 2.8 Mask of the inferior-fronto-occipital fasciculus: left (in blue) and right (in orange).

Uncinate fasciculus

The uncinate fasciculus connects the orbitofrontal lobe to the anterior

temporal lobe parahippocampal gyrus and the amygdala (Orrison 2008).

The uncinate fasciculus is associated with naming (Papagno et al 2011)

and temporal lobe-based mnemonic associations (e.g., associate the

name + face + voice of an individual) to modify behaviour (Von Der

Heide et al 2013). This tract is highly affected in FTD (Agosta et al 2011,

Galantucci et al 2011, Mahoney et al 2013, Matsuo et al 2008, Schwindt

et al 2013, Whitwell et al 2010, Zhang et al 2009).
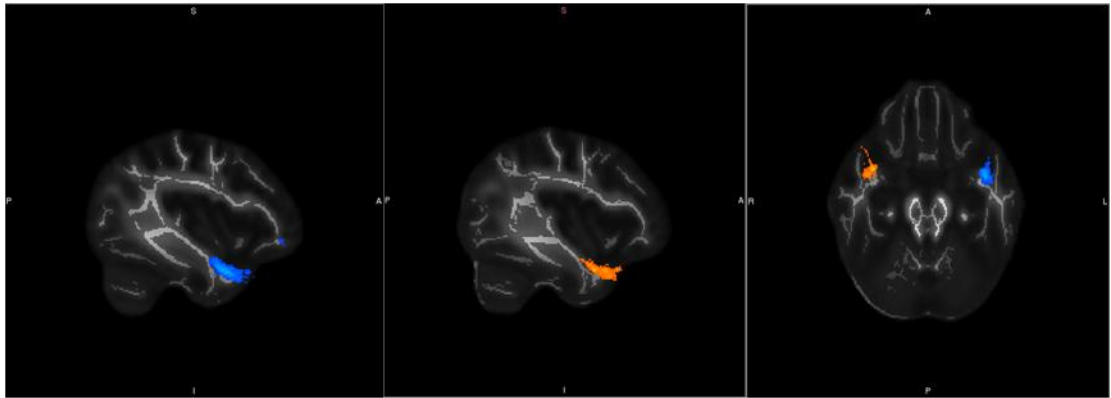
Figure 2.9 Mask of the uncinate fasciculus: left (in blue) and right (in orange).

Projection fibres

Anterior thalamic radiation

Anterior thalamic radiation refers to fibre pathways connecting the anterior and medial thalamic nuclei to the frontal lobe through the anterior limb of the internal capsule (Orrison 2008). Function of this tract is not clearly defined but shown to be correlated with speed processing, executive function and working memory (Duering et al 2011, Mamah et al 2010). This tract is less studied in FTD but also found to be affected (Zhang et al 2009).
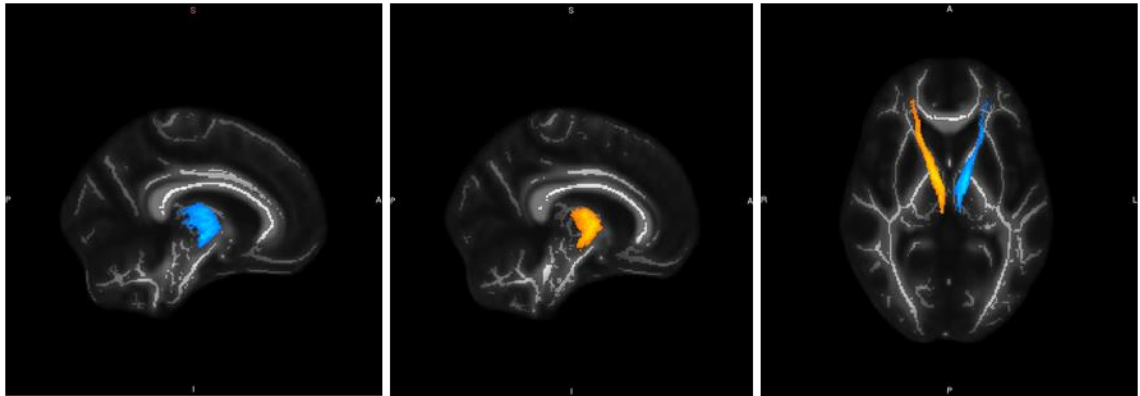
Figure 2.10 Mask of the anterior thalamic radiation: left (in blue) and right (in orange).

Brain stem fibres

Corticospinal tract

The corticospinal tract originates from the primary motor cortex, primary somatosensory cortex, premotor cortex and supplementary motor area and projects to the spinal cord. This tract can be further divided into anterior and lateral corticospinal tracts. Majority of the corticospinal tract runs laterally and crosses the pyramidal decussation to the spinal cord of the opposite side of the body. The remaining anterior corticospinal runs uncrossed to the spinal cord (Siegel & Sapru 2010). The corticospinal tract is measured as a whole in this thesis with reference to the mask in the JHU atlas (Mori et al 2008). The corticospinal tract is crucial for voluntary motor activities, control posture and muscle tone (Siegel & Sapru 2010). Loss of integrity has been shown on this tract in FTD (Lillo et al 2012, Whitwell et al 2010, Zhang et al 2009). Recent discovery has brought attention to this tract as

degeneration of the corticospinal tract is found to be associated with sv-PPA cases with FTLD-TDP type C and right temporal lobe atrophy (Josephs et al 2013).
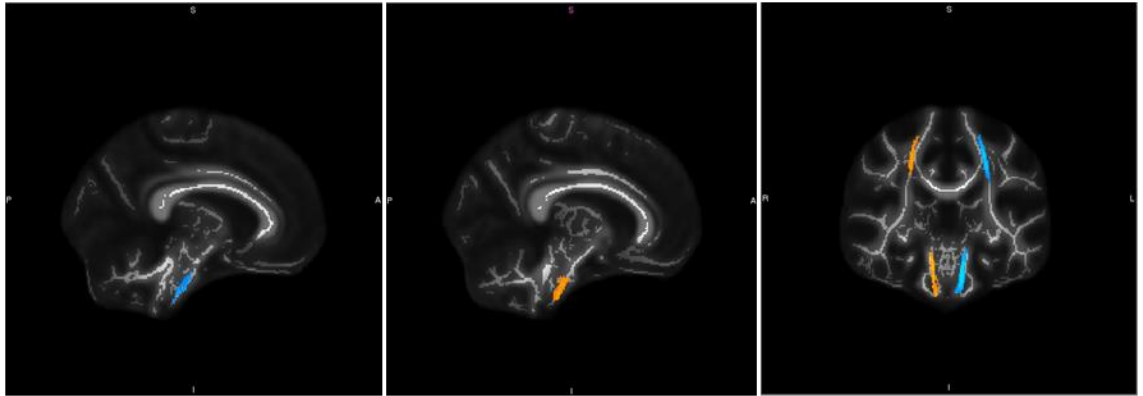
Figure 2.11 Mask of the corticospinal tract: left (in blue) and right (in orange).

2.8   Voxel based morphometry

Grey matter analysis was performed with voxel-based morphometry (VBM) from the FSL suite (Ashburner & Friston 2000, Good et al 2001). T1-weighted images underwent the Brain Extraction Tool to remove any non-brain matter (Smith 2002) and the brain was segmented into grey, white matter and cerebrospinal fluid using FMRIB's Automatic Segmentation Tool (Zhang et al 2001). The images were then registered into the MNI-152 standard space using non-linear registration (Andersson et al 2007a, Andersson et al 2007b). The space-transformed images were averaged and flipped along the x-axis to produce a symmetric, study-specific, grey matter template. All native T1 scans were non-linearly registered to the study-specific template for modulation to correct for local expansion or contraction due to non-linear component of the

spatial transformation. The resulting images were averaged and flipped along the x-axis to produce a left-right symmetric, study-specific grey matter template and were smoothed with an isotropic Gaussian kernel with a sigma of 3mm (full width half maximum = 8mm).

2.9   FreeSurfer

In addition to whole-brain voxelwise measures of the grey matter, cortical thickness and brain structure volumes were also determined by FreeSurfer version 4.2 which also uses T1-weighted images of MRI (Fischl & Dale 2000). The images were first automatically segmented into grey matter, white matter and cerebrospinal fluid. Visual inspection was done on the resulting image and manual corrections were made for segmentation error when necessary. Cortical thickness was calculated as "the shortest distance between two surfaces and each point across the cortical mantle which is determined by surface representations which is the grey/white matter and pial surface boundaries" (Dale et al 1999). The cortical thickness measurements were then mapped onto the inflated surface of each brain of the participant and aligned to a common spherical space according to cortical folding and thickness measurements (Fischl et al 1999). Cortical regions were identified by an automatic parcellation of the cerebral cortex (Fischl et al 2004). The resulting images were smoothed with a 20mm full-width at half height Gaussian kernel. The level of blurring was set to reduce the impact of imperfect alignment between cortices and to improve signal-to-noise ratio (Lerch & Evans 2005).

2.9.1   Grey matter atlas

Harvard-Oxford cortical and subcortical structural atlas was used in FSL derived by semi-automated segmentation of T1-weighted images of 37 healthy subjects. These images were registered to standard space. The atlas consists of 48 cortical and 21 subcortical structures.

Other in-house cortical atlases were used in FreeSurfer. The first one is a gyral-based atlas, whereby the gyrus is defined as running between the bottoms of two adjacent sulci (Desikan et al 2006). The other atlas is based on a parcellation scheme which divided the cortex into gyral and sulcal regions depending on the curvature of the surface (Destrieux et al 2010).

2.10 Voxelwise statistical analysis

In both TBSS and VBM, a voxelwise general linear model was applied and clusters were generated from a permutation-based (5000 permutations performed), non-parametric test with the threshold-free cluster enhancement option. The statistical threshold was set at $p < 0.05$ corrected for multiple comparisons (familywise error) for all analyses. In FreeSurfer, statistical significance was determined at $p < 0.05$ after Bonferroni correction.

Chapter 3: White matter changes in FTD syndromes

3 WHITE MATTER CHANGES IN FTD SYNDROMES

White matter undergoes significant damage in early FTD (Borroni et al 2007). Unlike grey matter atrophy in FTD which is well investigated, white matter integrity in FTD is relatively less researched. The study of white matter is essential to determine mechanisms of pathophysiology and to establish the patterns of disruption across FTD syndromes. Understanding the patterns of white matter change in FTD will also potentially assist clinical diagnosis and differentiation from other neurodegenerative diseases (Borroni et al 2007, Zhang et al 2009).

Early studies investigated white matter changes using signal intensity in T2- and proton density-weighted images. Visual inspection of increased signal intensity in the frontal and/or temporal lobes successfully distinguished FTD from Alzheimer's disease (Kitagaki et al 1997). Another pioneering study attempted to compare white matter atrophy to grey matter atrophy using volumetric change on T1-, T2- and proton density-weighted images in FTD (Chao et al 2007). White matter atrophy was found to largely parallel the patterns of grey matter atrophy in the study.

3.1 Deficiencies in the studies of white matter integrity in FTD

DTI findings in bvFTD, nfv-PPA and sv-PPA revealed decreased connectivity in different white matter tracts connecting the frontal and temporal lobes (Acosta-Cabronero et al 2011, Agosta et al 2011, Borroni et al 2007, Galantucci et al 2011, Mahoney et al 2013, Schwindt et al 2013, Zhang et al 2013) with some issues still unresolved. These studies have focussed on a tract or region of interest

without defining the global pattern of white matter change in FTD. Only a minority of the studies defined patterns of white matter change in FTD using a whole-brain voxelwise analysis to date (Acosta-Cabronero et al 2011, Agosta et al 2011, Mahoney et al 2013, Schwindt et al 2013). Even among the four studies investigating global white matter change in FTD, not all measured the full diffusion tensor behaviour in the FTD white matter (Acosta-Cabronero et al 2011, Agosta et al 2011, Mahoney et al 2013). Measuring all four DTI metrics (FA, MA, AxialD and RadialD) are advantageous as it increases sensitivity in detecting differential pathological states. Only one study measured global white matter change with the use of a complete set of DTI metrics, as well as investigated white matter change across the FTD spectrum (Agosta et al 2011). Given there is only one comprehensive study to date defining white matter change in the spectrum of FTD, it is important to confirm these findings with a slightly larger sample and at the same time attempt to answer more questions related to white matter degeneration in FTD.

3.2   Other uncertainties of white matter integrity in FTD

3.2.1   Current findings on white and grey matter relations

As reviewed in Chapter 1 Section 1.4.1, grey matter changes have been studied more extensively than white matter in FTD. In the behavioural-variant of FTD, grey matter atrophy is found in the mesial frontal and orbitofrontal regions, as well as anterior temporal regions (Schroeter et al 2008, Schroeter et al 2007, Seeley et al 2008, Vitali et al 2008). In nfv-PPA, grey matter atrophy is found predominately on the left posterior fronto-insular region (Gorno-Tempini et al

2004, Grossman et al 1996, Vitali et al 2008, Whitwell et al 2010). In sv-PPA, grey matter is more pronounced in the left anterior and inferior temporal lobe (Davies et al 2009, Davies et al 2004, Hodges & Patterson 2007, Vitali et al 2008).

Findings have been inconsistent amongst different studies regarding the severity and anatomical relation between white and grey matter changes. Some suggested grey matter changes match white matter changes with white matter changes developing as disease progresses (Acosta-Cabronero et al 2011, Hornberger et al 2010, Whitwell et al 2010). In contrast, others have argued that white matter changes are more extensive than grey matter changes and suggested white matter integrity could be an early marker for FTD (Agosta et al 2011, Mahoney et al 2013, Schwindt et al 2013, Zhang et al 2013).

3.2.2 DTI parameter and white matter tissue pathology

Traditionally, studies using DTI have mainly focused on a decrease in FA to represent a loss of white matter integrity (Borroni et al 2007, Matsuo et al 2008, Zhang et al 2009). Pathological changes, such as differential effects on glia and axonal degeneration may also alter other tensor behaviour in DTI, such as RadialD and AxialD, whilst FA may lack sensitivity if water diffusion changes proportionally along the direction of other DTI metrics (Acosta-Cabronero et al 2010). The combination of different DTI metrics (RadialD, AxialD, MD), which measure different aspects of diffusion behaviour in the white matter, appears more sensitive in detecting white matter changes in neurodegenerative conditions rather than the use of a single global diffusion measure such as FA. In addition, sensitivity of the DTI metrics appears to differ among different

diseases. For instance, RadialD may be the most sensitive measurement for sv-PPA (Acosta-Cabronero et al 2011) while MD and RadialD appear to be more sensitive measurements in Alzheimer's disease (Acosta-Cabronero et al 2010). These deficits in documenting white matter integrity in FTD leads to the study presented in this chapter. This study aims to:

1) define the patterns of white matter change in three major FTD subtypes (bvFTD, nfv-PPA and sv-PPA);

2) map the white matter changes relative to cortical grey matter atrophy in FTD subtypes; and

3) establish the sensitivity of different DTI metrics across these three clinical syndromes.

3.3   Methods

3.3.1   Participant and experimental procedures

Thirty-three individuals diagnosed with FTD (bvFTD = 12; nfv-PPA = 10; sv-PPA = 11) and 15 matched controls were recruited into this study. One nfv-PPA subject in this study was excluded for voxel-based morphometry analysis due to issues with the acquired T1-weighted image, but was included in the diffusion imaging analysis.

Details of patient recruitment procedure, image acquisition, imaging processing for tract-based spatial statistics and voxel-based morphometry and voxelwise analysis have been described previously in Chapter 2.

In brief, tract-based spatial statistics (TBSS) generates the FA data from diffusion-weighted images and the data are applied nonlinearly into standard

space which then creates a mean FA image and a mean FA skeleton; all FA data are then projected to the FA skeleton and entered into general linear modelling and thresholding for statistical analysis.

In voxel-based morphometry (VBM), T1-weighted images are first segmented into grey, white matter and cerebrospinal fluid, before being applied nonlinearly into standard space; a study specific grey matter template is produced in which all images are registered; at the last step images are smoothed with an isotropic Gaussian kernel with a sigma of 3mm (full width half maximum = 8mm) and entered into general linear modelling and thresholding for statistical analysis. The statistical threshold was set at $p < 0.05$ corrected for multiple comparisons (familywise error) for all analyses.

3.4 Results

3.4.1 Clinical demographics

Table 3.1 Demographic and clinical data of patients and control group at baseline.

	bvFTD	nfv-PPA	sv-PPA	Controls	p
Sex: M/F	8/4	6/4	9/2	8/7	NS
Mean age; yrs	63 ± 8 (28)	67 ± 11 (31)	62 ± 6 (28)	67 ± 6 (24)	NS
Education ; yrs	12 ± 3 (10)	12 ± 3 (9)	13 ± 3 (10)	14 ± 3 (7)	NS
ACE-R; max:100	74 ± 12 (39)	79 ± 11 (35)	63 ± 12 (44)	94 ± 4 (12)	#^
Disease duration; yrs	4.8 ± 2.8 (8)	3.0 ± 0.6 (2)	5.4 ± 3.0 (9)	N/A	^

Numerical values are illustrated in mean ± standard deviation (range of scores). # denotes significant differences in ACE-R between all FTD subtypes (bvFTD, nfv-PPA and sv-PPA) and controls (p < 0.001). ^ denotes significant differences between nfv-PPA and sv-PPA. Abbreviations: M = male; F = female; NS = not significant. ACE-R = Addenbrooke's Cognitive Examination-Revised; yrs = years; max = maximum; bvFTD = behavioural-variant

frontotemporal dementia; nfv-PPA= primary progressive aphasia non-fluent variant; sv-PPA = primary progressive aphasia semantic variant.

Demographic and clinical characteristics of study participants are presented in Table 3.1. Groups were well matched for age, years of education and sex. Not surprisingly, a significant group difference was observed on the ACE-R, with all FTD groups scoring significantly lower than controls determined by one-way ANOVA (F (3, 38) = 18.9, $p < 0.001$). A post-hoc Tukey revealed bvFTD (74 ± 12, $p < 0.001$), nfv-PPA (79 ± 11, $p < 0.001$) and sv-PPA (63 ± 12, $p < 0.001$) all scored significantly lower than controls (94 ± 4). In addition, the sv-PPA group also scored significantly lower than nfv-PPA on the ACE-R ($p < 0.035$), reflecting the semantic loading of this instrument. Furthermore, one-way ANOVA also showed difference in disease duration between groups (F (3, 44) = 19.8, $p < 0.00$). Post-hoc Tukey revealed that sv-PPA had a longer disease duration than nfv-PPA patients (5.4 ± 3.0 vs 3.0 ± 0.6 years, $p < 0.043$).

3.4.2   Patterns of white matter changes in FTD subtypes

Results from the TBSS analyses revealed different patterns of white matter changes in all the FTD subtypes (Figures 3.1-3.3) (Acosta-Cabronero et al 2011, Agosta et al 2011, Mahoney et al 2013, Schwindt et al 2013). Patterns of white matter change in the FTD differ slightly depending on the DTI metrics (Appendix Tables 3.2-3.5). The profiles for each subtype are described below.

3.4.2.1   Behavioural-variant FTD

All DTI measures revealed significant bilateral changes (reduced FA and increased MD, AxialD and RadialD) in similar locations, most pronounced in frontotemporal regions, in the bvFTD group compared to controls. The changes occurred in the anterior thalamic radiation, anterior cingulum, superior and inferior longitudinal, inferior frontal-occipital and uncinate fasciculi, as well as the genu of the corpus callosum. Abnormalities on MD and RadialD appeared the most extensive in this FTD group (Figure 3.1 and Appendix Tables 3.2-3.5).
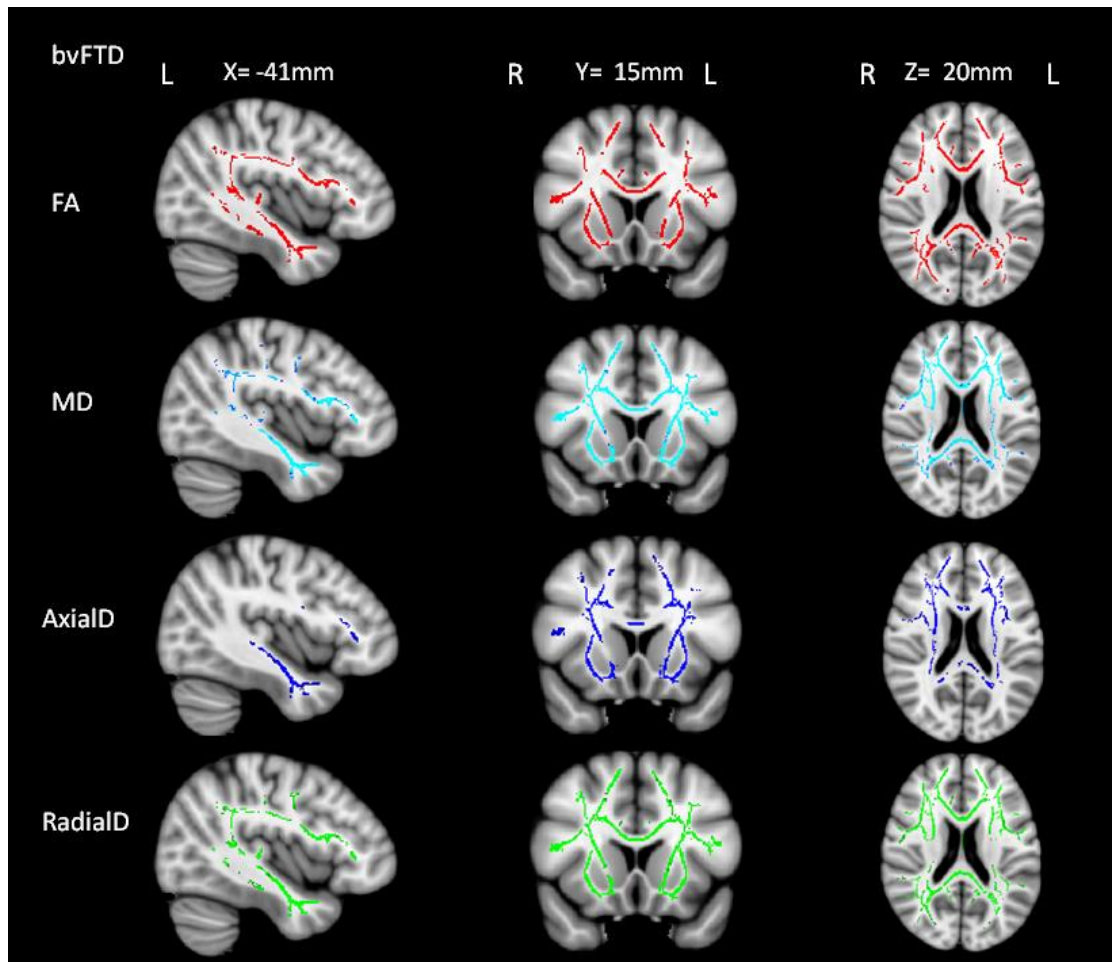
Figure 3.1 White matter changes in bvFTD compared to controls.

TBSS results of voxelwise group differences are shown for FA, MD, AxialD and RadialD at p < 0.05, corrected for multiple comparisons. Results are overlaid on sections of the MNI standard brain. L = left; R = right.

3.4.2.2 Nonfluent variant primary progressive aphasia

In nfv-PPA, left greater than right white matter changes were observed in the superior and inferior longitudinal fasciculi, as well as in the body and splenium of the corpus callosum. Abnormalities were generally more pronounced in the MD and RadialD DTI measures compared to the other metrics (Figure 3.2 and Appendix Tables 3.2-3.5).
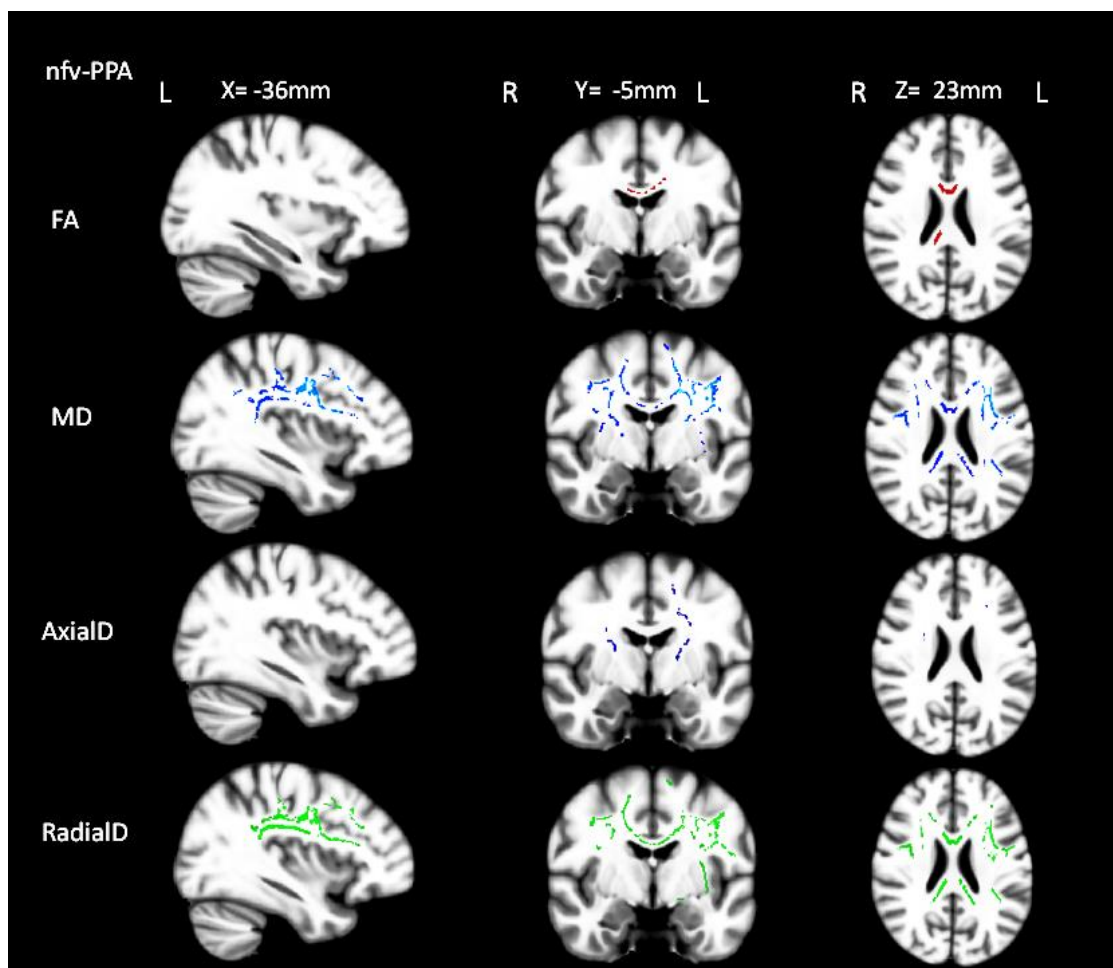
Figure 3.2 White matter changes in nfv-PPA compared to controls. *TBSS results of voxelwise group differences are shown for FA, MD, AxialD and RadialD at p < 0.05, corrected for multiple comparisons. Results are overlaid on sections of the MNI standard brain. L = left; R = right.*

3.4.2.3 Semantic variant primary progressive aphasia

In this group, white matter changes were identified only in the left hemisphere
(Figure 3.3). Regional white matter changes included the left cingulum, left
superior and inferior longitudinal and uncinate fasciculi. Similarly located
abnormalities were detected by all four DTI metrics, with most extensive
changes found in MD and AxialD (Appendix Tables 3.2-3.5).
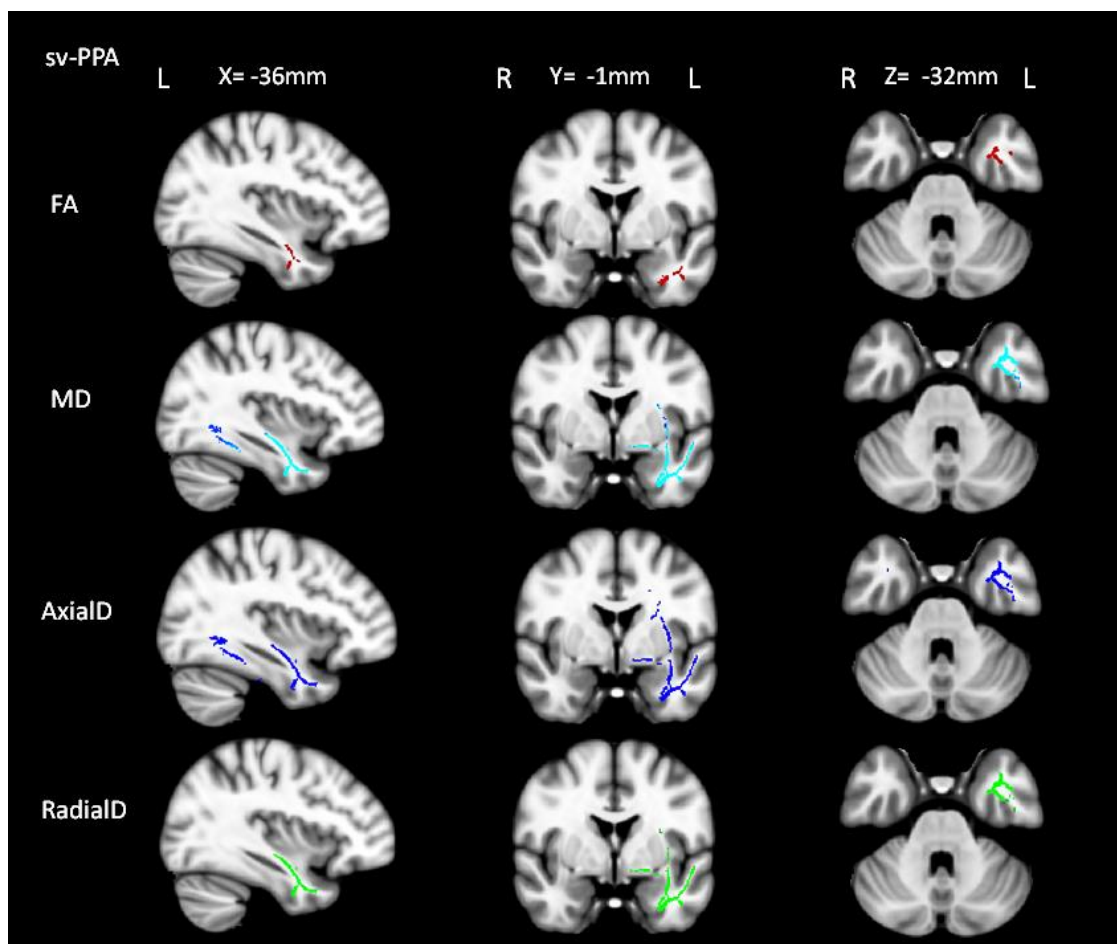
Figure 3.3 White matter changes in sv-PPA compared to controls
*TBSS results of voxelwise group differences are shown for FA, MD, AxialD and
RadialD at p < 0.05, corrected for multiple comparisons. Results are overlaid
on sections of the MNI standard brain. L = left; R = right.*

3.4.3 Grey matter changes in FTD subtypes and its relations to white matter alterations

VBM analyses revealed patterns of grey matter changes in all the FTD subtypes that were consistent with previous investigations (Figure 3.4 & Appendix Table 3.6). In brief, atrophy in the bilateral orbito-frontal and anterior temporal lobes are most prominent in bvFTD (Schroeter et al 2008, Schroeter et al 2007, Seeley et al 2008). In nfv-PPA, the atrophy is relatively focal and circumscribed to the left posterior fronto-insular region (Gorno-Tempini et al 2004, Grossman et al 1996, Whitwell et al 2010). Finally, sv-PPA is associated with an asymmetric pattern of atrophy involving the anterior temporal region, generally left more so than right (Davies et al 2009, Davies et al 2004, Hodges & Patterson 2007).

Importantly, white matter abnormalities were found to extend beyond the locations of grey matter atrophy in two of the three FTD subtypes.

This difference in the location of grey and white matter change was most pronounced in the nfv-PPA group. In this group, grey matter atrophy was observed only in the inferior frontal and insula regions. Whilst changes were found in the white matter overlying these regions with grey matter atrophy, additional white matter changes were also found in the temporal and parietal regions (superior longitudinal fasciculus)(Figure 3.2 & Figure 3.4).

In bvFTD, grey matter exhibits reductions in the frontal and anterior temporal lobes bilaterally, and with less predominant changes in the parietal and occipital lobes. White matter change maps grey matter atrophy but showed additional

changes in the left occipital regions (forceps major, inferior longitudinal fasciculus and inferior-fronto-occipital fasciculus) (Figure 3.1& Figure 3.4). In contrast, while grey matter atrophy was present in the temporal regions bilaterally with some changes in the frontal pole in sv-PPA, changes in white matter tract is more focal in the left temporal lobe (inferior longitudinal fasciculus) (Figure 3.3 & Figure 3.4).
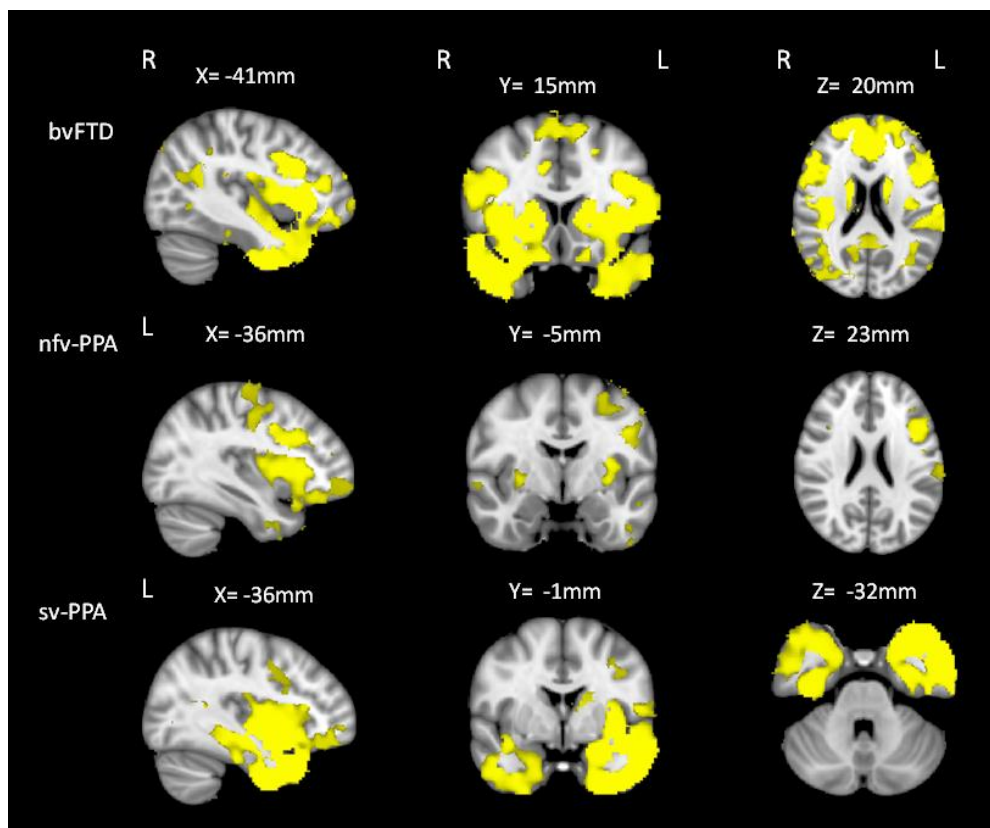
Figure 3.4 Cross-sectional grey matter changes in frontotemporal dementia groups compared to controls.

Reductions in grey matter density (in yellow) are shown for the bvFTD (top), nfv-PPA (middle) and sv-PPA (bottom) groups. Significant clusters were thresholded at p < 0.05, corrected for multiple comparisons. Results are overlaid on sagittal, axial and coronal sections of the MNI standard brain. L = left; R = right.

3.5 Discussion

This study investigated white matter changes in the three major subtypes of FTD with all four DTI metrics using a used a whole brain voxelwise approach. These findings demonstrated specific profiles of white matter changes in each FTD subtype. In two of the three FTD subtypes, white matter alterations extended beyond the grey matter cortical atrophy detected. Importantly, the location and severity of these changes varied depending on the DTI metrics used, indicating that white matter changes shown with different DTI measures may represent different pathological processes.

In bvFTD, severe white matter changes were observed in tracts connecting the orbitofrontal and anterior temporal regions (anterior thalamic radiation, anterior cingulum, superior and inferior longitudinal, inferior frontal-occipital and uncinate fasciculi, as well as the genu of the corpus callosum). In nfv-PPA, degeneration occurred bilaterally in frontotemporal white matter but with changes more predominant on the left (superior and inferior longitudinal fasciculi, as well as in the body and splenium of the corpus callosum). White matter changes in sv-PPA were circumscribed to the left temporal lobe (superior and inferior longitudinal fasciculi and the uncinate fasciculus).

3.5.1 White and grey matter relations

Co-localisation of white and grey matter abnormalities in FTD have been reported in some studies (Acosta-Cabronero et al 2011, Hornberger et al 2010, Whitwell et al 2010) but some found more widespread white than grey matter alternations (Agosta et al 2011, Mahoney et al 2013, Schwindt et al 2013, Zhang et al 2013). This study revealed changes in white matter integrity, as measured

by TBSS, extended beyond those changes in grey matter measured by VBM. These findings were most pronounced in nfv-PPA and were also observed in bvFTD. In contrast, bilateral temporal grey matter atrophy was observed in sv-PPA but only degeneration in left temporal white matter tracts were reported.

3.5.2 DTI parameter and white matter tissue pathology

In this study, MD and RadialD alterations were most severe in bvFTD and nfv-PPA, while MD and AxialD alterations were most prominent in sv-PPA. MD, the mean value of AxialD and RadialD, was consistently found to be most sensitive in detecting white matter changes across the three FTD groups. Animal studies have suggested that AxialD abnormalities correlate with axonal degeneration while RadialD abnormalities suggest myelin loss (Pierpaoli et al 2001, Song et al 2003) which leads to speculation of myelin loss to occur in bvFTD and nfv-PPA while axonal degeneration to occur in sv-PPA. The biological interpretations in human DTI data, however, is challenging given the structural heterogeneity using this indirect method compared with histopathological observations in animal models. Inclusion of grey matter, crossing fibres and residual misalignment may all cause changes to absolute diffusivities or eigenvalues which may not necessarily reflect underlying pathologies (Zhang et al 2013). In addition, given the complexity of pathological changes affecting the white matter (altered myelination, neurodegeneration, gliosis, calcification, etc.) (Sierra et al 2011), a single diffusion metric is unlikely to correlate best with a unique pathological process (Acosta-Cabronero et al 2010, Mahoney et al 2013, Pierpaoli et al 2001). Further, unlike other dementia syndromes, the neuropathology of FTD is complex and remains often unpredictable in life. FTD

subtypes share abnormal protein depositions of either tau (in bvFTD and nfv-PPA), TDP-43 (in bvFTD and sv-PPA) or, in a small proportion, fused in sarcoma (in bvFTD) (Davies et al 2005, Hodges et al 2004, Josephs et al 2006a, Knibb et al 2006, Lee et al 2011, Mackenzie et al 2010a, Mesulam et al 2008). The variability in protein deposition within and across FTD subtypes likely contributes to the complexity in interpreting changes identified on diffusion-weighted images.

3.6 Summary

- <u>Defined specific patterns of white matter changes:</u> This study defined changes in the white matter in three clinical subtypes of FTD: bvFTD, nfv-PPA and sv-PPA.

- <u>White matter change extend beyond grey matter atrophy:</u> These results confirmed previous findings of white matter change being more widespread than grey matter change. These findings are most prominent in nfv-PPA and bvFTD but not in sv-PPA.

- <u>White matter abnormalities differ depending on the DTI metrics used</u>: This suggests alterations in diffusion metrics may detect different pathological processes within each subtype. A full DTI tensor model is recommended to study and correlate pathological findings. Furthermore, pathological validation of these findings is needed.

- <u>Clinical implications of studying white matter abnormalities in FTD:</u> Confirming certain patterns of white matter change could potentially aid diagnosis of FTD, similar to the reference of frontotemporal atrophy using structural MRI scans.

Chapter 4: Longitudinal white matter changes in FTD

4 LONGITUDINAL WHITE MATTER CHANGES IN FTD SYNDROMES

4.1   The importance of longitudinal studies

Mapping progression of disease is essential to the understanding of disease mechanisms, improve disease management and also improve prediction of the disease course.

Mapping of disease progression can be addressed in certain ways. Firstly, disease progression can be inferred by comparing groups of patients at different stages of the disease. This approach allows for rapid collection of data in observable results and may include a large number of subjects in a study. The disadvantages, however, are the individual or environmental variabilities which could make group comparison difficult.

Alternatively, disease progression can be addressed using a true longitudinal design. Longitudinal study of continuous or repeated monitoring of subjects over time requires years to decades for progressive disorders and therefore, are usually less common. The undeniable advantage of such designs, however, is that they avoid the issue of inter-subject variability. As study participants act as their own control, they provide reliable indices of changes over time as the disease progresses. This approach provides the best direct indication of disease progression which is particularly useful for the study of development or progression of disease.

A true longitudinal prospective design to determine progression in FTD is used in this chapter.

4.2   Longitudinal grey matter changes in FTD

Due to the challenges described in the previous section, longitudinal studies are less common than cross-sectional studies in general. Limited studies in the literature assessed longitudinal grey matter alterations in FTD. Despite the distinctive patterns of grey matter atrophy shown early at disease stage, longitudinal findings displayed a convergent distribution of brain atrophy in all FTD subtypes. Changes in grey matter atrophy with disease progression are reviewed for each FTD subtype below:

4.2.1   Behavioural-variant frontotemporal dementia

In bvFTD, grey matter atrophy is present in bilateral frontal and temporal lobes, as well as the anterior cingulate, anterior insula and the thalamus. Grey matter atrophy measured overtime is rare but one study revealed disease progression in bvFTD and showed subsequent changes in bilateral frontal regions (left ventro-medial frontal and right medial superior frontal areas), anterior insular and other cortical structures (left amygdala/hippocampus) after a 12-month period. Furthermore, additional areas of atrophy were found in the middle and posterior cingulate gyrus (Brambati et al 2007).

4.2.2   Nonfluent variant primary progressive aphasia

The nfv-PPA is associated with bilateral grey matter atrophy but predominantly on the left. Structures affected included the inferior frontal lobe, insula and premotor cortex (Gorno-Tempini et al 2004, Josephs et al 2006a, Rogalski et al 2011, Rohrer et al 2009b). A cortical thickness study that measured nfv-PPA over a 2-year period showed peak atrophy sites spread beyond the initiative distinctive locations and subsequent atrophies are found in the frontal,

temporal, anterior parietal lobes and the caudate and thalamus. Despite the progression, atrophy remained predominately on the left hemisphere (Rogalski et al 2011).

4.2.3 Semantic variant primary progressive aphasia

The sv-PPA has asymmetric atrophy involving the anterior and inferior temporal lobes, predominantly on the left hemisphere (Davies et al 2009, Gorno-Tempini et al 2004, Hodges & Patterson 2007, Rohrer et al 2009b). One 8-year case study showing subtle atrophy at the left anterior temporal lobe initially and subsequent changes revealed more extensive regions of the left temporal lobe being affected and such changes extend to the right temporal regions (Czarnecki et al 2008). Another longitudinal study confirmed that the previously left-dominant changes in sv-PPA extend to the homologous regions in the right temporal lobe after 12-month (Brambati et al 2009).

4.3 Longitudinal white matter changes in FTD

In contrast to studies investigating grey matter integrity changes over time, there is no longitudinal investigation of white matter change in FTD regardless of volumetric measurement or diffusion tensor imaging. Evidence shows progressive loss of grey matter volume over time but white matter progression in FTD subtypes has not been researched. As such, the rate and locations of white matter changes with disease progression and the relationship with grey matter change overtime are unknown. Whether white and grey matter damage exhibit tight coupling over time with disease stage or type remains to be answered.

Similarly, the sensitivity of DTI measures as potential markers of disease progression in FTD remains unknown. DTI metrics reflect changes in white matter integrity and are potentially related to different underlying pathological processes. Differential effects on glia, mechanisms of axonal degeneration, inflammatory responses and rate of degeneration lead to different pathological states and alter diffusion tensor behaviours. DTI metrics have shown to be stage-specific in other dementias (Acosta-Cabronero et al 2012). Whether the sensitivity of DTI metrics differ with disease progression in FTD is yet to be determined.

Therefore, this chapter aims to:

1) establish the regional pattern and severity of white matter damage in the different FTD syndromes with disease progression over 12 months;

2) determine the relationship between white matter and grey matter change over the same time period;

3) study the sensitivity of different DTI metrics as markers of disease progression.

4.4 Methods

4.4.1 Participant

Thirty-three individuals diagnosed with FTD (bvFTD = 12; nfv-PPA = 10; sv-PPA = 11) were recruited. These participants are the same patients reported in Chapter 3, who all underwent an additional one-year follow-up. The time between baseline and follow-up scans for bvFTD, nfv-PPA and sv-PPA were 0.9 ± 0.2 years, 1.0 ± 0.0 years and 1.0 ± 0.3 years respectively. One nfv-PPA

subject in this study was excluded for voxel-based morphometry analysis due to issues with the acquired T1 image, but was included in the diffusion imaging analysis.

Controls participants were not included in this FTD disease progression study. Details of patient recruitment procedure, image acquisition, general imaging processing for the cross-sectional analysis have been described in Chapter 2. Longitudinal measurement and analysis of white matter specifically used for this study is detailed below.

4.4.2   Longitudinal measurement of white matter

Analysis of longitudinal data was conducted in a separate analysis in which FTD baseline and follow-up scans were used.

With the use of TBSS, all pre-processing steps are identical for the baseline and longitudinal images to those described in Chapter 2. Briefly, the following steps were used. Firstly, within each FTD subtype, all FA maps from baseline and follow-up scans were registered non-linearly to the FMRIB58 fractional anisotropy standard template; secondly, the mean FA skeleton was derived from baseline and follow-up FA maps within each FTD subtype; thirdly, each individual FA data point was projected on the mean FA skeleton with a threshold of 0.2 to minimize partial volume effects; and finally, AxialD, RadialD and MD data were also mapped onto the skeleton using projection vectors from the FA-to-skeleton transformation for each individual. This method has been used previously in other longitudinal studies (Acosta-Cabronero et al 2012, Barrick et al 2010, Teipel et al 2010, Weaver et al 2009).

For VBM, again processing steps were identical to those described in Chapter 2. In brief, T-1 images of baseline and follow-up scans were used to produce a grey matter study template. All native T1 scans were non-linearly registered to the study-specific template for modulation. The resulting images were averaged and smoothed with an isotropic Gaussian kernel with a sigma of 3mm (full width half maximum = 8mm).

4.4.3 Statistical analysis

Longitudinal analyses were conducted within each FTD subtype separately. In each group, TBSS and VBM data acquired were compared separately across the two time points (baseline and 12-month acquisition) with a paired t-test. The statistical threshold was set at $p < 0.05$ corrected for multiple comparisons (familywise error) for all analyses.

4.5 Results

4.5.1 Clinical demographics

Table 4.1 Demographic and clinical data of patients and control group with longitudinal assessment.

	bvFTD	nfv-PPA	sv-PPA	*p*
Sex: M/F	8/4	6/4	9/2	NS
Mean age; yrs	63 ± 8 (28)	67 ± 11 (31)	62 ± 6 (28)	NS
Education; yrs	12 ± 3 (10)	12 ± 3 (9)	13 ± 3 (10)	NS
ACE-R; max:100	74 ± 12 (39)	79 ± 11 (35)	63 ± 12 (44)	^
Disease duration; yrs	4.8 ± 2.8 (8)	3.0 ± 0.6 (2)	5.4 ± 3.0 (9)	^
Scan interval; yrs	0.9 ± 0.2 (0.5)	1.0 ± 0.0 (0)	1.0 ± 0.3 (1)	NS

Numerical values are illustrated in mean ± standard deviation (range of scores). ^ denotes significant differences between nfv-PPA and sv-PPA. Abbreviations: M = male; F = female; NS = not significant. ACE-R = Addenbrooke's Cognitive Examination-Revised; max = maximum; yrs = years; bvFTD = behavioural-variant frontotemporal dementia; nfv-PPA = nonfluent variant primary progressive aphasia; sv-PPA = semantic variant primary progressive aphasia.

Groups were well matched for age, years of education, sex and scan interval. FTD patients scored significantly different in ACE-R determined by one-way ANOVA ($F_{(3, 38)} = 18.9$, $p < 0.001$). A post-hoc Tukey revealed the sv-PPA group scored significantly lower in ACE-R than nfv-PPA (63 ± 12 vs 79 ± 11, $p < 0.035$) (Table 4.1).

The one-way ANOVA also showed difference in disease duration between the FTD groups ($F_{(3, 44)} = 19.8$, $p < 0.001$). Post-hoc Tukey revealed that sv-PPA

had a longer disease duration than nfv-PPA patients (5.4 ± 3.0 vs 3.0 ± 0.6 years, $p < 0.043$) (Table 4.1).

4.5.2   Patterns of longitudinal white matter changes in FTD subtypes

Results were collected using whole-brain voxelwise TBSS analysis (Figure 4.1-Figure 4.4) with a further regions-of-interest to obtain DTI values for statistical analysis (Table 4.2-Table 4.5).

Each FTD subtype exhibited specific patterns of white matter change over 12-month. All FTD groups showed continued progressive changes from baseline with additional involvement in other brain regions.

In bvFTD, baseline changes showed severe cross-sectional changes in orbitofrontal and anterior temporal tracts. Over 12-month, affected regions at baseline remained affected with additional changes in the posterior temporal and occipital white matter over the 12-months.

In nfv-PPA, baseline changes occurred bilaterally in frontotemporal white matter (left>right), with longitudinal changes more prominent on the right. Initial white matter changes in sv-PPA were circumscribed to the left temporal lobe, with longitudinal changes extending to bilateral frontotemporal tracts.

4.5.2.1   Behavioural-variant FTD

At 12 months, extensive bilateral changes continued in most white matter tracts across all DTI metrics compared to baseline measurements. Longitudinal changes in FA and RadialD were concordant with each other and showed the most extensive changes among all metrics (Table 4.2). Changes in FA and RadialD were found in bilateral anterior thalamic radiation, anterior cingulum, genu and splenium of corpus callosum, superior longitudinal fasciculus (superior-inferior and temporal), inferior-frontal-occipital fasciculus, inferior

longitudinal fasciculus and uncinate fasciculus. Variability in the extent of progression of white matter changes depend on the DTI metrics used. For example, some tracts were spared when measured using some DTI measures (right anterior cingulum and left superior longitudinal fasciculus in MD; bilateral anterior cingulum, superior and inferior longitudinal fasciculi in AxialD) (Figure 4.1 & Table 4.2).
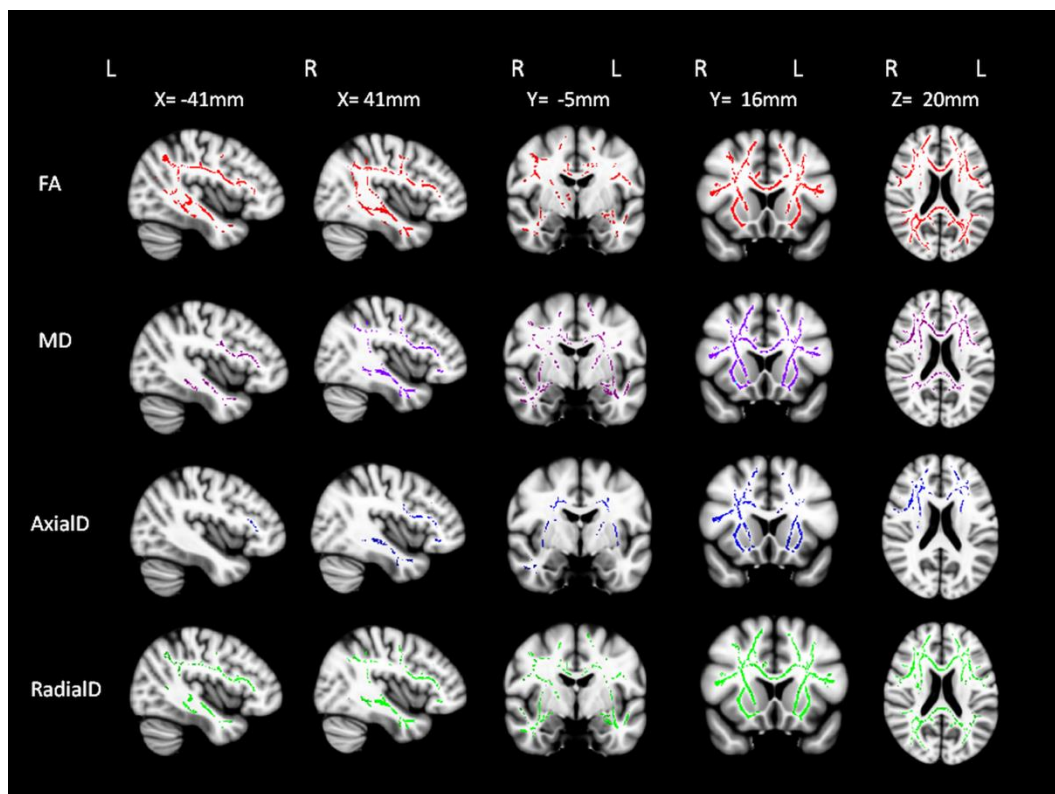
Figure 4.1 Longitudinal white matter changes in bvFTD.
Longitudinal assessments of white matter changes are shown for FA, MD, AxialD and RadialD (p < 0.05, corrected for multiple comparisons). Results are overlaid on sections of the MNI standard brain. L = left; R = right.

Table 4.2 Longitudinal white matter changes in bvFTD as illustrated in the four DTI metrics.

Tracts/Group	FA (Mean ± SD) Time 1	Time 2		MD (Mean ± SD) Time 1	Time 2		AxialD (Mean ± SD) Time 1	Time 2		RadialD (Mean ± SD) Time 1	Time 2	
Ant thal rad L	0.42 ± 0.03	0.41 ± 0.04	*	0.86 ± 0.11	0.92 ± 0.16	*	1.26 ± 0.11	1.32 ± 0.17	*	0.66 ± 0.11	0.72 ± 0.16	*
Ant thal rad R	0.43 ± 0.03	0.41 ± 0.04	*	0.84 ± 0.07	0.91 ± 0.11	**	1.24 ± 0.07	1.30 ± 0.11	*	0.63 ± 0.07	0.71 ± 0.12	**
Anterior cingulum L	0.41 ± 0.04	0.39 ± 0.05	**	0.89 ± 0.07	0.91 ± 0.08	*	1.31 ± 0.07	1.32 ± 0.10		0.67 ± 0.07	0.71 ± 0.09	**
Anterior cingulum R	0.37 ± 0.03	0.35 ± 0.04	**	0.90 ± 0.08	0.92 ± 0.08		1.27 ± 0.09	1.27 ± 0.09		0.71 ± 0.07	0.74 ± 0.08	*
Posterior cingulum L	0.38 ± 0.05	0.37 ± 0.04		0.85 ± 0.08	0.85 ± 0.08		1.21 ± 0.09	1.20 ± 0.09		0.67 ± 0.08	0.68 ± 0.08	
Posterior cingulum R	0.41 ± 0.04	0.39 ± 0.04		0.83 ± 0.08	0.82 ± 0.06		1.21 ± 0.09	1.17 ± 0.07		0.64 ± 0.08	0.64 ± 0.06	
Splenium of CC	0.57 ± 0.06	0.56 ± 0.06	***	0.85 ± 0.06	0.86 ± 0.06		1.50 ± 0.05	1.48 ± 0.05	*	0.53 ± 0.08	0.55 ± 0.08	**
Genu of CC	0.42 ± 0.06	0.40 ± 0.07	***	0.99 ± 0.14	1.04 ± 0.18	*	1.48 ± 0.12	1.52 ± 0.17		0.74 ± 0.16	0.80 ± 0.20	**
SLF (superior-inferior) L	0.41 ± 0.04	0.40 ± 0.04	**	0.80 ± 0.04	0.82 ± 0.06		1.18 ± 0.04	1.18 ± 0.06		0.62 ± 0.05	0.64 ± 0.06	*
SLF (superior-inferior) R	0.42 ± 0.04	0.41 ± 0.04	**	0.79 ± 0.06	0.80 ± 0.05	*	1.18 ± 0.06	1.18 ± 0.06		0.60 ± 0.07	0.61 ± 0.06	**
SLF (temporal) L	0.42 ± 0.03	0.41 ± 0.03	**	0.81 ± 0.04	0.82 ± 0.05		1.19 ± 0.05	1.19 ± 0.06		0.62 ± 0.05	0.63 ± 0.05	**
SLF (temporal) R	0.44 ± 0.04	0.43 ± 0.04	**	0.79 ± 0.05	0.80 ± 0.05	*	1.20 ± 0.05	1.20 ± 0.05		0.59 ± 0.06	0.60 ± 0.06	**
IFOF L	0.41 ± 0.04	0.39 ± 0.03	***	0.92 ± 0.10	0.96 ± 0.11	***	1.34 ± 0.10	1.37 ± 0.11	**	0.71 ± 0.11	0.75 ± 0.11	***
IFOF R	0.41 ± 0.03	0.40 ± 0.03	***	0.88 ± 0.05	0.91 ± 0.06	***	1.30 ± 0.05	1.32 ± 0.06	**	0.67 ± 0.06	0.71 ± 0.06	***
ILF L	0.41 ± 0.03	0.40 ± 0.03	**	0.88 ± 0.05	0.89 ± 0.06	*	1.29 ± 0.06	1.30 ± 0.07		0.67 ± 0.05	0.69 ± 0.06	**
ILF R	0.43 ± 0.03	0.42 ± 0.03	**	0.83 ± 0.06	0.85 ± 0.05	*	1.25 ± 0.07	1.26 ± 0.06		0.62 ± 0.06	0.65 ± 0.05	**
UF L	0.34 ± 0.05	0.32 ± 0.05	**	0.98 ± 0.19	1.03 ± 0.23	**	1.34 ± 0.18	1.38 ± 0.22	**	0.80 ± 0.19	0.85 ± 0.23	**
UF R	0.34 ± 0.05	0.32 ± 0.04	**	0.94 ± 0.10	0.99 ± 0.13	**	1.30 ± 0.09	1.35 ± 0.14	*	0.76 ± 0.11	0.81 ± 0.13	***
CST L	0.53 ± 0.03	0.53 ± 0.03		0.78 ± 0.03	0.79 ± 0.04		1.30 ± 0.05	1.31 ± 0.05		0.53 ± 0.03	0.53 ± 0.05	
CST R	0.57 ± 0.03	0.56 ± 0.04		0.77 ± 0.03	0.76 ± 0.03		1.32 ± 0.04	1.31 ± 0.06		0.49 ± 0.04	0.49 ± 0.04	

Asterisks show significant changes at Time 2 relative to Time 1: * $p < 0.05$, ** $p < 0.01$; *** $p < 0.001$. Values for MD, AxialD and RadialD were shown at $10^3 mm2s-1$. Abbreviations: FA = fractional anisotropy; MD = mean diffusivity; AxialD = axial diffusivity; RadialD = radial diffusivity; SD = standard deviation; CC = corpus callosum; SLF = superior longitudinal fasciculus; IFOF = inferior fronto-occipital fasciculus; ILF = inferior longitudinal fasciculus; UF = uncinate fasciculus; CST = corticospinal tract; L = left; R = right.

4.5.2.2 Nonfluent variant primary progressive aphasia

After 12 months, additional white matter abnormalities were observed in this group (anterior thalamic radiation, anterior cingulum, uncinate fasciculus and genu of corpus callosum), with the changes becoming more pronounced in the right compared to the left hemisphere (except for the anterior thalamic radiation which occurred on the left) (Figure 4.2).

Again, differences were found in the magnitude of change depending on the metrics used. Longitudinal changes in FA were most extensive and were found in the left anterior thalamic radiation, bilateral anterior cingulum, genu and splenium of the corpus callosum, the right superior longitudinal fasciculus (temporal), left inferior longitudinal fasciculus, right inferior longitudinal fasciculus and left uncinate fasciculus. An exception was the right inferior-fronto-occipital fasciculus which was affected in all other metrics but not FA. Moreover, tracts were spared in bilateral anterior cingulum and the corpus callosum in MD and RadialD (Figure 4.2 & Table 4.3).

Whole-brain voxelwise TBSS analysis showed AxialD alterations in the inferior-fronto-occipital fasciculus only when using a more liberal significance threshold ($p < 0.001$ uncorrected). This analysis is more stringent as signals are averaged across voxels of the whole brain rather than selected regions (Figure 4.2). In contrast, region-of-interest results as shown in Table 4.3 revealed AxialD alterations in the left anterior thalamic radiation and inferior-fronto-occipital fasciculus at $p < 0.05$.
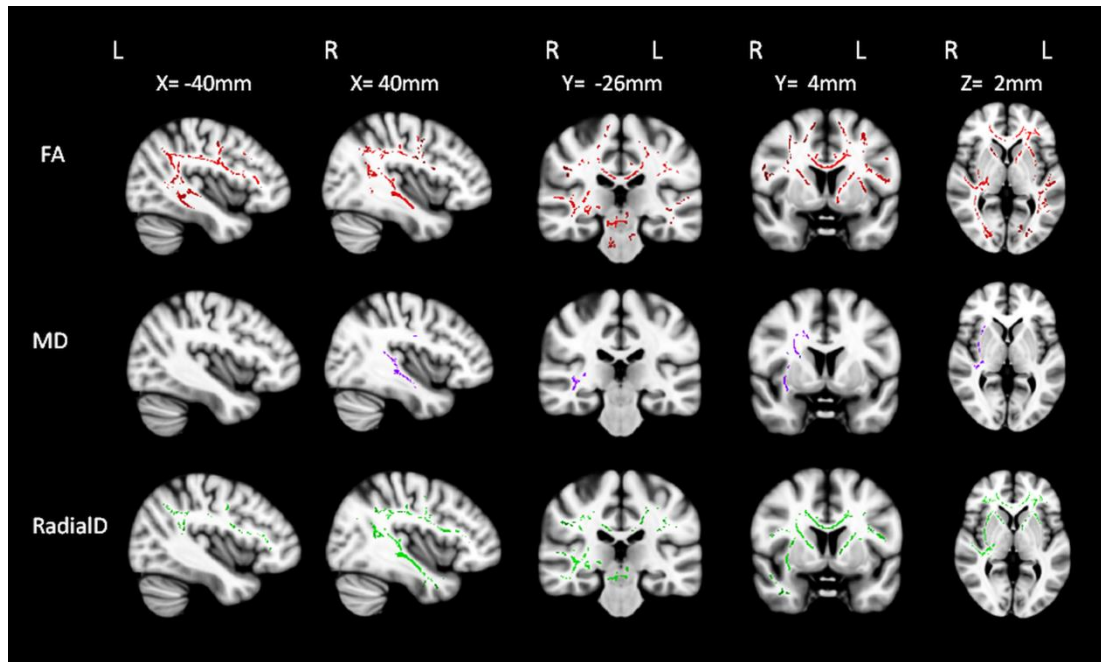
Figure 4.2 Longitudinal white matter changes in nfv-PPA.

Longitudinal assessments of white matter changes are shown for FA, MD and RadialD (p < 0.05, corrected for multiple comparisons). No significant change was found in AxialD. Results are overlaid on sections of the MNI standard brain. L = left; R = right.

Table 4.3 Longitudinal white matter changes in nfv-PPA as illustrated in the four DTI metrics.

Tracts/Group	FA (Mean ± SD)			MD (Mean ± SD)			AxialD (Mean ± SD)			RadialD (Mean ± SD)		
	Time 1	Time 2		Time 1	Time 2		Time 1	Time 2		Time 1	Time 2	
Ant thal rad L	0.44 ± 0.02	0.43 ± 0.03	*	0.77 ± 0.05	0.80 ± 0.06		1.16 ± 0.04	1.20 ± 0.06	*	0.58 ± 0.07	0.60 ± 0.07	
Ant thal rad R	0.43 ± 0.03	0.42 ± 0.03		0.81 ± 0.11	0.81 ± 0.06		1.20 ± 0.10	1.20 ± 0.06		0.62 ± 0.12	0.61 ± 0.06	
Anterior cingulum L	0.44 ± 0.04	0.43 ± 0.04	**	0.83 ± 0.04	0.84 ± 0.04		1.27 ± 0.04	1.27 ± 0.03		0.61 ± 0.05	0.63 ± 0.06	
Anterior cingulum_R	0.42 ± 0.05	0.41 ± 0.04	*	0.85 ± 0.04	0.86 ± 0.06		1.25 ± 0.08	1.26 ± 0.08		0.65 ± 0.06	0.66 ± 0.06	
Posterior cingulum L	0.41 ± 0.05	0.40 ± 0.06		0.81 ± 0.08	0.80 ± 0.07		1.16 ± 0.07	1.17 ± 0.08		0.63 ± 0.11	0.62 ± 0.07	
Posterior cingulum R	0.46 ± 0.05	0.44 ± 0.07		0.77 ± 0.19	0.73 ± 0.07		1.13 ± 0.17	1.09 ± 0.10		0.59 ± 0.21	0.55 ± 0.08	
Splenium of CC	0.60 ± 0.05	0.58 ± 0.06	**	0.84 ± 0.08	0.83 ± 0.06		1.48 ± 0.05	1.46 ± 0.04		0.52 ± 0.10	0.51 ± 0.08	
Genu of CC	0.50 ± 0.04	0.48 ± 0.05	*	0.83 ± 0.06	0.84 ± 0.06		1.34 ± 0.06	1.35 ± 0.06		0.58 ± 0.08	0.58 ± 0.07	
SLF (superior-inferior) L	0.40 ± 0.05	0.39 ± 0.05		0.82 ± 0.07	0.83 ± 0.09		1.18 ± 0.07	1.19 ± 0.08		0.65 ± 0.09	0.65 ± 0.10	
SLF (superior-inferior) R	0.43 ± 0.04	0.43 ± 0.04		0.77 ± 0.05	0.79 ± 0.05	*	1.16 ± 0.03	1.17 ± 0.04		0.58 ± 0.06	0.59 ± 0.05	*
SLF (temporal) L	0.42 ± 0.04	0.41 ± 0.04		0.81 ± 0.05	0.82 ± 0.06		1.19 ± 0.05	1.20 ± 0.05		0.62 ± 0.06	0.63 ± 0.07	
SLF (temporal) R	0.46 ± 0.03	0.45 ± 0.03	*	0.76 ± 0.04	0.77 ± 0.04	*	1.17 ± 0.04	1.19 ± 0.04		0.56 ± 0.05	0.57 ± 0.05	
IFOF L	0.42 ± 0.03	0.41 ± 0.03	*	0.86 ± 0.03	0.87 ± 0.04		1.27 ± 0.03	1.28 ± 0.03		0.65 ± 0.05	0.67 ± 0.06	
IFOF R	0.44 ± 0.04	0.43 ± 0.04		0.82 ± 0.05	0.84 ± 0.05	**	1.23 ± 0.05	1.26 ± 0.06	*	0.61 ± 0.06	0.63 ± 0.06	*
ILF L	0.43 ± 0.04	0.42 ± 0.04		0.85 ± 0.04	0.87 ± 0.05		1.27 ± 0.04	1.28 ± 0.04		0.65 ± 0.06	0.66 ± 0.06	
ILF R	0.46 ± 0.03	0.44 ± 0.04	*	0.79 ± 0.04	0.80 ± 0.05	*	1.20 ± 0.05	1.22 ± 0.05		0.59 ± 0.05	0.60 ± 0.05	
UF L	0.38 ± 0.03	0.36 ± 0.03	*	0.85 ± 0.05	0.86 ± 0.04		1.21 ± 0.03	1.22 ± 0.04		0.68 ± 0.07	0.68 ± 0.05	
UF R	0.40 ± 0.02	0.40 ± 0.03		0.82 ± 0.03	0.84 ± 0.04	*	1.21 ± 0.04	1.23 ± 0.06		0.63 ± 0.03	0.64 ± 0.04	*
CST L	0.55 ± 0.03	0.54 ± 0.03		0.78 ± 0.02	0.79 ± 0.03		1.31 ± 0.04	1.32 ± 0.04		0.51 ± 0.03	0.52 ± 0.04	
CST R	0.58 ± 0.03	0.57 ± 0.02	*	0.75 ± 0.02	0.76 ± 0.02	*	1.31 ± 0.03	1.32 ± 0.03		0.47 ± 0.03	0.48 ± 0.03	*

*Asterisks show significant changes at Time 2 relative to Time 1: * p < 0.05, ** p < 0.01; *** p < 0.001. Values for MD, AxialD and RadialD were shown at $10^3 mm^2 s^{-1}$. Abbreviations: FA = fractional anisotropy; MD = mean diffusivity; AxialD = axial diffusivity; RadialD = radial diffusivity; SD = standard deviation; CC = corpus callosum; SLF = superior longitudinal fasciculus; IFOF = inferior fronto-occipital fasciculus; ILF = inferior longitudinal fasciculus; UF = uncinate fasciculus; CST = corticospinal tract; L = left; R = right.*

4.5.2.3 Semantic variant primary progressive aphasia

Progressive longitudinal white matter changes in the sv-PPA group extended into frontal (inferior-fronto-occipital fasciculus) and commissural tracts (splenium of the corpus callosum) at 12 months, with less progression in left temporal regions (no progression in cingulum) (Figure 4.3).

Again, the magnitude of change varied among the DTI metrics used. Longitudinal alterations in FA were most extensive compared to the other metrics in sv-PPA, particularly in frontal white matter regions (genu and splenium of corpus callosum, left superior longitudinal fasciculus (superior-inferior), bilateral superior longitudinal fasciculus (temporal), bilateral inferior-fronto-occipital fasciculus, left inferior longitudinal fasciculus and bilateral uncinate fasciculus) (Table 4.4). The genu of the corpus callosum, superior longitudinal fasciculus and right inferior longitudinal fasciculus are relatively less affected in MD and RadialD.

Longitudinal changes in AxialD were found in the left temporal region only at the $p < 0.001$ uncorrected for multiple comparisons (Figure 4.3) while regions of interest analysis showed changes in AxialD in the splenium of corpus callosum, left inferior-fronto-occipital and uncinate fasciculi at $p < 0.05$ (Table 4.4).
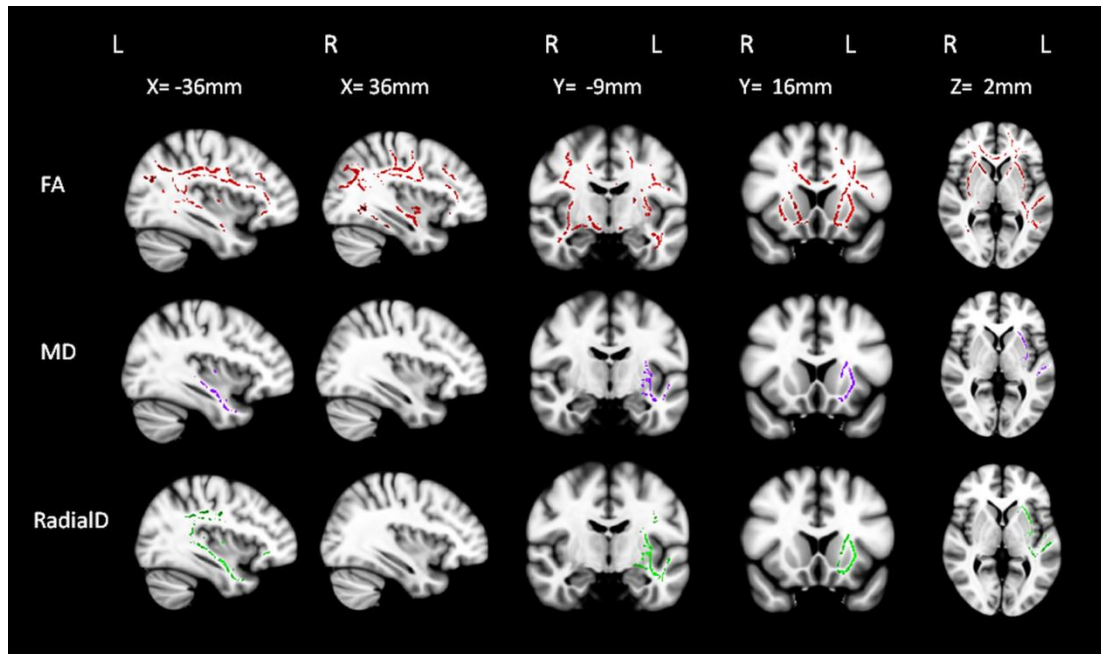
Figure 4.3 Longitudinal white matter changes in sv-PPA.

Longitudinal assessments of white matter changes are shown for FA, MD and RadialD (p < 0.05, corrected for multiple comparisons). No significant result was found in AxialD. Results are overlaid on sections of the MNI standard brain. L = left; R = right.

Table 4.4 Longitudinal white matter changes in sv-PPA as illustrated in the four DTI metrics.

Tracts/Group	FA (Mean ± SD)			MD (Mean ± SD)			AxialD (Mean ± SD)			RadialD (Mean ± SD)		
	Time 1	Time 2		Time 1	Time 2		Time 1	Time 2		Time 1	Time 2	
Ant thal rad L	0.43 ± 0.03	0.42 ± 0.03		0.75 ± 0.04	0.76 ± 0.04		1.14 ± 0.03	1.13 ± 0.04		0.56 ± 0.04	0.58 ± 0.04	
Ant thal rad R	0.42 ± 0.03	0.41 ± 0.03		0.76 ± 0.04	0.76 ± 0.05		1.12 ± 0.04	1.11 ± 0.05		0.57 ± 0.04	0.58 ± 0.05	
Anterior cingulum L	0.45 ± 0.03	0.44 ± 0.04		0.82 ± 0.04	0.82 ± 0.05		1.26 ± 0.05	1.26 ± 0.05		0.60 ± 0.04	0.61 ± 0.06	
Anterior cingulum R	0.43 ± 0.02	0.43 ± 0.03		0.83 ± 0.03	0.83 ± 0.04		1.25 ± 0.04	1.25 ± 0.06		0.62 ± 0.03	0.62 ± 0.04	
Posterior cingulum L	0.36 ± 0.06	0.35 ± 0.06		0.90 ± 0.11	0.93 ± 0.13		1.25 ± 0.10	1.27 ± 0.12		0.72 ± 0.12	0.77 ± 0.15	
Posterior cingulum R	0.43 ± 0.04	0.42 ± 0.06		0.78 ± 0.07	0.81 ± 0.05		1.15 ± 0.09	1.17 ± 0.05		0.59 ± 0.06	0.62 ± 0.07	
Splenium of CC	0.62 ± 0.03	0.60 ± 0.04	*	0.82 ± 0.02	0.83 ± 0.03		1.51 ± 0.04	1.50 ± 0.03	*	0.48 ± 0.04	0.50 ± 0.05	*
Genu of CC	0.52 ± 0.03	0.50 ± 0.04	*	0.79 ± 0.05	0.80 ± 0.06		1.32 ± 0.05	1.32 ± 0.06		0.53 ± 0.05	0.55 ± 0.07	
SLF (superior-inferior) L	0.44 ± 0.03	0.42 ± 0.03	*	0.78 ± 0.04	0.79 ± 0.07		1.18 ± 0.04	1.18 ± 0.08		0.58 ± 0.04	0.60 ± 0.07	
SLF (superior-inferior) R	0.47 ± 0.04	0.46 ± 0.04		0.75 ± 0.03	0.74 ± 0.04		1.17 ± 0.03	1.14 ± 0.04		0.53 ± 0.04	0.54 ± 0.05	
SLF (temporal) L	0.44 ± 0.02	0.43 ± 0.03	*	0.80 ± 0.03	0.81 ± 0.05		1.20 ± 0.04	1.21 ± 0.07		0.59 ± 0.03	0.61 ± 0.05	*
SLF (temporal) R	0.48 ± 0.03	0.47 ± 0.03	*	0.74 ± 0.03	0.74 ± 0.04		1.17 ± 0.03	1.16 ± 0.04		0.53 ± 0.03	0.53 ± 0.04	
IFOF L	0.44 ± 0.02	0.42 ± 0.03	*	0.87 ± 0.04	0.90 ± 0.06	*	1.31 ± 0.04	1.34 ± 0.05		0.65 ± 0.04	0.68 ± 0.06	*
IFOF R	0.46 ± 0.03	0.45 ± 0.03	**	0.81 ± 0.03	0.82 ± 0.04		1.25 ± 0.03	1.25 ± 0.04		0.59 ± 0.04	0.61 ± 0.05	*
ILF L	0.43 ± 0.02	0.42 ± 0.03		0.94 ± 0.06	0.98 ± 0.08	*	1.40 ± 0.07	1.45 ± 0.09	*	0.71 ± 0.05	0.75 ± 0.08	*
ILF R	0.48 ± 0.02	0.46 ± 0.03	*	0.81 ± 0.03	0.82 ± 0.04		1.28 ± 0.04	1.26 ± 0.05		0.58 ± 0.03	0.60 ± 0.04	
UF L	0.37 ± 0.03	0.35 ± 0.03	**	0.91 ± 0.07	0.95 ± 0.07	**	1.28 ± 0.07	1.31 ± 0.06	*	0.73 ± 0.08	0.78 ± 0.08	***
UF R	0.40 ± 0.03	0.38 ± 0.03	**	0.84 ± 0.06	0.88 ± 0.08	*	1.24 ± 0.05	1.26 ± 0.07		0.65 ± 0.06	0.69 ± 0.08	*
CST L	0.54 ± 0.02	0.53 ± 0.03		0.77 ± 0.02	0.77 ± 0.02	*	1.30 ± 0.03	1.30 ± 0.03		0.51 ± 0.02	0.53 ± 0.03	*
CST R	0.58 ± 0.02	0.57 ± 0.02		0.74 ± 0.01	0.74 ± 0.01		1.29 ± 0.02	1.28 ± 0.02		0.47 ± 0.02	0.47 ± 0.02	

*Asterisks show significant changes at Time 2 relative to Time 1: * $p < 0.05$, ** $p < 0.01$; *** $p < 0.001$. Values for MD, AxialD and RadialD were shown at $10^3 mm^2 s^{-1}$. Abbreviations: FA = fractional anisotropy; MD = mean diffusivity; AxialD = axial diffusivity; RadialD = radial diffusivity; SD = standard deviation; CC = corpus callosum; SLF = superior longitudinal fasciculus; IFOF = inferior fronto-occipital fasciculus; ILF = inferior longitudinal fasciculus; UF = uncinate fasciculus; CST = corticospinal tract; L = left; R = right.*

4.5.2.4 Overlaying white and grey matter changes in FTD subtypes after 12 months

In general, the progression of white matter abnormalities appeared more pronounced and widespread than the progression of grey matter atrophy in all FTD subtypes at the 12-month follow up (Figure 4.4).

In bvFTD, progressive white matter abnormalities were observed bilaterally while the progression of grey matter atrophy was localised only to the right frontotemporal region (Figure 4.4 & Table 4.5).

In nfv-PPA, only additional white matter changes were detected in the temporo-parieto-occipital regions bilaterally at 12 months. In contrast, no significant grey matter changes were found over the same time period. When using a more liberal significance threshold ($p < 0.001$ uncorrected for multiple comparisons), bilateral grey matter atrophy was observed in the left superior frontal and lateral occipital cortices (Figure 4.4 & Table 4.5).

In sv-PPA, while bilateral white matter changes were observed in frontotemporal regions, only circumscribed additional left hippocampal grey matter atrophy occurred over the same 12-month period (Figure 4.4 & Table 4.5).
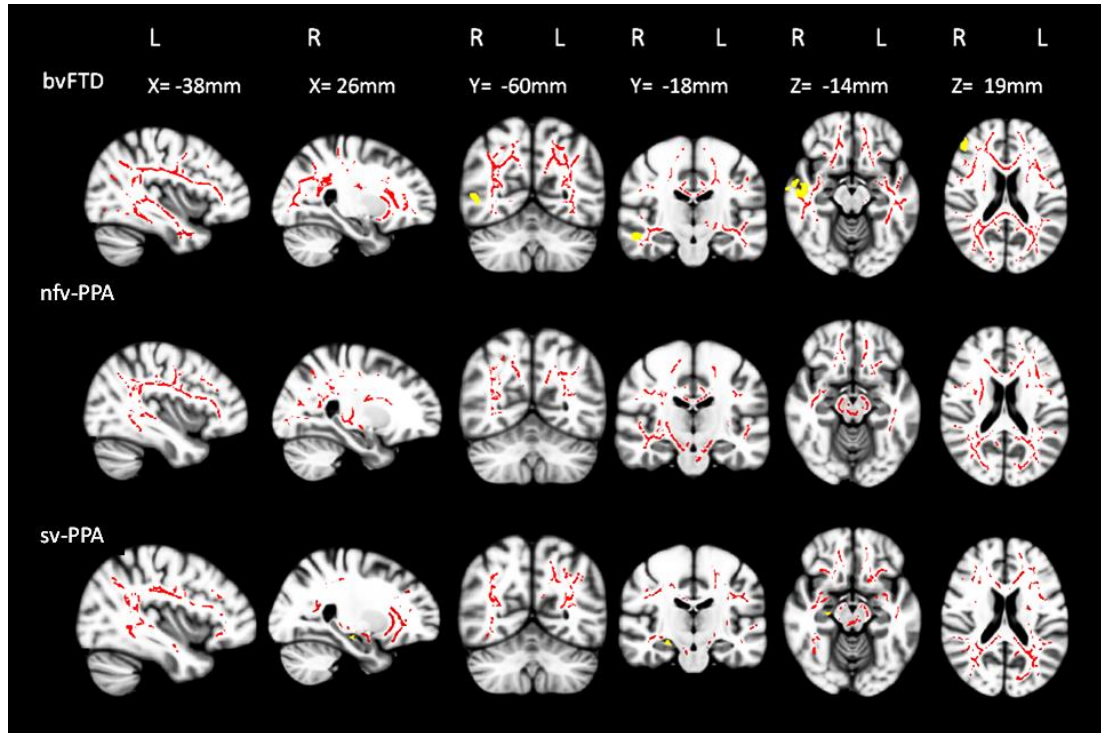
Figure 4.4 Longitudinal changes in white matter and grey matter in FTD subtypes.

Changes in FA (red) and grey matter density (yellow) over a 12-month period are illustrated for bvFTD, nfv-PPA and sv-PPA. All analyses were corrected for multiple comparisons at p < .05. No significant grey matter cluster was observed in nfv-PPA. Results are overlaid sections of the MNI standard brain. L = left; R = right.

Table 4.5 Longitudinal grey matter changes at each significant cluster in bvFTD and sv-PPA.

	Side (L/R)	Voxels	MNI coordinates (X-Y-Z)			t-stat
bvFTD						
Frontal pole	R	554	48	38	18	2.2
Precentral gyrus	R	188	50	10	30	1.87
Planum temporale	R	321	56	6	0	1.98
Anterior superior temporal gyrus	R	1741	58	-8	-6	2.1
Middle temporal gyrus	R	236	52	-58	3	1.83
Planum temporale	R	114	48	-26	10	1.9
sv-PPA						
Hippocampus	R	31	26	-18	-14	2

All clusters reported using threshold free cluster enhancement and corrected for multiple comparisons at p < 0.05. No significant cluster was observed at p < 0.05 in nonfluent variant primary progressive aphasia. Abbreviations: bvFTD = behavioural-variant frontotemporal dementia; sv-PPA = primary progressive aphasia semantic variant; L = left; R = right; MNI = Montreal Neurological Institute.

4.5.3   Discussion

This is the first study to report longitudinal white matter changes in FTD subtypes. The results demonstrated specific profiles of white matter changes in each FTD subtype over a 12-month period. Furthermore, white matter abnormalities were more extensive than grey matter changes over the course of 12 months, showing significant progression of white matter pathology in both initially affected regions and extended to include additional regions. Importantly, the location and severity of these changes varied depending on the DTI metrics used, indicating that white matter changes observed with different DTI measures may represent different pathological processes.

This study revealed that most white matter changes identified at follow up co-localised with the distribution of white matter abnormalities at baseline in all FTD subtypes. Importantly, the tissue abnormalities progressed to involve similar regions in the other hemisphere, giving rise to a bilateral, rather than focal, pattern of white matter change with disease progression. This progression is most pronounced in bvFTD where the orbitofrontal and anterior temporal regions, which were most affected at baseline, continue to progress bilaterally at follow-up, with additional posterior involvement, such as that of the splenium of the corpus callosum. Notably, this profile of white matter change was observed regardless of the metric used, and indicates a particularly rapidly progressive pathological change. The widespread and progressive white matter changes over time in bvFTD suggested that the rate of progression is rapid in this subtype and are consistent with the shorter life expectancy (Garcin et al 2009, Onyike 2011) and faster cognitive decline (i.e., ACE-R or frontotemporal dementia rating

scale) generally reported in these patients when compared to the other FTD subtypes (Kipps et al 2008, Piguet et al 2011). In contrast, the longitudinal white matter changes found in nfv-PPA were not as dramatic as those observed in bvFTD. Changes in this group appeared to remain relatively focal, even with progression, with the pattern of change over time involving tracts connected to the primary site of brain atrophy. Of note, while none of the patients displayed clinical features of progressive supranuclear palsy syndrome at baseline or at the 12-month review, significant white matter change was observed in the brainstem over the 1-year period in this group. In addition, the only nfv-PPA case coming to autopsy showed FTLD-tau pathology of the progressive supranuclear palsy subtype, consistent with previous studies highlighting the close relationship between these disorders (Josephs et al 2005, Rohrer et al 2010). These findings suggest that the brainstem may be particularly vulnerable with disease progression in nfv-PPA, even in the absence of clinical indicators, such as extrapyramidal or oculomotor disturbance. Finally, in sv-PPA, longitudinal white matter changes became widespread affecting white matter tracts bilaterally. Temporal regions continued to be affected, with additional frontal lobe involvement as disease progresses.

Given the age-related changes affecting the white matter previously reported (Bartzokis et al 2003, O'Sullivan et al 2001, Salat et al 2005), longitudinal analyses were also carried out in the control group in order to determine the ageing effect over 12 months. No significant changes in MD, AxialD and RadialD were observed between baseline and follow up scans. Small changes in FA were observed predominantly located in the frontal lobe white matter bilaterally

(superior and inferior longitudinal fasciculi, inferior-fronto-occipital fasciculi and uncinate fasciculi). The magnitude of these changes, however, was about 2 to 3-fold less compared to the changes found in FTD groups over the same time period. These analyses confirmed that the white matter changes found in the FTD groups reflected disease, rather than chronological ageing effects.

4.5.3.1   White and grey matter relations

This study also uncovered the spatial relations between white and grey matter changes varied over time in all FTD subtypes. At baseline, changes in white matter integrity, as measured by TBSS, mapped relatively closely to the reduction in grey matter measured by VBM. At 12 months, however, the rate and location of change in the white and grey matter became uncoupled. Atrophy of the grey matter progressed only minimally over that time period with the damage remaining relatively focal. In contrast, white matter changes became widespread with bilateral alterations in frontotemporal regions and the damage encroaching into the posterior white matter in all FTD subtypes.

In cross-sectional studies, co-localisation of white and grey matter abnormalities in FTD have been reported (Acosta-Cabronero et al 2011, Hornberger et al 2010, Whitwell et al 2010). In contrast, some studies suggested that white matter abnormalities act as an early marker of FTD as opposed to the volumetric grey matter loss occurring later in the disease (Agosta et al 2011, Mahoney et al 2013, Schwindt et al 2013, Zhang et al 2013). This study confirms the extensive pathological changes in white matter in FTD, changes that tend to extend beyond those observed grey matter atrophy, particularly with disease progression. The findings reveal different temporal and spatial patterns of white

and grey matter pathology over time in FTD. Direct comparisons of the longitudinal changes affecting the white and grey matter need to be approached with caution, given the different imaging modalities used to investigate these two types of tissue. Nevertheless, the magnitude of white matter change observed over 12 months using DTI indicates that this methodology is sensitive and appropriate to measure disease progression in FTD subtypes, regardless of the grey matter changes.

4.5.3.2 Sensitivity in DTI metrics and disease progression

Previous investigations of white matter changes in FTD have generally used FA as a single marker of white matter change. The combination of different DTI metrics (RadialD, AxialD, MD), which measure different aspects of diffusion behaviour in the white matter, appears more sensitive in detecting white matter changes in neurodegenerative conditions rather than the use of a single global diffusion measure such as FA (Acosta-Cabronero et al 2010). At baseline, MD and RadialD alterations were most severe in bvFTD and nfv-PPA, while MD and AxialD abnormalities were most prominent in sv-PPA. At follow-up, however, FA and RadialD revealed the most prominent changes in the white matter tracts in all three subtypes of FTD. These findings concord with those reported in Alzheimer's disease, where MD and AxialD were the first metrics to detect white matter alterations, while alterations in FA and RadialD became more pronounced with disease progression (Acosta-Cabronero et al 2012). Together, these data support the view that DTI metrics identify different underlying processes specific to the stage of the disease. These findings also likely explain

the variable co-localisation between white and grey matter changes reported above, given the single DTI measurement obtained in previous studies.

4.5.4 Summary

- Differential white matter changes in FTD subtypes: This study defined the patterns of longitudinal white matter change in FTD subtypes (bvFTD, nfv-PPA and sv-PPA) and revealed patterns of white matter change are specific to each group.

- White matter measurement more sensitive than grey matter: Longitudinal white matter changes extend beyond those observed in the grey matter during the same time period, indicating that imaging of the brain white matter is particularly sensitive to identifying the progression of pathology in FTD.

- Progression of white matter abnormalities differs depending on the DTI metrics used: This suggests alterations in diffusion metrics are sensitive to different pathological processes occurring at different disease stages. This is potentially useful as stage-specific markers to indicate disease progression.

Chapter 5: White matter changes in FTD with *C9orf72* gene expansions

5 WHITE MATTER CHANGES IN FTD WITH C9ORF72 GENE EXPANSIONS

5.1 Introduction

The recent discovery of the genetic abnormality in the chromosome 9 open reading frame 72 *(C9orf72)* has changed the understanding of the pathophysiology of FTD. The abnormality in the *C9orf72* gene involves the expansion of GGGGCC hexanucleotide repeats in the non-coding region of chromosome 9 between alternate 5 prime exons. Multiple transcript variants encoding different isoforms have been identified for this gene. The C9orf72 protein is predominately localised in the nucleus of human control fibroblast cell lines. The C9orf72 RNA is also present in multiple regions in the central nervous system in a neuropathologically normal individual (Renton et al 2011). Expansions in the *C9orf72* gene have received attention because they are the most common genetic abnormality linked to both FTD and motor neuron disease (MND) (also commonly referred to as amyotropic lateral sclerosis) (DeJesus-Hernandez et al 2011, Renton et al 2011) and account for about 30% of cases with familial FTD and about 40% of cases of familial MND (Boeve et al 2012, Hsiung et al 2012, Majounie et al 2012, Renton et al 2011, Simón-Sánchez et al 2012). All patients with expansions in the *C9orf72* gene have FTLD-TDP pathology (Bigio et al 2013, Hsiung et al 2012, Mahoney et al 2012b). Existing studies have examined the clinical (neuropsychiatric features, cognitive and motor deficits) and imaging characteristics in C9orf72 expansion carriers compared to non-carriers. The *C9orf72* expansion carriers have been compared

to healthy controls, sporadic cases or other gene mutations (i.e., *MAPT* &

progranulin) (Boeve et al 2012, Hsiung et al 2012, Kaivorinne et al 2013,

Mahoney et al 2012b, Simón-Sánchez et al 2012, Snowden et al 2012).

Variability in findings, however, differs among reports which may be due to the

clinical type of FTD sampled with *C9orf72* expansions which included a mixture

of bvFTD, MND, FTD-MND, MND-FTD, nfv-PPA or even sometimes sv-PPA

cases. The clinical and imaging characteristics of the *C9orf72* gene expansions

observed in mixed clinical samples are summarised in Appendix 5.7.8.

In order to understand the clinical and imaging characteristics of the *C9orf72*

gene expansions more accurately, expansion carriers and non-carriers from the

single largest clinical phenotype will be selected for this chapter.

The *C9orf72* gene expansions is most commonly found in bvFTD and less so in

the other subtypes within the FTD spectrum (Boeve et al 2012, Devenney et al

2014, Hsiung et al 2012, Kaivorinne et al 2013, Mahoney et al 2012b, Simón-

Sánchez et al 2012, Snowden et al 2012), therefore, bvFTD will be the focus of

study.

Patterns of white matter change were previously shown to be distinctive across

each subtype of FTD in Chapter 3 of this thesis. In bvFTD, significant white

matter alterations were observed in the frontotemporal tracts. It is of interest to

know how the *C9orf72* gene expansions contributes to the brain white matter

change and the FTLD-TDP pathology found in these cases, and how these white

matter abnormalities may predict any clinical changes between *C9orf72*

expansion carriers (with FTLD-TDP) and non-carriers (where more FTLD-tau

will occur) in bvFTD.

The following sections summarise the current findings on clinical and imaging differences between *C9orf72* expansions carriers and non-carriers in bvFTD.

5.2 Clinical features of bvFTD with *C9orf72* gene expansions

Among all clinical studies measuring the *C9orf72* gene expansions, only very few have contrasted the clinical features between *C9orf72* carriers and non-carriers within bvFTD (Devenney et al 2014, Sha et al 2012). These studies have shown that *C9orf72* expansion carriers and non-carriers within bvFTD exhibit similar but variable neuropsychiatric, cognitive and motor features (Devenney et al 2014, Sha et al 2012).

5.2.1 Neuropsychiatric features

Despite overall similar clinical characteristics in bvFTD with or without the *C9orf72* gene expansions, variability between groups was found. Two studies reported a high frequency of delusions in the *C9orf72* expansion carriers compared to non-carriers (Devenney et al 2014, Sha et al 2012). Hallucinations in *C9orf72* expansion carriers were also reported with higher frequency in one study (Devenney et al 2014) but not in another (Sha et al 2012). Whilst apathy was found to be significantly less frequent in the *C9orf72* expansion carriers (Devenney et al 2014), this was not a distinguishing feature between the two groups in another study (Sha et al 2012). A trend towards greater disinhibition and anxiety in *C9orf72* expansion carriers compared to non-carriers was also reported, although this group difference was not statistically significant (Sha et al 2012). When comparing eating behaviours, *C9orf72* expansion carriers

showed relatively mild abnormal eating habit than bvFTD patients without the gene expansion (Sha et al 2012).

These studies suggest that bvFTD *C9orf72* expansion carriers may have more delusions and less abnormal eating behaviour than non-carriers but variable in other neuropsychiatric features.

5.2.2   Cognitive features

With regard to cognitive function, bvFTD *C9orf72* expansion carriers have been reported to show greater impairment in working memory compared to non-carriers (Sha et al 2012), although this cognitive domain was not investigated in the other study (Devenney et al 2014). Other aspects of cognition, such as episodic memory and executive function were found not to differ between groups (Devenney et al 2014).

These studies suggest that bvFTD *C9orf72* expansion carriers may have greater difficulties with working memory than non-carriers, and margin difference in other cognitive features.

5.2.3   Motor features

No difference in movement abnormality, such as parkinsonism, apraxia and eye-movement abnormalities, have been reported between *C9orf72* expansion carriers and non-carriers (Devenney et al 2014, Sha et al 2012, Whitwell et al 2012). Nonetheless, it appears that bvFTD *C9orf72* expansion carriers may have a higher likelihood to develop parkinsonism throughout the disease than non-carriers (Devenney et al 2014).

5.3   Neuroimaging features of bvFTD with *C9orf72* gene expansions

Only four studies to date have investigated brain imaging features of *C9orf72*

carriers compared to non-carriers in bvFTD. Three have focused on brain

changes affecting the grey matter (Devenney et al 2014, Sha et al 2012, Whitwell

et al 2012) while only one has investigated white matter changes (Mahoney et al

2014).

5.3.1   Patterns of grey matter atrophy in bvFTD *C9orf72* expansion carriers and non-carriers

Comparison between these two groups with bvFTD showed that *C9orf72*

carriers had greater loss of posterior cortices, the thalamus and the cerebellum

than non-carriers (Sha et al 2012, Whitwell et al 2012), while another study

reported that *C9orf72* carriers lacked the typical imaging features associated

with bvFTD (Devenney et al 2014). On the other hand, non-carriers were

reported to exhibit greater atrophy of the medial frontal lobe than bvFTD

C9orf72 carriers (Sha et al 2012).

5.3.2   Patterns of white matter change in bvFTD *C9orf72* expansion carriers and non-carriers

The patterns of change in the white matter associated with the presence of the

C9orf72 gene expansions remains poorly defined. The only study to date to

contrast white matter integrity between bvFTD *C9orf72* expansion carriers with

non-carriers included only four *C9orf72* carriers (Mahoney et al 2014). This

study revealed that, compared to healthy controls, the *C9orf72* expansion

carriers had increased axial diffusivity in the corpus callosum and cingulum

bundle, while the direct comparison between bvFTD *C9orf72* carriers and sporadic bvFTD cases found no significant difference between groups (Mahoney et al 2014).

Overall, it is unclear if significant differences exist in the pattern of degeneration observed on neuroimaging between bvFTD with or without the *C9orf72* gene expansions, with some studies showing limited changes while others show no changes. The differences between studies could be due to analyses of mixed case types, although the lack of differences noted could be due to insufficient power in some analyses (too few case analysed) or comparisons between clinically (and potentially pathologically) similar bvFTD groups.

Since the discovery of the *C9orf72* gene expansions in 2011 (DeJesus-Hernandez et al 2011, Renton et al 2011), very few studies have examined the clinical and imaging characteristics of the *C9orf72* gene expansions in a clearly defined clinical phenotype. Furthermore, most reports to date have mostly focused on grey matter atrophy in bvFTD *C9orf72* carriers (Devenney et al 2014, Mahoney et al 2012b, Sha et al 2012, Whitwell et al 2012) with only one recent study investigating white matter tract damage in a relatively small sample (Mahoney et al 2014). More work is therefore required to determine the *in vivo* pattern of white matter change in larger cohorts of bvFTD with *C9orf72* genetic expansions as these cases are known to have homogenous underlying pathological changes. Comparisons between this homogeneous pathological group of bvFTD patients with a similar sized group of bvFTD with differences in

their clinical features (and potentially their underlying pathology) may identify imaging signatures for differentiating diverse pathologies in bvFTD.

This chapter aims to identify the differences in the presenting clinical features between those with the *C9orf72* gene expansions (and FTLD-TDP) and those without the expansion (and a greater likelihood of FTLD-tau), and determine any associated white matter changes in a homogeneous clinical sample of bvFTD (the most common subtype of FTD).

5.4 Aims

This study aims to:

1) define the patterns of white matter change in bvFTD *C9orf72* expansion carriers compared to bvFTD non-carriers; and

2) investigate the association between white matter tract changes and clinical features associated with the *C9orf72* genetic abnormality in a prospective, single-centre, single-protocol approach.

5.5 Methods

5.5.1 Participant and experimental procedures

Screening for *C9orf72* gene expansions was performed on all bvFTD patients (Chapter 2.1.2) who were subsequently divided into expansion carriers (C9pos) and those without any gene expansions (C9neg). Only patients with completed MRI and DTI images were included in this study. Nineteen bvFTD patients were included in this study (C9pos = 8; C9neg = 11). Two C9pos patients presented as bvFTD initially but developed MND features later in the disease course. Details of patient recruitment procedure, genetic expansion screening, image

acquisition, imaging processing for tract-based spatial statistics and voxelwise analysis have been described previously in Chapter 2.

5.5.2   Neuropsychological, language and behavioural assessments

Overall cognitive function was determined by ACE-R (Mioshi et al 2006). Additionally, all patients were assessed with the following 13 tests. The Trail Making Test (Part A, B and B-A) was used to assess executive function (Reitan & Wolfson 1985); the Digit Span (backward) acted as an index of verbal working memory (Wechsler 1997); the Doors (Part A) of the Doors and People Test was administered to measure visual recognition (Baddeley et al 1994); the Rey-Osterrieth Complex Figure (immediate recall) was used to assess episodic memory (Meyers & Meyers 1995). The Sydney Language Battery (naming, repetition, comprehension and semantic subtests) was used to test single-word processing (Savage et al 2013) while the Cambridge Behavioural Inventory (measures of eating habits, abnormal behaviour and stereotypical behaviour) was used to measure behavioural changes associated to dementia (Wear et al 2008).

In order to maximise use of data, missing values were imputed by linear multiple regression using existing clinical means for C9pos and C9neg patients. Three clinical scores, Trail Making Test (Part B-A), Sydney Language Battery (semantic association subtest) and Rey-Osterrieth Complex Copy figure (immediate recall), contained missing values in 3/19, 2/19 and 1/19 respectively. All 13 tests were further reduced down to 7 using Spearman's rank correlation to reduce variables that were highly correlated. Mann-Whitney U was performed

on the 7 tests to determine significant differences in clinical scores between

C9pos and C9neg patients ($p < 0.05$).

5.5.3 White matter analyses

DTI data were processed with Tract-based spatial statistics (TBSS v 1.1) (Smith

et al 2006), part FSL v 4.1.9 (Smith et al 2004) and whole-brain maps of white

matter change were generated. Details of the procedure are described in

Chapter 2.

Based on the whole-brain analysis, tracts of interests were selected and masks of

these tracts were created with reference to the Johns Hopkins University white

matter atlases for statistical analysis (Mori et al 2008, Oishi et al 2008). Mann-

Whitney U test was performed to test for significant tract differences between

C9pos and C9neg cases with a significant statistical threshold set at $p < 0.05$.

Among the DTI metrics, the FA, AxialD and RadialD were specifically

investigated because FA represents overall indication of white matter integrity

while AxialD and RadialD are suggestive of specific pathological changes such as

axonal and myelin loss (Pierpaoli et al 2001, Song et al 2003). As MD, the

average of AxialD and RadialD, reveals less specific pathological information

about white matter integrity, this particular measurement is not included in the

analysis to reduce the number of variables and the risk of type I errors.

 Given the small number of cases (n = 19), white matter tracts were further

reduced by a stepwise regression analysis to only include those relevant to the

clinical performance.

5.5.4 Grey matter analyses

As *C9orf72* expansion carriers showed smaller volumes in the thalamus and cerebellum than non-carriers (Sha et al 2012, Whitwell et al 2012), volumetric changes of these regions are of particular interest in this study. Therefore, FreeSurfer, the imaging software that provides accurate parcellation of subcortical structures and the cerebellum and derives quantitative regional estimates of the volumes of interest is used for the grey matter analysis. Volumetric measurements were obtained using FreeSurfer (version 4.2) (Fischl & Dale 2000) for the following structures: the thalamus, caudate nucleus, putamen, pallidum, and the cerebellum. Procedures to obtain these measurements have been described in Chapter 2. All brain volumes of interest were corrected for intracranial volume and are represented as % of total intracranial volume. Significant differences between C9pos and C9neg cases were determined by Mann-Whitney U test at $p < 0.005$ after Bonferroni correction.

5.5.5 Statistical analyses

Data were analysed with SPSS 22.0 (IBM Corp.). Data were first tested for normality using the Shapiro-Wilk tests. Parametric variables were compared between groups using the independent t-test while non-parametric variables were analysed with Mann-Whitney U tests. Multiple comparisons were adjusted with the Bonferroni correction. Categorical data were tested with a chi-square test. Hierarchical regression analysis was further carried out to identify the clinical variables that were significant predictors of white matter tract changes.

5.6 Results

5.6.1 Clinical demographics

Groups were well matched for sex (p = 0.54), age (p = 0.47), ACE-R (p = 0.12), disease duration (p = 0.24) and intracranial volume (p = 0.56) (Table 5.1). Years of education, however, has a trend to reach statistical significance (p = 0.053).

Table 5.1 Demographic information of *C9orf72* expansion carriers and non-carriers.

	C9neg	C9pos	*p*
Sex: M/F	7/4	6/2	0.54
Mean age; yrs	60.8± 7.3 (10)	58.9±4.3 (19)	0.47
Education; yrs	13.1 ± 3.2 (6)	10.5 ± 2.1 (10)	0.053
ACE-R; max:100	71.0 ± 11.8 (23)	78.5 ± 8.2 (42)	0.12
Disease duration; yrs	3.2 ± 1.7 (9)	4.8 ± 3.4 (8)	0.24
Intracranial volume ; x10^{4}mm^3	143±16 (59)	148±22 (62)	0.56

Numerical values are illustrated in mean ± standard deviation (range of scores). Abbreviations: M = male; F = female. ACE-R = Addenbrooke's Cognitive Examination-Revised; max = maximum; yrs = years.

5.6.2 Clinical features

Of the seven clinical features, two significantly differed between the *C9orf72* carriers and non-carriers. *C9orf72* carriers has fewer stereotypical behaviours ($U = 16.5$, Z = -2.3, p = 0.020) and had better semantic knowledge ($U = 16.5$, Z = -2.3, p = 0.020) than those without the gene abnormality (Table 5.2).

Table 5.2 Clinical features of *C9orf72* expansion carriers and non-carriers.

	C9neg	C9pos	*p*
Trail Making Test (B-A) (seconds)	135.7 ± 93.8	121.6 ± 71.4	NS
Digit span (backwards)	3.4 ± 0.8	3.6 ± 0.9	NS
Rey immediate recall (max: 36)	7.1 ± 5.4	8.5 ± 4.1	NS
Naming (max: 30)	20.3 ± 4.1	21.9 ± 3.3	NS
Semantic (max: 30)	21.1 ± 4.9	25.1 ± 1.7	*0.020*
Abnormal behaviour (max: 24)	5.7 ± 4.8	8.6 ± 4.4	NS
Stereotypical behaviour (max: 16)	8.6 ± 3.2	4.5 ± 3.7	*0.020*

Numerical values are illustrated in mean ± standard deviation. Abbreviation: NS = not significant; Rey = Rey-Osterrieth Complex Figure; max = maximum.

5.6.3 Comparing white matter changes between *C9orf72* expansion carriers and non-carriers

In all instances, when group differences were observed, white matter tracts were more affected in C9neg than in C9pos cases. No significant results were found denoting greater changes in C9pos compared with C9neg cases. In contrast, C9neg cases showed greater alterations in the left anterior thalamic radiation, bilateral anterior cingulum, inferior-fronto-occipital fasciculi, inferior longitudinal fasciculi and uncinate fasciculi than C9pos cases. White matter integrity only varied slightly depending on the DTI metrics used. Measurements of FA and RadialD were mostly concordant to each other. However, change in the left superior longitudinal fasciculus (temporal) was observed in RadialD but not FA. Of the three DTI metrics, AxialD was the one that was found to be least sensitive to white matter changes. AxialD revealed a loss of white matter

integrity in frontotemporal tracts that were concurrent to those affected in FA and RadialD. Changes in AxialD, however, were confined to the left hemisphere and fronto-parietal regions of the brain (Figure 5.1 & Table 5.3).
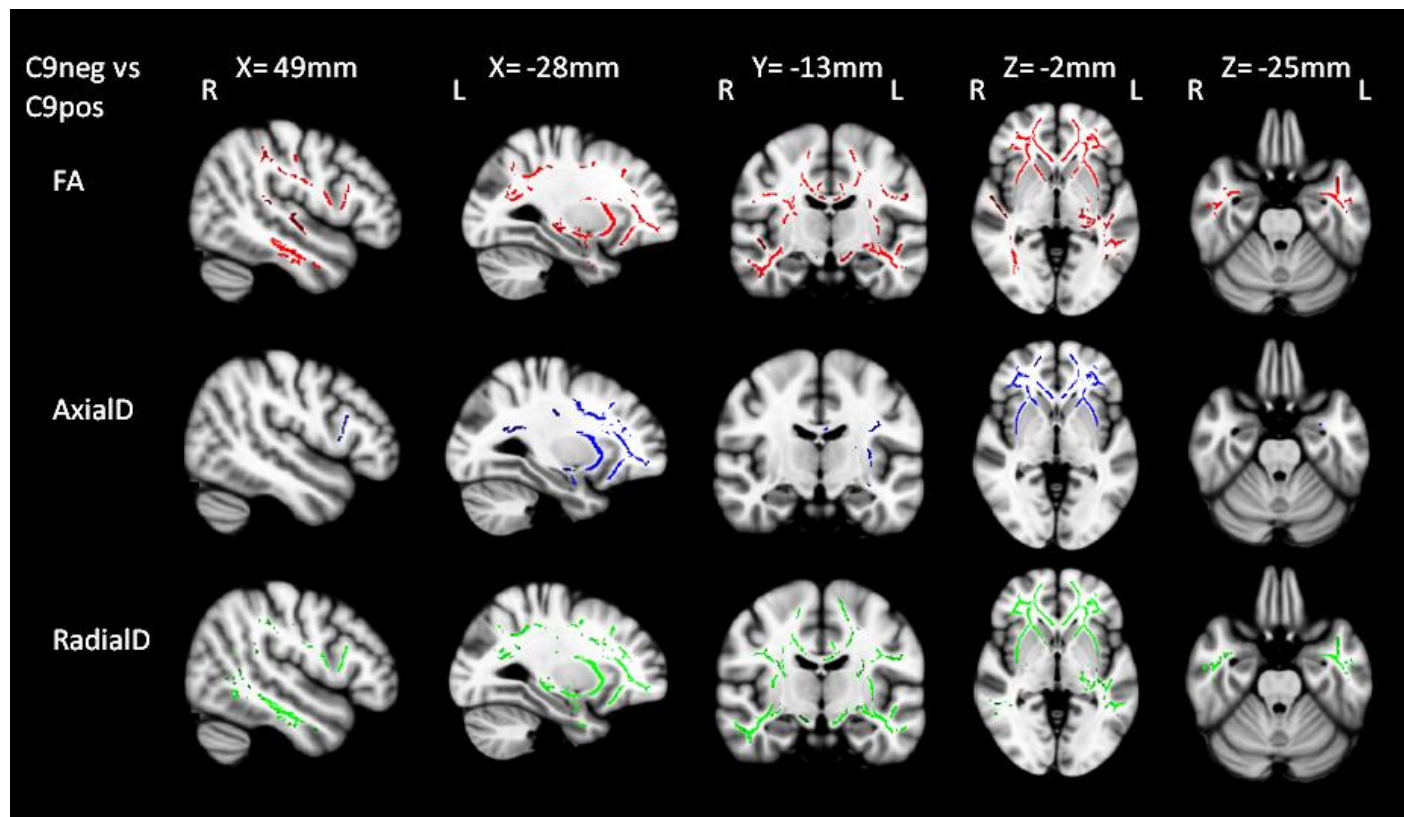
Figure 5.1 White matter changes in C9orf72 expansion carriers compared to non-carriers.

Voxelwise analyses are shown for FA (red), AxialD (blue) and RadialD (green). Coloured voxels are shown at p < 0.05, corrected for multiple comparisons.

No significant clusters were found when overlaying C9pos over C9neg cases. Results are overlaid on sections of the MNI standard brain. L = left; R = right.

Table 5.3 FA, AxialD and RadialD changes in white matter tracts of *C9orf72* expansion carriers compared to non-carriers (Mean ± SD).

Tracts/Group	FA			AxialD (x10³mm²s⁻¹)			RadialD (x10³mm²s⁻¹)		
	C9neg	C9pos		C9neg	C9pos		C9neg	C9pos	
Ant thal rad L	0.40 ± 0.04	0.43 ± 0.02	*	1.26 ± 0.10	1.19 ± 0.06	*	0.69 ± 0.11	0.59 ± 0.03	*
Ant thal rad R	0.40 ± 0.04	0.42 ± 0.03		1.27 ± 0.07	1.21 ± 0.10		0.69 ± 0.08	0.62 ± 0.08	
Ant cing L	0.39 ± 0.04	0.46 ± 0.03	***	1.32 ± 0.08	1.24 ± 0.04	*	0.72 ± 0.08	0.58 ± 0.04	***
Ant cing R	0.38 ± 0.03	0.44 ± 0.05	**	1.30 ± 0.10	1.24 ± 0.05		0.72 ± 0.08	0.61 ± 0.06	**
SLF (superior-inferior) L	0.41 ± 0.04	0.45 ± 0.04	*	1.20 ± 0.08	1.14 ± 0.03		0.64 ± 0.08	0.55 ± 0.04	*
SLF (superior-inferior) R	0.42 ± 0.05	0.46 ± 0.04		1.18 ± 0.06	1.16 ± 0.06		0.60 ± 0.08	0.54 ± 0.05	
SLF (temporal) L	0.42 ± 0.03	0.45 ± 0.03		1.21 ± 0.06	1.16 ± 0.03	*	0.63 ± 0.06	0.56 ± 0.03	*
SLF (temporal) R	0.44 ± 0.05	0.47 ± 0.03		1.20 ± 0.05	1.16 ± 0.04		0.58 ± 0.08	0.53 ± 0.04	
IFOF L	0.40 ± 0.04	0.45 ± 0.03	**	1.36 ± 0.08	1.28 ± 0.02	**	0.74 ± 0.10	0.62 ± 0.04	**
IFOF R	0.41 ± 0.04	0.46 ± 0.02	**	1.31 ± 0.05	1.26 ± 0.03	*	0.68 ± 0.07	0.59 ± 0.03	**
ILF L	0.41 ± 0.03	0.45 ± 0.03	*	1.31 ± 0.06	1.27 ± 0.04		0.68 ± 0.05	0.61 ± 0.04	*
ILF R	0.43 ± 0.03	0.48 ± 0.03	**	1.25 ± 0.09	1.24 ± 0.05		0.62 ± 0.06	0.56 ± 0.04	*
UF L	0.31 ± 0.04	0.39 ± 0.03	***	1.38 ± 0.17	1.22 ± 0.03	***	0.86 ± 0.18	0.64 ± 0.04	**
UF R	0.32 ± 0.04	0.41 ± 0.04	***	1.31 ± 0.10	1.23 ± 0.06		0.79 ± 0.10	0.63 ± 0.07	***
CST L	0.53 ± 0.03	0.53 ± 0.04		1.30 ± 0.05	1.26 ± 0.04		0.53 ± 0.04	0.51 ± 0.04	
CST R	0.56 ± 0.04	0.57 ± 0.02		1.31 ± 0.04	1.30 ± 0.03		0.49 ± 0.05	0.47 ± 0.02	

*Asterisks show significant changes in white matter tracts in between C9neg and C9pos cases. * $p < 0.05$, ** $p < 0.01$; *** $p < 0.001$. Abbreviations: FA = fractional anisotropy; AxialD = axial diffusivity; RadialD = radial diffusivity; SD = standard deviation; Ant thal rad = anterior thalamic radiation; Ant cing = anterior cingulum; SLF = superior longitudinal fasciculus; IFOF = inferior fronto-occipital fasciculus; ILF = inferior longitudinal fasciculus; UF = uncinate fasciculus; CST = corticospinal tract; L = left; R = right.*

5.6.4 Subcortical and cerebellar volumetric measurements in *C9orf72* expansion carriers and non-carriers

Among all grey matter structures measured, none of the volumetric measurement reached statistical significance after corrected for Bonferroni correction at p < 0.005 (Table 5.4).

Table 5.4 Grey matter changes in *C9orf72* expansion carriers compared to non-carriers.

Brain structure	C9neg	C9pos	*U*	Z	*p*
Thalamus L	4.29 ± 0.77	4.78 ± 0.80	31.00	-1.07	0.31
Thalamus R	4.21 ± 0.74	4.52 ± 0.79	36.00	-0.66	0.55
Caudate L	1.84 ± 0.56	2.10 ± 0.37	33.00	-0.91	0.40
Caudate R	1.77 ± 0.39	2.09 ± 0.35	26.00	-1.49	0.15
Putamen L	2.86 ± 0.81	2.97 ± 0.49	43.00	-0.08	0.97
Putamen R	2.58 ± 0.47	2.81 ± 0.55	34.00	-0.83	0.44
Pallidum L	1.15 ± 0.25	0.87 ± 0.32	20.00	-1.98	0.05
Pallidum R	1.03 ± 0.17	0.87 ± 0.25	30.00	-1.16	0.27
Cerebellum L	4.56 ± 0.68	4.62 ± 0.60	42.00	-0.17	0.90
Cerebellum R	4.58 ± 0.63	4.75 ± 0.57	36.00	-0.66	0.55

Numerical values are illustrated in mean ± standard deviation. Abbreviations: L = left; R = right. All volumes were corrected for intracranial volume (which was presented and shown not significantly different between C9neg and C9pos groups in Table 5.1).

5.6.5 Regression model

Dependent variables

Scores of stereotypical behaviour and semantic knowledge were fitted into the regression model as dependent variables as these scores significantly differentiated C9pos and C9neg patients as previously reported in Table 5.2.

Independent variables (predictor variables)

The independent variables were the white matter tracts. Tracts that significantly differentiated C9pos and C9neg patients as previously reported were the left anterior thalamic radiation, bilateral anterior cingulum, inferior-fronto-occipital fasciculi, inferior longitudinal fasciculi and uncinate fasciculi. FA values of these tracts were fitted into a stepwise regression model to identify the tract integrity changes associated with either stereotypical behaviour or semantic knowledge.

For stereotypical behaviour, changes in the integrity of two tracts, the left cingulum and left anterior thalamic radiation ($F_{(2, 16)} = 13.91$, $p < 0.001$; adjusted $R^2 = 0.59$), were identified as predicting changes in the severity of stereotypical behaviour $(p < 0.005)$.

For semantic knowledge, changes in the integrity of one tract, the left uncinate fasciculus ($F_{(1, 17)} = 4.56$, $p = 0.048$; adjusted $R^2 = 0.17$), was identified as predicting changes in the severity of semantic deficits.

5.6.6   Hierarchical regression model

To determine structural changes predicting clinical differences between bvFTD with and without *C9orf72* gene expansions, a 2-step hierarchical regression model was used with the clinical indices as the dependent variables. **In the first step**, the white matter tract was entered as a single predictor, as it is the main focus to determine any structural changes associated with clinical score. **In the second step,** two additional predictors were added. Firstly, the diagnostic group, which is a categorical variable indicating the presence or absence of the *C9orf72* gene abnormality (C9pos = 1; C9neg = 0), was added to the model (Table 5.5). This variable reflected any group differences in the changes in clinical score. Secondly, the interaction between the white matter tract change and the diagnostic group was added. This variable was included to test the combined effects of white matter change and gene abnormality on the clinical score and how these effects differ between *C9orf72* expansion carriers and non-carriers (Table 5.5).

Table 5.5 Hierarchical regression model.

Independent variables:	
Step 1	White matter tract metric
Step 2	White matter tract metric
	Diagnostic group
	White matter tract metric x Diagnostic group interaction

* Note: Dependent variable: clinical score

5.6.7   Prediction of DTI tract changes from clinical variables

Results for each step of the regression model are presented below.

The constant described the mean response value of the dependent variable (clinical score) when all independent variables (white matter tract and/or diagnostic group) are set to zero.

The unstandardised coefficient b and its standard error indicate the average change in white matter tract with a one unit increase in the independent variable, when all other independent variables are held constant. Standardised coefficient β is used to compare the strength of each independent variable on the white matter measurement where the independent variable with the largest β has the strongest effect.

Stereotypical behaviour and the left cingulum bundle

FA

In step 1, FA decrease in the left cingulum was a significant predictor of stereotypical behaviour and explained 34% of the score variance ($F_{(1, 17)}$ = 10.40, p = 0.005; adjusted R^2 = 0.34). In step 2, FA decrease in the left cingulum, diagnostic group and the interaction between these two variables acted as significant predictors of the model and explained 59% of variance in stereotypical behaviour ($F_{(3, 15)}$ = 9.60, p = 0.001; adjusted R^2 = 0.59). Diagnostic group and the interaction variables are the significant contributors and explained the increase in percentage of variance in the regression model (Table 5.6).

AxialD

The change in AxialD of the left cingulum was tested in the model but was not a significant predictor of stereotypical behaviour.

RadialD

In step 1, RadialD increase in the left cingulum is a significant predictor and explained 26% of variance in stereotypical behaviour ($F_{(1, 17)} = 7.16$, $p = 0.016$; adjusted $R^2 = 0.26$).

In step 2, RadialD increase in the left cingulum, diagnostic group and the interaction between these two variables acted as significant predictors of the model and explained 57% of variance in stereotypical behaviour ($F_{(3, 15)} = 8.85$, $p = 0.001$; adjusted $R^2 = 0.57$). Despite overall significance in step 2, only the diagnostic group and the interaction variable contribute significantly to the increase in percentage of variance explained in the regression model (Table 5.6).

Table 5.6 Regression analysis of changes in the left cingulum to stereotypical behaviour.

		FA				RadialD x 10^3mm²s⁻¹			
		b	SE b	β	*p*	b	SE b	β	*p*
Step 1	Constant	26.26	6.05			-7.87	5.57		
	Left cingulum	-46.53	14.43	-0.62	0.00	22.44	8.38	0.54	0.02
Step 2	Constant	15.54	6.42			4.66	6.85		
	Left cingulum	-17.85	16.50	-0.24	0.30	5.56	9.52	0.13	0.57
	Diagnostic group	-6.96	2.26	-0.90	0.01	-7.71	2.32	-1.00	0.00
	Tract x Diagnostic group Interaction	0.91	0.27	0.75	0.00	0.96	0.27	0.79	0.00

Table5.6 illustrates prediction of stereotypical behaviour from the left cingulum in a regression analysis. Unstandardised coefficient b and its standard error, standardised coefficient β and p-value of the regression model were listed. Abbreviations: FA = fractional anisotropy; RadialD = radial diffusivity.

Stereotypical behaviour and the left anterior thalamic radiation

AxialD

In step 1, AxialD increase in the left anterior thalamic radiation is a significant predictor and explained 20% of variance in stereotypical behaviour ($F_{(1, 17)} = 5.37$, $p = 0.03$; adjusted $R^2 = 0.20$).

In step 2, AxialD increase in the left anterior thalamic radiation, diagnostic group and the interaction between these two variables acted as significant predictors of the model and explained 57% of variance in stereotypical behaviour ($F_{(3, 15)} = 8.93$, $p = 0.001$; adjusted $R^2 = 0.57$). Despite overall significance in step 2, the diagnostic group and the interaction variable were the only significant contributors to the increase in percentage of variance explained in the regression model (Table 5.7).

FA and RadialD

No prediction of stereotypical behaviour was observed from changes in FA and RadialD of the left anterior thalamic radiation (Table 5.7).

Table 5.7 Regression analysis of changes in the left anterior thalamic radiation to stereotypical behaviour.

		AxialD x 10^3mm²s⁻¹			
		b	SE b	β	*p*
Step 1	Constant	-19.13	11.26		
	Left ant thal rad	21.13	9.12	0.49	0.03
Step 2	Constant	2.18	9.95		
	Left ant thal rad	5.11	7.84	0.12	0.52
	Diagnostic group	-7.97	1.97	-1.03	0.00
	Tract x Diagnostic group Interaction	0.94	0.28	0.78	0.00

Table5.7 illustrates prediction of stereotypical behaviour from the left anterior thalamic radiation in a regression analysis. Unstandardised coefficient b and its standard error, standardised coefficient β and p-value of the regression model were listed. Abbreviations: ant thal rad = anterior thalamic radiation; AxialD = axial diffusivity.

Semantic deficits and the left uncinate fasciculus

FA

Regression results showed only significance in step 1 where a FA decrease in the left uncinate fasciculus is a significant predictor and explained 17% of variance in semantic knowledge scores ($F_{(1, 17)} = 4.56$, $p = 0.048$; adjusted $R^2 = 0.17$) (Table 5.8).

AxialD

In step 1, AxialD increase in the left uncinate fasciculus is a significant predictor and explained 26% of variance in semantic knowledge ($F_{(1, 17)} = 7.29$, $p = 0.02$; adjusted $R^2 = 0.26$).

In step 2, AxialD increase in the left uncinate fasciculus, diagnostic group and the interaction between these two variables acted as significant predictors of the model and explained 57% of variance in semantic knowledge ($F_{(3, 15)} = 4.00$, $p = 0.03$; adjusted $R^2 = 0.5$). Despite overall significance in step 2, the individual predictors, left uncinate fasciculus, diagnostic group and the interaction variable, did not yield statistical significance (Table 5.8).

RadialD

In step 1, RadialD increase in the left uncinate fasciculus is a significant predictor and explained 16% of variance in semantic knowledge ($F_{(1, 17)} = 4.46$, $p = 0.050$; adjusted $R^2 = 0.16$).

However, the predictors did not contribute significantly to the change in semantic knowledge scores in step 2 (Table 5.8).

Table 5.8 Regression analysis of changes in the left uncinate fasciculus to semantic knowledge.

		FA				AxialD x 10^3mm²s⁻¹				RadialD x 10^3mm²s⁻¹			
		b	SE b	β	*p*	b	SE b	β	*p*	b	SE b	β	*p*
Step 1	Constant	26.26	6.05			-11.46	6.84			-7.87	5.57		
	Left uncinate fasciculus	-46.53	14.43	-0.62	0.00	14.00	5.19	0.55	0.02	22.44	8.38	0.54	0.02
Step 2	Constant				NS	-4.07	8.08						NS
	Left uncinate fasciculus					9.21	5.82	0.36	0.13				
	Diagnostic group					20.14	17.72	2.60	0.27				
	Tract x Diagnostic group Interaction					-0.91	0.70	-2.95	0.22				

Table 5.8 illustrates prediction of semantic knowledge from the left uncinate fasciculus in a regression analysis. Unstandardised coefficient b and its standard error, standardised coefficient β and p-value of the regression model were listed. Abbreviations: FA = fractional anisotropy; AxialD = axial diffusivity; RadialD = radial diffusivity; NS = not significant.

5.7 Discussion

This study assessed bvFTD cases under the influences of the *C9orf72* repeat expansions and identified differences in some clinical characteristics that associate with changes in white matter integrity. Stereotypical behaviour was less severe in *C9orf72* expansion carriers than in non-carriers and the left cingulum and anterior thalamic radiation were predictive of the changes in stereotypical behaviour scores. Semantic knowledge was less affected in *C9orf72* expansion carriers than in non-carriers and the left uncinate fasciculus was predictive of this change in semantic knowledge. These predictions significantly differentiated between bvFTD patients with and without the *C9orf72* gene expansions. Overall, white matter changes in bvFTD *C9orf72* expansion carriers (known to have FTLD-TDP) do not exhibit the typical frontotemporal tract changes in non-carriers, suggesting that greater white matter damage distinguishes non-carriers more likely to have FTLD-tau.

5.7.1 Clinical characteristics in bvFTD with *C9orf72* gene expansions

As expected, many of the typical clinical characteristics of patients with bvFTD were similarly affected in *C9orf72* expansion carriers and non-carriers, otherwise they would not have the clinical syndrome targeted. In particular, executive function, verbal working memory, episodic memory and naming, as well as behavioural features were affected to a similar degree in bvFTD *C9orf72* expansion carriers and non-carriers. This finding is consistent with the previous study comparing clinical features in bvFTD *C9orf72* expansion carriers and non-carriers that showed no significant differences in episodic memory and

executive function (Devenney et al 2014) Importantly, findings in this chapter highlighted differences in stereotypical behaviour and semantic knowledge, features that were significantly less affected in those with *C9orf72* repeat expansions than those without these expansions.

However, the issue of small number of cases included in each study requires further studies with larger samples of clinically defined FTD cases to validate these findings and potentially identify additional subtle clinical features. The number of cases examined in this chapter suggests that the clinical differences noted may be sufficiently robust to identify bvFTD patients with *C9orf72* repeat expansions.

5.7.2   White matter measurement in bvFTD with *C9orf72* gene expansions

White matter, measured using whole-brain voxelwise analysis, showed subtle tract changes in *C9orf72* expansion carriers compared to non-carriers. In contrast, a substantial diffuse pattern of white matter changes was observed in non-*C9orf72* expansion carriers compared to the expansion carriers. These changes, as measured by decrease in FA, and increases in AxialD and RadialD, were observed in the left anterior thalamic radiation, bilateral anterior cingulum, inferior-fronto-occipital fasciculi, inferior longitudinal fasciculi and uncinate fasciculi.

Comparison of these results to the other existing white matter studies (Mahoney et al 2012b, Mahoney et al 2014) need to be made with caution because of the mixed clinical phenotypes and small sample size used in previous studies. One study compared *C9orf72* expansion carriers to controls and illustrated white matter alterations in FA and RadialD in the bilateral anterior thalamic

radiations, uncinate fasciculi, anterior cingulum and anterior corpus callosum; and in the right posterior corpus callosum, posterior inferior longitudinal fasciculus and superior longitudinal fasciculus. However, *C9orf72* expansion carriers sampled in the study comprised of different clinical phenotypes, including bvFTD, FTD-MND and nfv-PPA (Mahoney et al 2012b), making direct comparisons with the current findings difficult. The other study revealed no differences in white matter integrity in *C9orf72* expansion carriers compared to sporadic bvFTD cases, however, these results are likely to be underpowered due to the small sample size used (n = 4)(Mahoney et al 2014).

5.7.3 Grey matter measurement in bvFTD with *C9orf72* expansion carriers

None of the grey matter subcortical or cerebellum volumes measured differed between *C9orf72* expansion carriers and non-carriers after Bonferroni correction. The subcortical structure closest to statistical difference was the left globus pallidus where a smaller left pallidum in the *C9orf72* expansion carriers was observed compared to the non-carriers. The pallidum or globus pallidus is a component of the extrapyramidal system which could explain the propensity for an increase in extrapyramidal symptoms reported in some *C9orf72* patients (Boeve et al 2012, Kaivorinne et al 2013, Mahoney et al 2012b).
Other studies have highlighted significant atrophy in the thalamus and cerebellum in *C9orf72* expansion carriers (Devenney et al 2014, Mahoney et al 2012b) but these were not found in the current study analysing only bvFTD cases.

5.7.4   Prediction of clinical features from white matter change

Both *C9orf72* expansion carriers and non-carriers shared the same clinical diagnosis of bvFTD and these groups also performed similarly using many neuropsychological assessments except for minor deviations in language and behaviour. Interestingly, however, brain white matter integrity differed in association with these clinical differences between the two bvFTD groups with or without the *C9orf72* gene expansions.

5.7.4.1   White matter changes in the prediction of stereotypical behaviour

White matter abnormalities in the left cingulum (FA decrease and RadialD increase) and also in the left anterior thalamic radiation (AxialD increase) were predictive of greater severity in stereotypical behaviours.

Greater abnormalities in the FA and RadialD of the left cingulum predicted more severe stereotypical behaviour and this prediction significantly differentiated bvFTD *C9orf72* expansion carriers from non-carriers (Table 5.6). In contrast, the prediction that the AxialD change in the left anterior thalamic radiation was greater with worse stereotypical behaviour did not significantly differentiated *C9orf72* expansion carriers from non-carriers (Table 5.7). These results showed group membership (having *C9orf72* gene expansions or not) has a different impact on tract integrity and the prediction of stereotypical behaviour. Furthermore, group membership combined with tract integrity has a differential effect in predicting stereotypical behaviour in bvFTD patients.

The prediction that the cingulum is important for stereotypical behaviour is supported by findings in other diseases. The cingulum is commonly affected in

135

autism spectrum disorders and the loss of integrity in this white matter tract has been correlated with the presence of stereotypical behaviours (Ha 2012, Kumar et al 2010). The anterior thalamic radiation was found to be affected in both *C9orf72* expansion carriers and non-carriers in this thesis and also in other studies (Mahoney et al 2012b, Zhang et al 2009) but this white matter tract has not been associated with any clinical characteristics. This is the first study to confirm this white matter association with stereotypical behaviour in bvFTD.

5.7.4.2 White matter changes in the prediction of semantic knowledge

Alterations in the structure of the uncinate fasciculus (FA decrease, AxialD and RadialD increase) were predictive of worse semantic knowledge.

Although all DTI metrics measured were predictive of worse semantic knowledge, only changes in AxialD successfully differentiated *C9orf72* expansion carriers from non-carriers. Furthermore, the interaction variable of group membership (having *C9orf72* gene expansions or not) combined with tract integrity in predicting semantic performances further emphasised the differences between *C9orf72* expansion carriers from non-carriers.

Previous studies have shown uncinate fasciculus impairment in semantic variant patients (Agosta et al 2010) and that this tract was associated with problems in semantic processing (Han et al 2013). This is the first study to demonstrate a predictive relation between the uncinate fasciculus and the semantic system.

The DTI metrics, FA, AxialD and RadialD, have different sensitivities in predicting these clinical features in bvFTD. These results can provide direction for pathological studies in the study of a specific tract (i.e. the left cingulum,

anterior thalamic radiation or uncinate fasciculus) to investigate whether the DTI parameters correlate with a specific pathological processes, such as axonal or myelin loss as suggested in previous studies (Pierpaoli et al 2001, Song et al 2003) or protein/genetic abnormality (present study).

5.7.5   Relation to phenocopy bvFTD cases

It is noteworthy to mention a clinical subgroup of bvFTD called the phenocopy due to the absence of significant tissue degeneration on imaging and the relative lack of a progressive course years (Davies et al 2006, Hornberger et al 2009, Piguet et al 2009). This group of patients meet the clinical diagnostic criteria for possible bvFTD and symptom profiles as reported by carers, except for the less disrupted activities of daily living. The clinical features of phenocopy patients remain stable over many years (Davies et al 2006, Hornberger et al 2009, Piguet et al 2009).

A recent study reported two very slowly progressive cases with the *C9orf72* gene expansions (Khan et al 2012). Questions of whether clinically defined phenocopy cases are more likely to have the *C9orf72* gene expansions have been raised. Undeniably, phenocopy patients progress slowly and often lack apparent atrophy on MRI scans (Brodtmann et al 2013, Kipps et al 2010). Similarly, these attributes are observed in the *C9orf72* expansion carriers in the present study. In contrast, phenocopy cases exhibit normal or marginal impairment on neuropsychological tests of executive function and have preserved memory and social cognition (Kipps et al 2010) while *C9orf72* expansion carriers showed behavioural characteristics similar to typical bvFTD patients to a certain extend (Devenney et al 2014, Mahoney et al 2012b, Sha et al 2012, Simón-Sánchez et al

2012). Further longitudinal studies on disease progression with pathological validation are required to determine if a significant association exists between bvFTD phenocopy and bvFTD with *C9orf72* repeat expansions.

5.7.6   Strengths and limitations

Strengths of this study design are that the patients were from the same centre, same clinical tools were administered by the same personnel allowing matching of clinical phenotypes, and the same imaging data collection protocols were used.

Previous studies of the *C9orf72* expansion carriers compared such cases against other genetic mutations, such as MAPT, progranulin and also to sporadic bvFTD, resulting in study groups comprised of a mixture of different clinical groups (i.e. bvFTD, FTD-MND and MND, etc.). While clinical symptoms and neuroimaging can be used to identify *C9orf72* gene cases from other genetic groups, clinical differentiation from sporadic FTD subtypes is less easy.

Very few papers have separated bvFTD and MND, and further differentiated those with or without *C9orf72* gene expansions in their analyses (Devenney et al 2014, Mahoney et al 2014, Sha et al 2012, Whitwell et al 2012), a strategy which could potentially assist diagnosis and tracking of disease progression. However, this strategy leaves groups with relatively low numbers and reduced statistical power for analyses. The same issue of small sample size is one of the limitations of this study, particularly when *C9orf72* expansion carriers and non-carriers were assessed within the same clinical subgroup, bvFTD. The rigorous threshold set in the present study for statistical significance may be over conservative for

results with non-significant trends which may reflect true underlying differences between the *C9orf72* expansion carrier and non-carrier groups. This chapter provides data to further understand this neurodegenerative disease via three different aspects: genetically, clinically and radiologically. This is aligned with the aim of the thesis which is to understand FTD for early detection of the disease and accurate diagnosis for a more effective management and better control of symptoms.

5.7.7   Summary

- <u>Similar clinical profiles in bvFTD *C9orf72* expansion carriers and non-carriers but with deviation</u>: The overall clinical profiles of *C9orf72* expansion carriers are similar to those without the expansion. *C9orf72* expansion carriers have less stereotypical behaviour and semantic knowledge abnormalities.

- <u>White matter change is less evident in bvFTD *C9orf72* expansion carriers than non-carriers:</u> White matter was generally less affected in frontotemporal tracts in *C9orf72* carriers.

- <u>White matter tract changes predicted clinical scores and differentiated *C9orf72* expansion carriers from non-carriers:</u> The left cingulum and anterior thalamic radiation were predictive of changes in stereotypical behaviour. The association between FA and RadialD changes of the left cingulum and stereotypical behaviour statistically differentiated between *C9orf72* expansion carriers and non-carriers.

  The left uncinate fasciculus was predictive of changes in semantic knowledge. The association between AxialD of the left uncinate fasciculus and semantic knowledge statistically differentiated between *C9orf72* expansion carriers and non-carriers.

Chapter 6 General discussion

Chapter Six

6 GENERAL DISCUSSION

6.1 Summary

The objectives of this thesis were to investigate brain white matter alterations *in vivo* in the main subtypes of FTD, namely bvFTD, nfv-PPA and sv-PPA. Using diffusion tensor imaging, the investigations presented in Chapters 3-5 have resulted in an improved understanding of the white matter alterations in FTD. These findings includes patterns of white matter changes in FTD subtypes at the time of presentation to the clinic (Chapter 3), following a 12-month interval (Chapter 4), and in a cohort of patients presenting with genetic FTD due to abnormal *C9orf72* gene expansions and a known underlying pathology (Chapter 5).

In Chapter 3, the patterns of white matter changes in each FTD subtype were identified using four different DTI metrics. Each FTD subtype was found to exhibit its own signature of white matter change. White matter alterations were observed in orbitofrontal and anterior temporal tracts in bvFTD, bilateral (left>right) frontotemporal tracts in the nfv-PPA and circumscribed left temporal lobe in sv-PPA. Findings showed white matter alterations largely overlap with grey matter atrophy and even extended beyond the grey matter cortical atrophy in two of the three subtypes: bvFTD and nfv-PPA. In contrast, sv-PPA had bilateral grey matter atrophy but focal tract changes in the left anterior temporal lobe. The location and severity of these changes varied depending on the DTI metrics used, indicating that white matter changes shown with different DTI measures may represent different pathological processes.

In Chapter 4, white matter changes were measured in the same groups of participants after 12 months. Analyses demonstrated that white matter alterations continued in regions identified at baseline, but with additional changes that extended beyond the original regions affected. Furthermore, white matter damage in all FTD subtypes extended far beyond the site of atrophy in grey matter. These results demonstrated that FTD is a dynamic process with ongoing changes taking place over the course of the disease.

The sensitivity of DTI parameters used to measure white matter change varied along different disease stages. As discussed in Chapter 3, analyses of baseline measurements revealed that the DTI metrics, MD and AxialD, were the most sensitive indicators of change in bvFTD and nfv-PPA while MD and RadialD were most sensitive in sv-PPA. In contrast, Chapter 4 showed that FA and RadialD DTI measurements were more sensitive parameters as the disease progresses. As the FA and MD give an overall indication of white matter integrity and AxialD and RadialD reflect diffusion properties more specifically in a particular direction in the white matter tract and these metrics are sensitive at different disease stages, measuring all four metrics are needed in order to get a full picture of the changes in the white matter.

In Chapter 5, investigations of clinical features and white matter changes in FTD cases carrying the *C9orf72* gene expansions, which explains one-third of familial FTD cases, were conducted based on the findings from the previous chapters. *C9orf72* expansion carriers and non-carriers with the same clinical subtype, bvFTD, showed similar clinical profiles, with two exceptions: bvFTD expansion carriers exhibited milder clinical symptoms in stereotypical behaviour and

better performance in semantic knowledge compared to non-carriers. In addition, brain white matter alterations in *C9orf72* expansion carriers showed significantly less pronounced frontotemporal tract changes than non-carriers. Regression analyses were carried out to identify the white matter tracts that best predicted changes in the clinical features that differed between expansion carriers and non-carriers. Given the limited information currently available on the biological/clinical associations between *C9orf72* expansion carriers and non-carriers within a single phenotype, these results improved the understanding of this progressive neurodegenerative condition.

6.2 The significance of studying the brain white matter

Axonal fibres of the white matter are an important means of neural communication among neurons. In many disorders of the brain, the structural integrity and connectivity of white matter pathways *in vivo* have been much less studied compared to grey matter until the relatively recent development of DTI which allows sensitive measurement of tract integrity (Basser et al 1994, Le Bihan et al 2001). The studies in this thesis have demonstrated that DTI is a sensitive measurement to detect white matter alterations. The DTI findings reflect integrity of these connecting fibres in the brain and will further the understanding on imaging and pathological changes in neuronal fibres in neurodegenerative diseases. Findings arising from this thesis demonstrated that patterns of white matter changes were also reflective of clinical characteristics of FTD subtypes. For example, bvFTD patients who experienced changes in personality, social behaviour and loss of insight showed degeneration

predominantly in frontotemporal white matter tracts, while the two language variants of FTD showed predominant brain changes on the left hemisphere which are responsible for language.

Comparing white matter to grey matter changes, bvFTD and nfv-PPA have frontotemporal white matter tracts affected that are more distal to the primary sites grey matter atrophy, suggesting grey and white matter changes have different contributions to the clinical phenotypes.

As disease progresses, both grey and white matter alterations tend to become more diffuse across different lobes and across both hemispheres of the brain, these findings are also in line with the overlapping clinical symptoms in different FTD subtypes as disease progress. Grey matter atrophy progressed relatively focal in contrast to white matter changes which became widespread with bilateral alterations in frontotemporal regions and the damage encroaching into the posterior white matter in all FTD subtypes. This shows uncoupling between grey and white matter as disease progresses and suggests independent processes underlying the grey and white matter changes.

Studying the white matter will be useful in clinical trials when monitoring the impact of novel drug compounds as the extensive involvement of the white matter pathology and its rapid progression over time will help the development of therapeutic treatments in FTD syndromes over a relatively short time period.

6.3 Structural and functional correlations

The pattern of widespread white matter change compared to the relatively focal grey matter atrophy indicates that DTI is a sensitive tool to detect brain changes

underlying the degenerative disease. Direct conclusion, however, cannot yet be drawn concerning whether white or grey matter changes appear first in FTD because these changes are measured using different imaging modalities. However, the combined information of white matter connectivity, together with structural grey matter data, and functional MRI data have the potential to generate comprehensive models of the brain architecture. The Human Connectome Project (http://www.humanconnectomeproject.org/) is such a project. It combines functional and structural connectivity across all cortical and subcortical brain regions, with the aim to map the neural connections of the human nervous system. By investigating the whole brain networks with anatomical and functional components, the human connectomes will greatly benefit the understanding of the circuits of the brain, regardless of being at a healthy or disease state.

6.4 Implication of different sensitivity in DTI metrics

In this thesis, white matter integrity was measured using four different DTI metrics: two providing overall indices of changes (FA and MD) and two reflecting changes along a particular direction (AxialD-diffusion along the main axis of diffusion, generally thought to reflect axonal diffusion; RadialD-diffusion perpendicular to the axon, generally thought to reflect myelin loss) (Song et al 2003, Song et al 2002, Sun et al 2006). White matter alterations did not overlap fully among the different metrics. The four DTI metrics have variable sensitivities at different disease stages. Although DTI is a sensitive tool to detect white matter alterations, its implications from the DTI parameters are less

specific. Difficulty arises when it comes to identifying the many different components of the white matter tissue which include axonal length, axonal density, altered myelination and glial cell proliferation that all contribute to the white matter alteration observed. Improved diffusion models with high sensitivity and specificity and also *postmortem* pathological investigations will be able to establish the association between DTI measurements *in vivo* and different pathological processes accurately.

6.5   Genetic influence on patterns of brain changes

There are clear genetic influences on brain structures of patients with FTD (Mahoney et al 2012b, Rohrer et al 2011, Whitwell et al 2012) but little is known about the impact of the *C9orf72* gene expansions on brain white matter. Chapter 5 in this thesis adds important information to the understanding of the white matter alterations associated with the *C9orf72* gene abnormality. Of importance, less damage in certain frontotemporal white matter tracts was shown to be predictive of specific clinical features such as less stereotypical behaviour and better semantic knowledge and can be used to differentiate non-carriers from carriers of the *C9orf72* gene expansions.

Understanding the genetic influence on brain pathology has important clinical implications. Presence of the repeat expansion in the *C9orf72* gene in patients diagnosed with bvFTD correlated with reduced symptoms compared to patients who did not carry the expansion. This poses challenging issues for clinical management as *C9orf72* expansion carriers of bvFTD may present with behavioural symptoms and not satisfy the "probable bvFTD" classification due

to the lack of clinical and imaging changes. Considerations of atypical brain changes due to such genetic influences may need to be included in future revision of the clinical diagnostic criteria for FTD.

6.6 Limitations and future directions

Pathological validation

DTI is developed to investigate the underlying pathological changes in the white matter tissue. Animal studies have suggested that a decrease in AxialD correlates with axonal degeneration while an increase in RadialD suggests myelin loss (Song et al 2003, Song et al 2002, Sun et al 2006). Given the complexity of pathological changes affecting the white matter (altered myelination, neurodegeneration, gliosis, calcification, etc.) (Sierra et al 2011), it is unlikely that one metric is reflecting only one type of pathological change. *Postmortem* histopathological confirmation of the type of change being detected *in vivo* with DTI overtime is needed in order to establish whether the relationships reported in animal studies hold true in humans.

Improvement on specificity of studying the white matter

Since DTI assumes that each voxel contains a single, coherently oriented bundle of white matter axons, situations where voxels containing multiple fibre orientation and with crossing-fibres are not optimally assessed by the present DTI measurements. The specificity of studying the white matter tissue structure can be improved by other diffusion models. The high angular resolution diffusion-weighted imaging is one alternative way to extract more information

from the diffusion-weighted images by capturing a much larger number of uniformly distributed diffusion-weighted gradient directions to capture the high angular frequency feature that are not adequately modelled by a single diffusion tensor (Tuch et al 2002).

Another way to improve specificity of investigating white matter change is to use a reliable and interpretable measurement to assess white matter tracts. FA is the most common DTI-derived measurement to study white matter integrity at present. Sensitivity and accuracy of this measurement, however, have been challenged. FA recorded no change in value when water diffusion changes proportionally along the direction of other DTI metrics (Acosta-Cabronero et al 2010). Researchers have been exploring alternative measurements to investigate white matter integrity. One of the proposed approaches is the "apparent fibre density" which is based on higher-order information provided by fibre orientation distributions computed using spherical deconvolution. The "apparent fibre density" is more reliable and interpretable in identifying differences along single fibre bundles containing multiple fibre populations than traditionally DTI-derived measures (Raffelt et al 2012).

6.7 Conclusions

This thesis has highlighted the differential white matter changes at baseline and over a 12-month period in the three FTD subtypes and also the influence on the white matter by the *C9orf72* gene expansions. Together, these results demonstrated the importance of studying white matter for the classification and disease monitoring of this devastating degenerative disease.

The improving diffusion imaging techniques provide hope for detecting white matter changes early at the disease stage and changes in the white matter may one day become a biomarker for FTD diagnosis.

The longitudinal study assessed white matter changes along disease progression. Continuous collection of multiple longitudinal scans has its potential to map disease progression more extensively for better monitoring and management of FTD.

Lastly, the study of FTD under the influence of the *C9orf72* gene expansions provided important information about the imaging-clinical associations which further the understanding of the complex relations between clinical, pathological and genetic components of FTD.

REFERENCES

Acosta-Cabronero J, Alley S, Williams G, B. , Pengas G, Nestor P, J. . 2012. Diffusion Tensor Metrics as Biomarkers in Alzheimer's Disease. *PLoS ONE* 7: e49072

Acosta-Cabronero J, Patterson K, Fryer TD, Hodges JR, Pengas G, et al. 2011. Atrophy, hypometabolism and white matter abnormalities in semantic dementia tell a coherent story. *Brain* 134: 2025-35

Acosta-Cabronero J, Williams GB, Pengas G, Nestor PJ. 2010. Absolute diffusivities define the landscape of white matter degeneration in Alzheimer's disease. *Brain* 133: 529-39

Agosta F, Canu E, Sarro L, Comi G, Filippi M. 2012. Neuroimaging findings in frontotemporal lobar degeneration spectrum of disorders. *Cortex* 48: 389-413

Agosta F, Henry RG, Migliaccio R, Neuhaus J, Miller BL, et al. 2010. Language networks in semantic dementia. *Brain* 133: 286-99

Agosta F, Scola E, Canu E, Marcone A, Magnani G, et al. 2011. White Matter Damage in Frontotemporal Lobar Degeneration Spectrum. *Cerebral Cortex* 22: 2075-14

Ahmed Z, Doherty K, Silveira-Moriyama L, Bandopadhyay R, Lashley T, et al. 2011. Globular glial tauopathies (GGT) presenting with motor neuron disease or frontotemporal dementia: an emerging group of 4-repeat tauopathies. *Acta Neuropathologica* 122: 415-28

Alzheimer A. 1911. Über eigenartige Krankheitsfälle des späteren Alters. *Zentralbl Gesamte Neurol Psychiatr* 4: 356-85

Andersson J, Jenkinson M, Smith S. 2007a. Non-linear optimisation. FMRIB technical report TR07JA1 from www.fmrib.ox.ac.uk/analysis/techrep.

Andersson J, Jenkinson M, Smith S. 2007b. Non-linear registration, aka Spatial normalisation. FMRIB technical report TR07JA2 from www.fmrib.ox.ac.uk/analysis/techrep.

Arfanakis K, Haughton VM, Carew JD, Rogers BP, Dempsey RJ, Meyerand ME. 2002. Diffusion Tensor MR Imaging in Diffuse Axonal Injury. *American Journal of Neuroradiology* 23: 794-802

Ashburner J, Friston KJ. 2000. Voxel-Based Morphometry—The Methods. *NeuroImage* 11: 805-21

Avants BB, Cook PA, Ungar L, Gee JC, Grossman M. 2010. Dementia induces correlated reductions in white matter integrity and cortical thickness: A multivariate neuroimaging study with sparse canonical correlation analysis. *NeuroImage* 50: 1004-16

Ayala YM, Pantano S, D'Ambrogio A, Buratti E, Brindisi A, et al. 2005. Human, Drosophila, and C. elegans TDP43: Nucleic Acid Binding Properties and Splicing Regulatory Function. *Journal of Molecular Biology* 348: 575-88

Baddeley AD, Emslie H, Nimmo-Smith I. 1994. *Doors and People: A Test of Visual and Verbal Recall and Recognition*. Suffolk, England: Thames Valley Test Company.

Barrick TR, Charlton RA, Clark CA, Markus HS. 2010. White matter structural decline in normal ageing: A prospective longitudinal study using tract-based spatial statistics. *NeuroImage* 51: 565-77

Bartzokis G, Cummings JL, Sultzer D, Henderson VW, Nuechterlein KH, Mintz J. 2003. White matter structural integrity in healthy aging adults and patients with alzheimer disease: A magnetic resonance imaging study. *Archives of Neurology* 60: 393-98

Basser PJ, Mattiello J, LeBihan D. 1994. MR diffusion tensor spectroscopy and imaging. *Biophysical Journal* 66: 259-67

Basser PJ, Pierpaoli C. 1996. Microstructural and Physiological Features of Tissues Elucidated by Quantitative-Diffusion-Tensor MRI. *Journal of Magnetic Resonance, Series B* 111: 209-19

Beaulieu C. 2002. The basis of anisotropic water diffusion in the nervous system – a technical review. *NMR in Biomedicine* 15: 435-55

Beaulieu C, Does MD, Snyder RE, Allen PS. 1996. Changes in water diffusion due to Wallerian degeneration in peripheral nerve. *Magnetic Resonance in Medicine* 36: 627-31

Behrens TEJ, Berg HJ, Jbabdi S, Rushworth MFS, Woolrich MW. 2007. Probabilistic diffusion tractography with multiple fibre orientations: What can we gain? *NeuroImage* 34: 144-55

Bernal B, Ardila A. 2009. The role of the arcuate fasciculus in conduction aphasia. *Brain* 132: 2309-16

Bigio EH, Weintraub S, Rademakers R, Baker M, Ahmadian SS, et al. 2013. Frontotemporal lobar degeneration with TDP-43 proteinopathy and chromosome 9p repeat expansion in C9ORF72: clinicopathologic correlation. *Neuropathology* 33: 122-33

Bird TD, Nochlin D, Poorkaj P, Cherrier M, Kaye J, et al. 1999. A clinical
pathological comparison of three families with frontotemporal dementia
and identical mutations in the tau gene (P301L). *Brain* 122: 741-56

Boccardi M, Sabattoli F, Laakso MP, Testa C, Rossi R, et al. 2005.
Frontotemporal dementia as a neural system disease. *Neurobiology of
Aging* 26: 37-44

Boeve BF, Boylan KB, Graff-Radford NR, DeJesus-Hernandez M, Knopman DS,
et al. 2012. Characterization of frontotemporal dementia and/or
amyotrophic lateral sclerosis associated with the GGGGCC repeat
expansion in C9ORF72. *Brain* 135: 765-83

Borroni B, Bonvicini C, Alberici A, Buratti E, Agosti C, et al. 2009. Mutation
within TARDBP leads to Frontotemporal Dementia without motor
neuron disease. *Human Mutation* 30: 974-83

Borroni B, Brambati SM, Agosti C, Gipponi S, Bellelli G, et al. 2007. Evidence of
White Matter Changes on Diffusion Tensor Imaging in Frontotemporal
Dementia. *Arch Neurol* 64: 246-51

Bossù P, Salani F, Alberici A, Archetti S, Bellelli G, et al. 2011. Loss of function
mutations in the progranulin gene are related to pro-inflammatory
cytokine dysregulation in frontotemporal lobar degeneration patients.
Journal of Neuroinflammation 8: 65-70

Brambati SM, Rankin KP, Narvid J, Seeley WW, Dean D, et al. 2009. Atrophy
progression in semantic dementia with asymmetric temporal
involvement: A tensor-based morphometry study. *Neurobiology of Aging*
30: 103-11

Brambati SM, Renda NC, Rankin KP, Rosen HJ, Seeley WW, et al. 2007. A tensor based morphometry study of longitudinal gray matter contraction in FTD. *NeuroImage* 35: 998-1003

Brodtmann A, Cowie T, McLean C, Darby D. 2013. Phenocopy or variant: a longitudinal study of very slowly progressive frontotemporal dementia. *BMJ Case Reports* 2013: doi: 10.1136/bcr-2012-008077

Brooks B, Miller R, Swash M, Munsat T. 2000. El Escorial revisited: revised criteria for the diagnosis of amyotrophic lateral sclerosis. *Amyotrophic lateral sclerosis and other motor neuron disorders* 1: 293-9

Brown R. 1828. A brief account of microscopical observations made in the months of June, July, August, 1827, on the particles contained in the pollen of plants; and on the general existence of active molecules in organic and inorganic bodies. *Phil Mag* 4: 161-73

Bugiani O, Murrell JR, Giaccone G, Hasegawa M, Ghigo G, et al. 1999. Frontotemporal Dementia and Corticobasal Degeneration in a Family with a P301S Mutation in Tau. *Journal of Neuropathology & Experimental Neurology* 58: 667-77

Cairns N, Bigio E, Mackenzie I, Neumann M, Lee V, et al. 2007. Neuropathologic diagnostic and nosologic criteria for frontotemporal lobar degeneration: Consensus of the consortium for frontotemporal lobar degeneration. *Acta Neurol* 114: 5-22

Chao LL, Schuff N, Clevenger EM, Mueller SG, Rosen HJ, et al. 2007. Patterns of White Matter Atrophy in Frontotemporal Lobar Degeneration. *Arch Neurol* 64: 1619-24

Chare L, Hodges JR, Leyton CE, McGinley C, Tan RH, et al. 2014. New criteria for frontotemporal dementia syndromes: clinical and pathological diagnostic implications. *Journal of Neurology, Neurosurgery & Psychiatry* 85: 865-70

Czarnecki K, Duffy JR, Nehl CR, et al. 2008. Very early semantic dementia with progressive temporal lobe atrophy: An 8-year longitudinal study. *Archives of Neurology* 65: 1659-63

Dale AM, Fischl B, Sereno MI. 1999. Cortical Surface-Based Analysis: I. Segmentation and Surface Reconstruction. *NeuroImage* 9: 179-94

Davies R, Scahill V, Graham A, Williams G, Graham K, Hodges J. 2009. Development of an MRI rating scale for multiple brain regions: comparison with volumetrics and with voxel-based morphometry. *Neuroradiology* 51: 491-503

Davies RR, Graham KS, Xuereb JH, Williams GB, Hodges JR. 2004. The human perirhinal cortex and semantic memory. *European Journal of Neuroscience* 20: 2441-46

Davies RR, Hodges JR, Kril JJ, Patterson K, Halliday GM, Xuereb JH. 2005. The pathological basis of semantic dementia. *Brain* 128: 1984-95

Davies RR, Kipps CM, Mitchell J, Kril JJ, Halliday GM, Hodges JR. 2006. Progression in frontotemporal dementia: Identifying a benign behavioral variant by magnetic resonance imaging. *Archives of Neurology* 63: 1627-31

DeJesus-Hernandez M, Mackenzie Ian R, Boeve Bradley F, Boxer Adam L, Baker M, et al. 2011. Expanded GGGGCC Hexanucleotide Repeat in

Noncoding Region of C9ORF72 Causes Chromosome 9p-Linked FTD and ALS. *Neuron* 72: 245-56

Delano-Wood L, Stricker NH, Sorg SF, Nation DA, Jak AJ, et al. 2012. Posterior Cingulum White Matter Disruption and Its Associations with Verbal Memory and Stroke Risk in Mild Cognitive Impairment. *Journal of Alzheimer's Disease* 29: 589-603

Desikan RS, Ségonne F, Fischl B, Quinn BT, Dickerson BC, et al. 2006. An automated labeling system for subdividing the human cerebral cortex on MRI scans into gyral based regions of interest. *NeuroImage* 31: 968-80

Destrieux C, Fischl B, Dale A, Halgren E. 2010. Automatic parcellation of human cortical gyri and sulci using standard anatomical nomenclature. *NeuroImage* 53: 1-15

Devenney E, Hornberger M, Irish M, et al. 2014. Frontotemporal dementia associated with the c9orf72 mutation: A unique clinical profile. *JAMA Neurology* 71: 331-9

Dickson D, Kouri N, Murray M, Josephs K. 2011. Neuropathology of Frontotemporal Lobar Degeneration-Tau (FTLD-Tau). *Journal of Molecular Neuroscience* 45: 384-89

Diehl-Schmid J, Pohl C, Perneczky R, Förstl H, Kurz A. 2006. Behavioral Disturbances in the Course of Frontotemporal Dementia. *Dementia and Geriatric Cognitive Disorders* 22: 352-57

Duering M, Zieren N, Hervé D, Jouvent E, Reyes S, et al. 2011. Strategic role of frontal white matter tracts in vascular cognitive impairment: a voxel-based lesion-symptom mapping study in CADASIL. *Brain* 134: 2366-75

Duffau H, Gatignol P, Denvil D, Lopes M, Capelle L. 2003. The articulatory loop: study of the subcortical connectivity by electrostimulation. *NeuroReport* 14: 2005-08

Einstein A. 1905. Über die von der molekularkinetischen Theorie der Wärme geforderte Bewegung von in ruhenden Flüssigkeiten suspendierten Teilchen. *Annalen der Physik* 322: 549-60

Farg MA, Sundaramoorthy V, Sultana JM, Yang S, Atkinson RAK, et al. 2014. C9ORF72, implicated in amytrophic lateral sclerosis and frontotemporal dementia, regulates endosomal trafficking. *Human Molecular Genetics*: doi:10.1093/hmg/ddu068

Fischl B, Dale AM. 2000. Measuring the thickness of the human cerebral cortex from magnetic resonance images. *Proceedings of the National Academy of Sciences* 97: 11050-55

Fischl B, Sereno MI, Dale AM. 1999. Cortical Surface-Based Analysis: II: Inflation, Flattening, and a Surface-Based Coordinate System. *NeuroImage* 9: 195-207

Fischl B, van der Kouwe A, Destrieux C, Halgren E, Ségonne F, et al. 2004. Automatically Parcellating the Human Cerebral Cortex. *Cerebral Cortex* 14: 11-22

Frackowiak RSJ, Friston KJ, Frith C., Dolan R, Mazziotta CJ. 1997. Human brain function. USA: Academic Press

Galantucci S, Tartaglia MC, Wilson SM, Henry ML, Filippi M, et al. 2011. White matter damage in primary progressive aphasias: a diffusion tensor tractography study. *Brain* 134: 3011-29

Garcin B, Lillo P, Hornberger M, Piguet O, Dawson K, et al. 2009. Determinants of survival in behavioral variant frontotemporal dementia. *Neurology* 73: 1656-61

Goedert M, Spillantini MG, Jakes R, Rutherford D, Crowther RA. 1989. Multiple isoforms of human microtubule-associated protein tau: sequences and localization in neurofibrillary tangles of Alzheimer's disease. *Neuron* 3: 519-26

Goedert M, Wischik CM, Crowther RA, Walker JE, Klug A. 1988. Cloning and sequencing of the cDNA encoding a core protein of the paired helical filament of Alzheimer disease: identification as the microtubule-associated protein tau. *Proceedings of the National Academy of Sciences* 85: 4051-55

Goldman JS, Farmer JM, Wood EM, Johnson JK, Boxer A, et al. 2005. Comparison of family histories in FTLD subtypes and related tauopathies. *Neurology* 65: 1817-19

Good CD, Johnsrude IS, Ashburner J, Henson RNA, Friston KJ, Frackowiak RSJ. 2001. A Voxel-Based Morphometric Study of Ageing in 465 Normal Adult Human Brains. *NeuroImage* 14: 21-36

Gorno-Tempini ML, Dronkers NF, Rankin KP, Ogar JM, Phengrasamy L, et al. 2004. Cognition and anatomy in three variants of primary progressive aphasia. *Annals of Neurology* 55: 335-46

Gorno-Tempini ML, Hillis AE, Weintraub S, Kertesz A, Mendez M, et al. 2011. Classification of primary progressive aphasia and its variants. *Neurology* 76: 1006-14

Gorno-Tempini ML, Ogar JM, Brambati SM, Wang P, Jeong JH, et al. 2006. Anatomical correlates of early mutism in progressive nonfluent aphasia. *Neurology* 67: 1849-51

Grossman M, Mickanin J, Onishi K, Hughes E, D'Esposito M, et al. 1996. Progressive Nonfluent Aphasia: Language, Cognitive, and PET Measures Contrasted with Probable Alzheimer's Disease. *Journal of Cognitive Neuroscience* 8: 135-54

Grossman M, Powers J, Ash S, McMillan C, Burkholder L, et al. 2013. Disruption of large-scale neural networks in non-fluent/agrammatic variant primary progressive aphasia associated with frontotemporal degeneration pathology. *Brain and Language* 127: 106-20

Gydesen S, Brown JM, Brun A, Chakrabarti L, Gade A, et al. 2002. Chromosome 3 linked frontotemporal dementia (FTD-3). *Neurology* 59: 1585-94

Ha J. 2012. *Impaired white matter integrity and social cognition in high functioning autism spectrum disorders: A diffusion tensor imaging study*. Yonsei University, South Korea

Han Z, Ma Y, Gong G, He Y, Caramazza A, Bi Y. 2013. White matter structural connectivity underlying semantic processing: Evidence from brain damaged patients. *Brain*: doi: 10.1093/brain/awt205

Hodges JR, Davies RR, Xuereb JH, Casey B, Broe M, et al. 2004. Clinicopathological correlates in frontotemporal dementia. *Ann Neurol* 56: 399-406

Hodges JR, Patterson K. 1996. Nonfluent progressive aphasia and semantic dementia: A comparative neuropsychological study. *Journal of the International Neuropsychological Society* 2: 511-24

Hodges JR, Patterson K. 2007. Semantic dementia: a unique clinicopathological syndrome. *The Lancet Neurology* 6: 1004-14

Hodges JR, Patterson K, Oxbury S, Funnell E. 1992. Semantic dementia: Progressive fluent aphasia with temporal lobe atrophy. *Brain* 115: 1783-806

Hornberger M, Savage S, Hsieh S, Mioshi E, Piguet O, Hodges JR. 2010. Orbitofrontal Dysfunction Discriminates Behavioral Variant Frontotemporal Dementia from Alzheimer's Disease. *Dementia and Geriatric Cognitive Disorders* 30: 547-52

Hornberger M, Shelley BP, Kipps CM, Piguet O, Hodges JR. 2009. Can progressive and non-progressive behavioural variant frontotemporal dementia be distinguished at presentation? *Journal of Neurology, Neurosurgery & Psychiatry* 80: 591-93

Hsiung G-YR, DeJesus-Hernandez M, Feldman HH, Sengdy P, Bouchard-Kerr P, et al. 2012. Clinical and pathological features of familial frontotemporal dementia caused by C9ORF72 mutation on chromosome 9p. *Brain* 135: 709-22

Hutton M, Lendon CL, Rizzu P, Baker M, Froelich S, et al. 1998. Association of missense and 5[prime]-splice-site mutations in tau with the inherited dementia FTDP-17. *Nature* 393: 702-05

Jbabdi S, Behrens TEJ, Smith SM. 2010. Crossing fibres in tract-based spatial
    statistics. *NeuroImage* 49: 249-56

Jenkinson M, Beckmann CF, Behrens TEJ, Woolrich MW, Smith SM. 2012.
    FSL. *NeuroImage* 62: 782-90

Josephs KA, Boeve BF, Duffy JR, Smith GE, Knopman DS, et al. 2005. Atypical
    progressive supranuclear palsy underlying progressive apraxia of speech
    and nonfluent aphasia. *Neurocase* 11: 283-96

Josephs KA, Duffy JR, Strand EA, Whitwell JL, Layton KF, et al. 2006a.
    Clinicopathological and imaging correlates of progressive aphasia and
    apraxia of speech. *Brain* 129: 1385-98

Josephs KA, Petersen RC, Knopman DS, Boeve BF, Whitwell JL, et al. 2006b.
    Clinicopathologic analysis of frontotemporal and corticobasal
    degenerations and PSP. *Neurology* 66: 41-48

Josephs KA, Whitwell JL, Murray ME, Parisi JE, Graff-Radford NR, et al. 2013.
    Corticospinal tract degeneration associated with TDP-43 type C
    pathology and semantic dementia. *Brain* 136: 455-70

Kaivorinne AL, Bode MK, Paavola L, Tuominen H, Kallio M, et al. 2013. Clinical
    Characteristics of C9ORF72-Linked Frontotemporal Lobar Degeneration.
    Dementia and Geriatric Cognitive Disorders Extra 3: 251-62

Kertesz A, Martinez-Lage P, Davidson W, Munoz DG. 2000. The corticobasal
    degeneration syndrome overlaps progressive aphasia and frontotemporal
    dementia. *Neurology* 55: 1368-75

Kertesz A, McMonagle P, Blair M, Davidson W, Munoz DG. 2005. The evolution
    and pathology of frontotemporal dementia. *Brain* 128: 1996-2005

Khan BK, Yokoyama JS, Takada LT, Sha SJ, Rutherford NJ, et al. 2012. Atypical, slowly progressive behavioural variant frontotemporal dementia associated with C9ORF72 hexanucleotide expansion. *Journal of Neurology, Neurosurgery & Psychiatry* 83: 358-64

Kim JW, Lee DY, Choo ILH, Seo EH, Kim SG, et al. 2011. Microstructural Alteration of the Anterior Cingulum is Associated With Apathy in Alzheimer Disease. *The American Journal of Geriatric Psychiatry* 19: 644-53

Kipps CM, Davies RR, Mitchell J, Kril JJ, Halliday GM, Hodges JR. 2007. Clinical Significance of Lobar Atrophy in Frontotemporal Dementia: Application of an MRI Visual Rating Scale. *Dementia and Geriatric Cognitive Disorders* 23: 334-42

Kipps CM, Hodges JR, Hornberger M. 2010. Nonprogressive behavioural frontotemporal dementia: recent developments and clinical implications of the 'bvFTD phenocopy syndrome'. *Current Opinion in Neurology* 23: 628-32 10.1097/wco.0b013e3283404309

Kipps CM, Nestor PJ, Dawson CE, Mitchell J, Hodges JR. 2008. Measuring progression in frontotemporal dementia: Implications for therapeutic interventions. *Neurology* 70: 2046-52

Kitagaki H, Mori E, Hirono N, Ikejiri Y, Ishii K, et al. 1997. Alteration of white matter MR signal intensity in frontotemporal dementia. *AJNR Am J Neuroradiol* 18: 367-78

Knibb JA, Xuereb JH, Patterson K, Hodges JR. 2006. Clinical and pathological characterization of progressive aphasia. *Annals of Neurology* 59: 156-65

Kril J, Halliday G. 2011. Pathological Staging of Frontotemporal Lobar Degeneration. *Journal of Molecular Neuroscience* 45: 379-83

Kril JJ, Halliday GM. 2004. Clinicopathological Staging of Frontotemporal Dementia Severity: Correlation with Regional Atrophy. *Dementia and Geriatric Cognitive Disorders* 17: 311-15

Kumar A, Sundaram SK, Sivaswamy L, Behen ME, Makki MI, et al. 2010. Alterations in Frontal Lobe Tracts and Corpus Callosum in Young Children with Autism Spectrum Disorder. *Cerebral Cortex* 20: 2103-13

Kumfor F, Miller L, Lah S, Hsieh S, Savage S, et al. 2011. Are you really angry? The effect of intensity on facial emotion recognition in frontotemporal dementia. *Social Neuroscience* 6: 502-14

Le Ber I, Camuzat A, Hannequin D, Pasquier F, Guedj E, et al. 2008. Phenotype variability in progranulin mutation carriers: a clinical, neuropsychological, imaging and genetic study. *Brain* 131: 732-46

Le Bihan D. 1995. Molecular diffusion, tissue microdynamics and microstructure. *NMR in Biomedicine* 8: 375-86

Le Bihan D, Mangin J-F, Poupon C, Clark CA, Pappata S, et al. 2001. Diffusion tensor imaging: Concepts and applications. *Journal of Magnetic Resonance Imaging* 13: 534-46

Lee SE, Seeley WW, Poorzand P, Rademakers R, Karydas A, et al. 2011. Clinical characterization of bvFTD due to FUS neuropathology. *Neurocase*: 1-13

Lerch JP, Evans AC. 2005. Cortical thickness analysis examined through power analysis and a population simulation. *NeuroImage* 24: 163-73

Lillo P, Mioshi E, Burrell JR, Kiernan MC, Hodges JR, Hornberger M. 2012. Grey and White Matter Changes across the Amyotrophic Lateral Sclerosis-Frontotemporal Dementia Continuum. *PLoS ONE* 7: e43993

Lillo P, Mioshi E, Zoing MC, Kiernan MC, Hodges JR. 2011. How common are behavioural changes in amyotrophic lateral sclerosis? *Amyotrophic Lateral Sclerosis* 12: 45-51

Litvan I, Agid Y, Calne D, Campbell G, Dubois B, et al. 1996. Clinical research criteria for the diagnosis of progressive supranuclear palsy (Steele-Richardson-Olszewski syndrome): Report of the NINDS-SPSP International Workshop*. *Neurology* 47: 1-9

Mackenzie I, Neumann M, Bigio E, Cairns N, Alafuzoff I, et al. 2010a. Nomenclature and nosology for neuropathologic subtypes of frontotemporal lobar degeneration: an update. *Acta Neuropathologica* 119: 1-4

Mackenzie IA, Munoz D, Kusaka H, Yokota O, Ishihara K, et al. 2011a. Distinct pathological subtypes of FTLD-FUS. *Acta Neuropathologica* 121: 207-18

Mackenzie IA, Neumann M, Baborie A, Sampathu D, Plessis D, et al. 2011b. A harmonized classification system for FTLD-TDP pathology. *Acta Neuropathologica* 122: 111-13

Mackenzie IRA, Rademakers R, Neumann M. 2010b. TDP-43 and FUS in amyotrophic lateral sclerosis and frontotemporal dementia. *The Lancet Neurology* 9: 995-1007

Mahoney C, Downey L, Ridgway G, Beck J, Clegg S, et al. 2012a. Longitudinal neuroimaging and neuropsychological profiles of frontotemporal

dementia with C9ORF72 expansions. *Alzheimer's Research & Therapy* 4: 41

Mahoney CJ, Beck J, Rohrer JD, Lashley T, Mok K, et al. 2012b. Frontotemporal dementia with the C9ORF72 hexanucleotide repeat expansion: clinical, neuroanatomical and neuropathological features. *Brain* 135: 736-50

Mahoney CJ, Malone IB, Ridgway GR, Buckley AH, Downey LE, et al. 2013. White matter tract signatures of the progressive aphasias. *Neurobiology of Aging* 34: 1687-99

Mahoney CJ, Ridgway GR, Malone IB, Downey LE, Beck J, et al. 2014. Profiles of white matter tract pathology in frontotemporal dementia. *Human Brain Mapping*: doi: 10.1002/hbm.22468

Majounie E, Renton AE, Mok K, Dopper EGP, Waite A, et al. 2012. Frequency of the C9orf72 hexanucleotide repeat expansion in patients with amyotrophic lateral sclerosis and frontotemporal dementia: a cross-sectional study. *The Lancet Neurology* 11: 323-30

Mamah D, Conturo TE, Harms MP, Akbudak E, Wang L, et al. 2010. Anterior thalamic radiation integrity in schizophrenia: A diffusion-tensor imaging study. *Psychiatry Research: Neuroimaging* 183: 144-50

Mandonnet E, Nouet A, Gatignol P, Capelle L, Duffau H. 2007. Does the left inferior longitudinal fasciculus play a role in language? A brain stimulation study. *Brain* 130: 623-29

Matsuo K, Mizuno T, Yamada K, Akazawa K, Kasai T, et al. 2008. Cerebral white matter damage in frontotemporal dementia assessed by diffusion tensor tractography. *Neuroradiology* 50: 605-11

Mesulam M, Wicklund A, Johnson N, Rogalski E, Léger GC, et al. 2008.
Alzheimer and frontotemporal pathology in subsets of primary
progressive aphasia. *Annals of Neurology* 63: 709-19

Meyers JE, Meyers KR. 1995. Rey Complex FigureTest and Recognition Trial:
Professional manual. Odessa, FL: Psychological Assessment Resources.

Mioshi E, Dawson K, Mitchell J, Arnold R, Hodges JR. 2006. The
Addenbrooke's Cognitive Examination Revised (ACE-R): a brief cognitive
test battery for dementia screening. *Int J Geriatr Psych* 21: 1078-85

Mori S, Frederiksen K, van Zijl PCM, Stieltjes B, Kraut MA, et al. 2002. Brain
white matter anatomy of tumor patients evaluated with diffusion tensor
imaging. *Annals of Neurology* 51: 377-80

Mori S, Oishi K, Jiang H, Jiang L, Li X, et al. 2008. Stereotaxic white matter
atlas based on diffusion tensor imaging in an ICBM template.
NeuroImage 40: 570-82

Morris JC. 1997. Clinical Dementia Rating: A Reliable and Valid Diagnostic and
Staging Measure for Dementia of the Alzheimer Type. *International
Psychogeriatrics* 9: 173-76

Mountcastle VB, Lynch JC, Georgopoulos A, Sakata H, Acuna C. 1975. Posterior
parietal association cortex of the monkey: command functions for
operations within extrapersonal space. *Journal of Neurophysiology* 38:
871-908

Munoz DG, Ros R, Fatas M, Bermejo F, de Yebenes JG. 2007. Progressive
Nonfluent Aphasia Associated With a New Mutation V363I in Tau Gene.

American Journal of Alzheimer's Disease and Other Dementias 22: 294-99

Murphy JM, Henry RG, Langmore S, Kramer JH, Miller BL, Lomen-Hoerth C. 2007. Continuum of frontal lobe impairment in amyotrophic lateral sclerosis. *Archives of Neurology* 64: 530-34

Nagy Z, Weiskopf N, Alexander D.C., Deichmann R. 2007. A method for improving the performance of gradient systems for diffusion-weighted MRI. *Magnetic Resonance in Medicine* 58: 763-68

Neary D, Snowden JS, Gustafson L, Passant U, Stuss D, et al. 1998. Frontotemporal lobar degeneration: A consensus on clinical diagnostic criteria. *Neurology* 51: 1546-54

Neumann M, Kwong L, Lee E, Kremmer E, Flatley A, et al. 2009a. Phosphorylation of S409/410 of TDP-43 is a consistent feature in all sporadic and familial forms of TDP-43 proteinopathies. *Acta Neuropathologica* 117: 137-49

Neumann M, Kwong LK, Truax AC, Vanmassenhove B, et al. 2007. TDP-43-Positive White Matter Pathology in Frontotemporal Lobar Degeneration With Ubiquitin-Positive Inclusions. *Journal of Neuropathology and Experimental Neurology* 66: 177-83

Neumann M, Rademakers R, Roeber S, Baker M, Kretzschmar HA, Mackenzie IRA. 2009b. A new subtype of frontotemporal lobar degeneration with FUS pathology. *Brain* 132: 2922-31

O'Sullivan M, Jones DK, Summers PE, Morris RG, Williams SCR, Markus HS. 2001. Evidence for cortical "disconnection" as a mechanism of age-related cognitive decline. *Neurology* 57: 632-38

Oishi K, Zilles K, Amunts K, Faria A, Jiang H, et al. 2008. Human brain white matter atlas: Identification and assignment of common anatomical structures in superficial white matter. *NeuroImage* 43: 447-57

Onyike CU. 2011. What Is the Life Expectancy in Frontotemporal Lobar Degeneration? *Neuroepidemiology* 37: 166-67

Orrison WW. 2008. Atlas of brain function. New York: Thieme Medical Publishers

Ortibus ELS, Verhoeven J, Sunaert S, Casteels I, De Cock P, Lagae L. 2012. Integrity of the inferior longitudinal fasciculus and impaired object recognition in children: a diffusion tensor imaging study. *Developmental Medicine & Child Neurology* 54: 38-43

Papagno C, Miracapillo C, Casarotti A, Romero Lauro LJ, Castellano A, et al. 2011. What is the role of the uncinate fasciculus? Surgical removal and proper name retrieval. *Brain* 134: 405-14

Pesiridis GS, Lee VM-Y, Trojanowski JQ. 2009. Mutations in TDP-43 link glycine-rich domain functions to amyotrophic lateral sclerosis. *Human Molecular Genetics* 18: 156-62

Philips T, Robberecht W. 2011. Neuroinflammation in amyotrophic lateral sclerosis: role of glial activation in motor neuron disease. *The Lancet Neurology* 10: 253-63

Pick A. 1892. Über die Beziehungen der senilen Hirnatrophie zur Aphasie. *Prager Medizinische Wochenschrift* 17: 165-7

Pierpaoli C, Barnett A, Pajevic S, Chen R, Penix L, et al. 2001. Water Diffusion Changes in Wallerian Degeneration and Their Dependence on White Matter Architecture. *NeuroImage* 13: 1174-85

Piguet O, Hornberger M, Mioshi E, Hodges JR. 2011. Behavioural-variant frontotemporal dementia: diagnosis, clinical staging, and management. *The Lancet Neurology* 10: 162-72

Piguet O, Hornberger M, Shelley BP, Kipps CM, Hodges JR. 2009. Sensitivity of current criteria for the diagnosis of behavioral variant frontotemporal dementia. *Neurology* 72: 732-37

Raffelt D, Tournier JD, Rose S, Ridgway GR, Henderson R, et al. 2012. Apparent Fibre Density: A novel measure for the analysis of diffusion-weighted magnetic resonance images. *NeuroImage* 59: 3976-94

Rascovsky K, Hodges JR, Knopman D, Mendez MF, Kramer JH, et al. 2011. Sensitivity of revised diagnostic criteria for the behavioural variant of frontotemporal dementia. *Brain* 134: 2456-77

Ratnavalli E, Brayne C, Dawson K, Hodges JR. 2002. The prevalence of frontotemporal dementia. *Neurology* 58: 1615-21

Rebeiz JJ, Kolodny EH, Richardson EP, Jr. 1968. Corticodentatonigral degeneration with neuronal achromasia. *Archives of Neurology* 18: 20-33

Reitan RM, Wolfson D. 1985. The Halstead–Reitan Neuropsycholgical Test

Battery: Therapy and clinical interpretation. Tucson, Arizona:

Neuropsychological Press

Renton Alan E, Majounie E, Waite A, Simón-Sánchez J, Rollinson S, et al. 2011.

A Hexanucleotide Repeat Expansion in C9ORF72 Is the Cause of

Chromosome 9p21-Linked ALS-FTD. *Neuron* 72: 257-68

Ringholz GM, Appel SH, Bradshaw M, Cooke NA, Mosnik DM, Schulz PE. 2005.

Prevalence and patterns of cognitive impairment in sporadic ALS.

Neurology 65: 586-90

Rogalski E, Cobia D, Harrison TM, Wieneke C, Thompson CK, et al. 2011.

Anatomy of Language Impairments in Primary Progressive Aphasia. *The

Journal of Neuroscience* 31: 3344-50

Rohrer JD, Guerreiro R, Vandrovcova J, Uphill J, Reiman D, et al. 2009a. The

heritability and genetics of frontotemporal lobar degeneration.

Neurology 73: 1451-56

Rohrer JD, Lashley T, Schott JM, Warren JE, Mead S, et al. 2011. Clinical and

neuroanatomical signatures of tissue pathology in frontotemporal lobar

degeneration. *Brain* 134: 2565-81

Rohrer JD, Paviour D, Bronstein AM, O'Sullivan SS, Lees A, Warren JD. 2010.

Progressive supranuclear palsy syndrome presenting as progressive

nonfluent aphasia: A neuropsychological and neuroimaging analysis.

Movement Disorders 25: 179-88

Rohrer JD, Rosen HJ. 2013. Neuroimaging in frontotemporal dementia.

International Review of Psychiatry 25: 221-29

Rohrer JD, Warren JD, Modat M, Ridgway GR, Douiri A, et al. 2009b. Patterns

    of cortical thinning in the language variants of frontotemporal lobar

    degeneration. *Neurology* 72: 1562-69

Rosen HJ, Gorno–Tempini ML, Goldman WP, Perry RJ, Schuff N, et al. 2002.

    Patterns of brain atrophy in frontotemporal dementia and semantic

    dementia. *Neurology* 58: 198-208

Rosenbloom MAM, Sullivan EV, Pfefferbaum A. 2003. Using Magnetic

    Resonance Imaging and Diffusion Tensor Imaging to Assess Brain

    Damage in Alcoholics. *Alcohol Res Health.* 27: 146-52

Rosso SM, Kaat LD, Baks T, Joosse M, de Koning I, et al. 2003. Frontotemporal

    dementia in The Netherlands: patient characteristics and prevalence

    estimates from a population-based study. *Brain* 126: 2016-22

Salat DH, Tuch DS, Greve DN, van der Kouwe AJW, Hevelone ND, et al. 2005.

    Age-related alterations in white matter microstructure measured by

    diffusion tensor imaging. *Neurobiology of Aging* 26: 1215-27

Savage S, Hsieh S, Leslie F, Foxe D, Piguet O, Hodges JR. 2013. Distinguishing

    Subtypes in Primary Progressive Aphasia: Application of the Sydney

    Language Battery. *Dementia and Geriatric Cognitive Disorders* 35: 208-

    18

Schermuly I, Fellgiebel A, Wagner S, Yakushev I, Stoeter P, et al. 2010.

    Association between cingulum bundle structure and cognitive

    performance: An observational study in major depression. *European*

    Psychiatry 25: 355-60

Schroeter ML, Raczka K, Neumann J, von Cramon DY. 2008. Neural networks
in frontotemporal dementia—A meta-analysis. *Neurobiology of Aging*
29: 418-26

Schroeter ML, Raczka K, Neumann J, Yves von Cramon D. 2007. Towards a
nosology for frontotemporal lobar degenerations--A meta-analysis
involving 267 subjects. *NeuroImage* 36: 497-510

Schwindt GC, Graham NL, Rochon E, Tang-Wai DF, Lobaugh NJ, et al. 2013.
Whole-brain white matter disruption in semantic and nonfluent variants
of primary progressive aphasia. *Human Brain Mapping* 34: 973-84

Seelaar H, Kamphorst W, Rosso SM, Azmani A, Masdjedi R, et al. 2008.
Distinct genetic forms of frontotemporal dementia. *Neurology* 71: 1220-
26

Seeley WW, Crawford R, Rascovsky K, Kramer JH, Weiner M, et al. 2008.
Frontal Paralimbic Network Atrophy in Very Mild Behavioral Variant
Frontotemporal Dementia. *Arch Neurol* 65: 249-55

Sha SJ, Takada LT, Rankin KP, Yokoyama JS, Rutherford NJ, et al. 2012.
Frontotemporal dementia due to C9ORF72 mutations: Clinical and
imaging features. *Neurology* 79: 1002-11

Siegel A, Sapru HN. 2010. Essential Neuroscience. Baltimore, Maryland:
Lippincott Williams & Wilkins

Sierra A, Laitinen T, Lehtimäki K, Rieppo L, Pitkänen A, Gröhn O. 2011.
Diffusion tensor MRI with tract-based spatial statistics and histology
reveals undiscovered lesioned areas in kainate model of epilepsy in rat.
Brain Structure and Function 216: 123-35

Simón-Sánchez J, Dopper EGP, Cohn-Hokke PE, Hukema RK, Nicolaou N, et al. 2012. The clinical and pathological phenotype of C9ORF72 hexanucleotide repeat expansions. *Brain* 135: 723-35

Skibinski G, Parkinson NJ, Brown JM, Chakrabarti L, Lloyd SL, et al. 2005. Mutations in the endosomal ESCRTIII-complex subunit CHMP2B in frontotemporal dementia. *Nat Genet* 37: 806-08

Smith SM. 2002. Fast robust automated brain extraction. *Human Brain Mapping* 17: 143-55

Smith SM, Jenkinson M, Johansen-Berg H, Rueckert D, Nichols TE, et al. 2006. Tract-based spatial statistics: Voxelwise analysis of multi-subject diffusion data. *NeuroImage* 31: 1487-505

Smith SM, Jenkinson M, Woolrich MW, Beckmann CF, Behrens TEJ, et al. 2004. Advances in functional and structural MR image analysis and implementation as FSL. *NeuroImage* 23, Supplement 1: S208-S19

Snowden JS, Pickering-Brown SM, Mackenzie IR, Richardson AMT, Varma A, et al. 2006. Progranulin gene mutations associated with frontotemporal dementia and progressive non-fluent aphasia. *Brain* 129: 3091-102

Snowden JS, Rollinson S, Thompson JC, Harris JM, Stopford CL, et al. 2012. Distinct clinical and pathological characteristics of frontotemporal dementia associated with C9ORF72 mutations. *Brain* 135: 693-708

Song S-K, Sun S-W, Ju W-K, Lin S-J, Cross AH, Neufeld AH. 2003. Diffusion tensor imaging detects and differentiates axon and myelin degeneration in mouse optic nerve after retinal ischemia. *NeuroImage* 20: 1714-22

Song S-K, Sun S-W, Ramsbottom MJ, Chang C, Russell J, Cross AH. 2002. Dysmyelination Revealed through MRI as Increased Radial (but Unchanged Axial) Diffusion of Water. *NeuroImage* 17: 1429-36

Spillantini MG, Goedert M. 1998. Tau protein pathology in neurodegenerative diseases. *Trends in Neurosciences* 21: 428-33

Stejskal EO, Tanner JE. 1965. Spin Diffusion Measurements: Spin Echoes in the Presence of a Time-Dependent Field Gradient. *The Journal of Chemical Physics* 42: 288-92

Sun S-W, Liang H-F, Trinkaus K, Cross AH, Armstrong RC, Song S-K. 2006. Noninvasive detection of cuprizone induced axonal damage and demyelination in the mouse corpus callosum. *Magnetic Resonance in Medicine* 55: 302-08

Suzuki M, Lee H-C, Kayasuga Y, Chiba S, Nedachi T, et al. 2009. Roles of Progranulin in Sexual Differentiation of the Developing Brain and Adult Neurogenesis. *Journal of Reproduction and Development* 55: 351-55

Tanner JE, Stejskal EO. 1968. Restricted Self-Diffusion of Protons in Colloidal Systems by the Pulsed-Gradient, Spin-Echo Method. *The Journal of Chemical Physics* 49: 1768-77

Teipel SJ, Meindl T, Wagner M, Stieltjes B, Reuter S, et al. 2010. Longitudinal Changes in Fiber Tract Integrity in Healthy Aging and Mild Cognitive Impairment: A DTI Follow-Up Study. *Journal of Alzheimer's Disease* 22: 507-22

Torrey HC. 1956. Bloch equations with diffusion terms. *Phys Rev* 104: 563-65

Tuch DS, Reese TG, Wiegell MR, Makris N, Belliveau JW, Wedeen VJ. 2002.
High angular resolution diffusion imaging reveals intravoxel white
matter fiber heterogeneity. *Magnetic Resonance in Medicine* 48: 577-82

Van Damme P, Van Hoecke A, Lambrechts D, Vanacker P, Bogaert E, et al.
2008. Progranulin functions as a neurotrophic factor to regulate neurite
outgrowth and enhance neuronal survival. *The Journal of Cell Biology*
181: 37-41

Van Langenhove T, van der Zee J, Gijselinck I, et al. 2013. DIstinct clinical
characteristics of c9orf72 expansion carriers compared with grn, mapt,
and nonmutation carriers in a flanders-belgian ftld cohort. *JAMA
Neurology* 70: 365-73

Vitali P, Migliaccio R, Agosta F, Rosen HJ, Geschwind MD. 2008.
Neuroimaging in Dementia. *Semin Neurol* 28: 467-83

Von Der Heide RJ, Skipper LM, Klobusicky E, Olson IR. 2013. Dissecting the
uncinate fasciculus: disorders, controversies and a hypothesis. *Brain* 136:
1692-707

Warach S, Chien D, Li W, Ronthal M, RR. E. 1992. Fast magnetic resonance
diffusion-weighted imaging of acute human stroke. *Neurology* 42: 1717-
23

Watson PE, Watson ID, Batt RD. 1980. Total body water volumes for adult
males and females estimated from simple anthropometric
measurements. *The American Journal of Clinical Nutrition* 33: 27-39

Watts GDJ, Wymer J, Kovach MJ, Mehta SG, Mumm S, et al. 2004. Inclusion
body myopathy associated with Paget disease of bone and frontotemporal

dementia is caused by mutant valosin-containing protein. *Nat Genet* 36: 337-81

Wear HJ, Wedderburn CJ, Mioshi E, Williams-Gray CH, Mason SL, et al. 2008. The Cambridge Behavioural Inventory revised. *Dement. Neuropsychol.* 2: 102-07

Weaver KE, Richards TL, Liang O, Laurino MY, Samii A, Aylward EH. 2009. Longitudinal diffusion tensor imaging in Huntington's Disease. *Experimental Neurology* 216: 525-29

Wechsler D. 1997. WAIS-III: Administration and scoring manual : Wechsler adult intelligence scale--third edition. San Antonio, Texas: The Psychological Corporation

Whitwell JL, Avula R, Senjem ML, Kantarci K, Weigand SD, et al. 2010. Gray and white matter water diffusion in the syndromic variants of frontotemporal dementia. *Neurology* 74: 1279-87

Whitwell JL, Weigand SD, Boeve BF, Senjem ML, Gunter JL, et al. 2012. Neuroimaging signatures of frontotemporal dementia genetics: C9ORF72, tau, progranulin and sporadics. *Brain* 135: 794-806

Winston GP. 2012. The physical and biological basis of quantitative parameters derived from diffusion MRI. *Quantitative Imaging in Medicine and Surgery* 2: 254-65

Zhang Y, Brady M, Smith S. 2001. Segmentation of brain MR images through a hidden Markov random field model and the expectation-maximization algorithm. *Medical Imaging, IEEE Transactions on* 20: 45-57

Zhang Y, Schuff N, Du A-T, Rosen HJ, Kramer JH, et al. 2009. White matter damage in frontotemporal dementia and Alzheimer's disease measured by diffusion MRI. *Brain* 132: 2579-92

Zhang Y, Tartaglia MC, Schuff N, Chiang GC, Ching C, et al. 2013. MRI Signatures of Brain Macrostructural Atrophy and Microstructural Degradation in Frontotemporal Lobar Degeneration Subtypes. *Journal of Alzheimer's Disease* 33: 431-44

APPENDICES

Figure has been removed due to Copyright restrictions.

Appendix 2.3.1
Door test (Part A) is a visual recognition test in which participants were given pictures of different doors to look at and were then asked to point out the door which was shown previously in the test phase.

Figure has been removed due to Copyright restrictions.

Appendix 2.3.4

The above shows the example items of the Sydney Language Battery word comprehension and semantic association tasks. Left figure shows comprehension item for "cigarette" with visually and semantically related foils. Right figure shows semantic item for "bicycle" with visually and semantically related foils.

Appendix Table 3.2 Fractional anisotropy changes in FTD at baseline (Mean ± SD).

Tracts	Controls			bvFTD				nfv-PPA				sv-PPA			
Ant thal rad L	.42	±	.02	.42	±	.03		.43	±	.02		.44	±	.03	
Ant thal rad R	.43	±	.03	.40	±	.03	*	.42	±	.03	*	.43	±	.03	
Anterior cingulum L	.45	±	.04	.40	±	.04	*	.44	±	.04		.45	±	.03	
Anterior cingulum R	.42	±	.04	.38	±	.03	*	.41	±	.05		.43	±	.02	
Posterior cingulum L	.42	±	.06	.37	±	.05	*	.41	±	.05		.36	±	.06	*
Posterior cingulum R	.45	±	.06	.40	±	.04	*	.46	±	.05		.43	±	.04	
Splenium of CC	.62	±	.03	.58	±	.06	*	.60	±	.05		.61	±	.03	
Genu of CC	.51	±	.03	.41	±	.06	***	.50	±	.04		.52	±	.03	
SLF (superior-inferior) L	.44	±	.03	.41	±	.04	*	.39	±	.05	*	.44	±	.03	
SLF (superior-inferior) R	.45	±	.03	.42	±	.04		.44	±	.04		.47	±	.04	
SLF (temporal) L	.45	±	.02	.42	±	.03	*	.42	±	.04	*	.45	±	.02	
SLF (temporal) R	.47	±	.03	.44	±	.04	*	.46	±	.03		.48	±	.03	
IFOF L	.45	±	.03	.41	±	.03	*	.43	±	.03		.44	±	.03	
IFOF R	.46	±	.03	.41	±	.03	**	.44	±	.04		.47	±	.03	
ILF L	.44	±	.03	.41	±	.03	*	.42	±	.04		.43	±	.02	
ILF R	.47	±	.03	.43	±	.03	*	.46	±	.04		.47	±	.02	
UF L	.39	±	.03	.34	±	.05	*	.37	±	.03		.37	±	.03	
UF R	.41	±	.03	.34	±	.04	***	.40	±	.02		.40	±	.03	
CST L	.55	±	.02	.53	±	.03		.55	±	.03		.54	±	.02	
CST R	.58	±	.02	.57	±	.03		.59	±	.03		.58	±	.02	

Asterisks show significant changes of white matter tracts in FTD subtypes (bvFTD, nfv-PPA and sv-PPA) relative to control. * p < 0.05, ** p < 0.01; *** p < 0.001. Abbreviations: FA = fractional anisotropy; MD = mean diffusivity; AxialD = axial diffusivity; RadialD = radial diffusivity; SD = standard deviation; CC = corpus callosum; SLF = superior longitudinal fasciculus; IFOF = inferior fronto-occipital fasciculus; ILF = inferior longitudinal fasciculus; UF = uncinate fasciculus; CST = corticospinal tract; L = left; R = right.

Appendix Table 3.3 Mean diffusivity (MD x 10³mm²s⁻¹) changes in FTD at baseline (Mean ± SD).

Tracts	Controls			bvFTD				nfv-PPA				sv-PPA			
Ant thal rad L	.77	±	.03	.84	±	.08	*	.77	±	.04		.75	±	.04	
Ant thal rad R	.77	±	.04	.88	±	.08	***	.80	±	.05		.75	±	.04	
Anterior cingulum L	.83	±	.05	.89	±	.07	*	.84	±	.04		.83	±	.04	
Anterior cingulum R	.85	±	.06	.89	±	.08	*	.86	±	.04		.83	±	.03	
Posterior cingulum L	.77	±	.06	.86	±	.08	*	.79	±	.03		.90	±	.10	***
Posterior cingulum R	.76	±	.05	.84	±	.08	*	.74	±	.09		.79	±	.06	
Splenium of CC	.81	±	.03	.85	±	.06	*	.82	±	.05		.82	±	.02	
Genu of CC	.81	±	.06	.98	±	.14	***	.83	±	.05		.79	±	.05	
SLF (superior-inferior) L	.77	±	.04	.80	±	.04	*	.82	±	.07	*	.77	±	.04	
SLF (superior-inferior) R	.75	±	.03	.79	±	.06	*	.77	±	.05		.74	±	.03	
SLF (temporal) L	.77	±	.03	.81	±	.04	*	.81	±	.05	*	.80	±	.03	
SLF (temporal) R	.75	±	.02	.79	±	.05	*	.76	±	.04		.74	±	.03	
IFOF L	.84	±	.04	.92	±	.10	*	.85	±	.03		.87	±	.04	*
IFOF R	.81	±	.04	.88	±	.05	**	.82	±	.05		.81	±	.03	
ILF L	.83	±	.04	.87	±	.05	*	.85	±	.04		.94	±	.06	***
ILF R	.79	±	.04	.83	±	.06	*	.79	±	.04		.81	±	.03	
UF L	.83	±	.04	.98	±	.19	*	.85	±	.03		.92	±	.07	***
UF R	.81	±	.04	.94	±	.10	***	.82	±	.03		.85	±	.06	*
CST L	.75	±	.03	.79	±	.03	**	.77	±	.02	*	.77	±	.02	*
CST R	.73	±	.02	.76	±	.03	***	.75	±	.02	*	.75	±	.02	*

*Asterisks show significant changes of white matter tracts in FTD subtypes (bvFTD, nfv-PPA and sv-PPA) relative to control. * p < 0.05, ** p < 0.01; *** p < 0.001. Abbreviations: FA = fractional anisotropy; MD = mean diffusivity; AxialD = axial diffusivity; RadialD = radial diffusivity; SD = standard deviation; CC = corpus callosum; SLF = superior longitudinal fasciculus; IFOF = inferior fronto-occipital fasciculus; ILF = inferior longitudinal fasciculus; UF = uncinate fasciculus; CST = corticospinal tract; L = left; R = right.*

Appendix Table 3.4 Axial diffusivity (AxialD x 10³mm²s⁻¹) changes in FTD at baseline (Mean ± SD).

Tracts	Controls	bvFTD	nfv-PPA	sv-PPA
Ant thal rad L	1.15 ± .03	1.24 ± .08 **	1.16 ± .05	1.13 ± .03
Ant thal rad R	1.15 ± .04	1.26 ± .09 **	1.18 ± .06	1.13 ± .04 *
Anterior cingulum L	1.28 ± .07	1.30 ± .07	1.28 ± .04	1.28 ± .05
Anterior cingulum R	1.27 ± .09	1.28 ± .09	1.27 ± .07	1.24 ± .04
Posterior cingulum L	1.14 ± .08	1.21 ± .09 *	1.16 ± .07	1.25 ± .09 *
Posterior cingulum R	1.14 ± .07	1.21 ± .09 *	1.13 ± .14	1.15 ± .08
Splenium of CC	1.49 ± .04	1.50 ± .05	1.48 ± .05	1.50 ± .03
Genu of CC	1.34 ± .08	1.47 ± .12 *	1.35 ± .06	1.32 ± .04
SLF (superior-inferior) L	1.16 ± .06	1.18 ± .04	1.18 ± .07	1.17 ± .05
SLF (superior-inferior) R	1.14 ± .06	1.18 ± .06	1.17 ± .04	1.17 ± .03
SLF (temporal) L	1.18 ± .05	1.19 ± .05	1.20 ± .05	1.21 ± .04
SLF (temporal) R	1.17 ± .04	1.20 ± .05	1.18 ± .04	1.17 ± .03
IFOF L	1.28 ± .05	1.34 ± .09 *	1.27 ± .02	1.30 ± .04 *
IFOF R	1.25 ± .04	1.30 ± .05 *	1.24 ± .05	1.25 ± .03
ILF L	1.27 ± .05	1.29 ± .06	1.27 ± .04	1.40 ± .07 ***
ILF R	1.24 ± .05	1.25 ± .07	1.21 ± .04	1.27 ± .04
UF L	1.20 ± .05	1.34 ± .18 *	1.21 ± .03	1.29 ± .07 ***
UF R	1.19 ± .05	1.30 ± .09 **	1.21 ± .04	1.24 ± .05 *
CST L	1.27 ± .04	1.31 ± .05	1.31 ± .04 *	1.30 ± .03
CST R	1.27 ± .04	1.32 ± .04 *	1.32 ± .03 **	1.29 ± .02

*Asterisks show significant changes of white matter tracts in FTD subtypes (bvFTD, nfv-PPA and sv-PPA) relative to control. * $p < 0.05$, ** $p < 0.01$; *** $p < 0.001$. Abbreviations: FA = fractional anisotropy; MD = mean diffusivity; AxialD = axial diffusivity; RadialD = radial diffusivity; SD = standard deviation; CC = corpus callosum; SLF = superior longitudinal fasciculus; IFOF = inferior fronto-occipital fasciculus; ILF = inferior longitudinal fasciculus; UF = uncinate fasciculus; CST = corticospinal tract; L = left; R = right.*

Appendix Table 3.5 Radial diffusivity (RadialD x 10³mm²s⁻¹) changes in FTD at baseline (Mean ± SD).

Tracts	Controls			bvFTD				nfv-PPA				sv-PPA			
Ant thal rad L	.58	±	.03	.65	±	.08	*	.58	±	.04		.56	±	.04	
Ant thal rad R	.58	±	.04	.69	±	.08	***	.60	±	.05	*	.57	±	.04	
Anterior cingulum L	.61	±	.05	.68	±	.07	*	.62	±	.06		.60	±	.05	
Anterior cingulum R	.64	±	.06	.70	±	.07	*	.65	±	.05		.62	±	.03	
Posterior cingulum L	.58	±	.06	.68	±	.08	*	.60	±	.04		.73	±	.11	***
Posterior cingulum R	.56	±	.06	.65	±	.08	*	.55	±	.08		.60	±	.06	
Splenium of CC	.47	±	.04	.52	±	.08	*	.49	±	.07		.48	±	.04	
Genu of CC	.55	±	.06	.74	±	.15	***	.57	±	.06		.53	±	.05	
SLF (superior-inferior) L	.57	±	.04	.62	±	.05	*	.64	±	.08	*	.58	±	.04	
SLF (superior-inferior) R	.55	±	.03	.60	±	.06	*	.58	±	.05		.53	±	.04	
SLF (temporal) L	.57	±	.03	.61	±	.05	*	.62	±	.06	*	.59	±	.03	
SLF (temporal) R	.54	±	.03	.58	±	.06	*	.55	±	.05		.53	±	.03	
IFOF L	.62	±	.05	.71	±	.10	*	.64	±	.04		.65	±	.04	
IFOF R	.59	±	.04	.67	±	.06	***	.60	±	.06		.58	±	.04	
ILF L	.61	±	.04	.67	±	.06	*	.64	±	.05		.71	±	.05	***
ILF R	.57	±	.04	.62	±	.06	*	.58	±	.05		.58	±	.03	
UF L	.64	±	.05	.80	±	.19	*	.66	±	.04		.73	±	.08	**
UF R	.61	±	.05	.76	±	.11	***	.62	±	.04		.66	±	.06	*
CST L	.49	±	.02	.53	±	.03	**	.50	±	.03		.51	±	.02	*
CST R	.45	±	.02	.49	±	.04	**	.46	±	.03		.47	±	.02	*

*Asterisks show significant changes of white matter tracts in FTD subtypes (bvFTD, nfv-PPA and sv-PPA) relative to control. * p < 0.05, ** p < 0.01; *** p < 0.001. Abbreviations: FA = fractional anisotropy; MD = mean diffusivity; AxialD = axial diffusivity; RadialD = radial diffusivity; SD = standard deviation; CC = corpus callosum; SLF = superior longitudinal fasciculus; IFOF = inferior fronto-occipital fasciculus; ILF = inferior longitudinal fasciculus; UF = uncinate fasciculus; CST = corticospinal tract; L = left; R = right.*

Appendix Table 3.6 Significant clusters of grey matter change in FTD subgroups.

	Side (L/R)	Voxels	MNI coordinates (X-Y-Z)			t-stats
bvFTD						
Superior frontal gyrus	R	1032	18	-12	80	1.85
Precentral gyrus	L	441	-26	-22	68	1.79
Temporal fusiform cortex	R	466430	30	-10	-52	3.45
Occipital pole	L	1336	-14	-104	-4	1.97
Lateral occipital cortex	L	212	-16	-64	72	1.80
Lateral occipital cortex	R	126	52	-78	4	1.73
nfv-PPA						
Frontal pole	R	567	10	64	2	1.98
Putamen	L	88988	-34	2	2	3.48
Thalamus	L	284	-18	-14	12	1.82
Supramarginal gyrus	L	7716	-60	-24	30	2.25
Temporal pole	R	154	38	16	-30	1.82
sv-PPA						
Frontal pole	R	939	24	50	-6	1.96
Temporal pole	R	39418	44	8	-20	3.47
Temporal fusiform cortex	L	140749	-28	-4	-52	3.47

All clusters were reported using threshold free cluster enhancement and corrected for multiple comparisons at p < 0.05. Abbreviations: L = left; R = right; MNI = Montreal Neurological Institute.

Appendix 5.7.8 Supplementary information

Clinical features of FTD with C9orf72 expansions

Neuropsychiatric features

The most prominent neuropsychiatric feature in *C9orf72* expansion carriers are apathy and disinhibition (Hsiung et al 2012, Kaivorinne et al 2013, Mahoney et al 2012b, Simón-Sánchez et al 2012, Van Langenhove et al 2013). Other features include depression (Mahoney et al 2012b) and anxiety (Kaivorinne et al 2013). The presence of psychotic features, including delusions and/or hallucinations, has also been reported in *C9orf72* expansion carriers (Boeve et al 2012, Devenney et al 2014, Kaivorinne et al 2013, Sha et al 2012, Snowden et al 2012). Variation in findings, however, exist as some studies demonstrated *C9orf72* expansion carriers with low frequency in psychotic symptoms (Hsiung et al 2012, Mahoney et al 2012b, Simón-Sánchez et al 2012).

Cognitive features

Behavioural changes, such as obsessive-compulsive behaviour or stereotyped behaviour, are also reported in *C9orf72* expansion carriers (Kaivorinne et al 2013, Simón-Sánchez et al 2012, Snowden et al 2012). Frequency of the reported behavioural change, however, also varied among studies. For example, eating behavioural changes were reported less common in *C9orf72* expansion carriers (Snowden et al 2012) while another study showed abnormal eating behaviour in all *C9orf72* expansion carriers (Boeve et al 2012).

One of the most common neuropsychological features in *C9orf72* expansion carriers is impairment in executive function (Boeve et al 2012, Hsiung et al 2012, Kaivorinne et al 2013, Mahoney et al 2012b, Snowden et al 2012). Other features include impairment in episodic memory (Mahoney et al 2012b), and reduced speed of processing (Boeve et al 2012). There are no deficit, however, in object recognition (Mahoney et al 2012b, Snowden et al 2012) and visuospatial skills (Hsiung et al 2012).

Not surprisingly, language deficits reported in *C9orf72* expansion carriers also varies. In one study, deficits in naming, semantic association and word fluency were found in about one-third of the bvFTD patients (10/34) who harboured the *C9orf72* gene expansions (Simón-Sánchez et al 2012) while naming was found to be impaired in half of the *C9orf72* expansion carriers (6/12) with bvFTD and FTD-MND cases. In contrast, naming, semantic and phonological processing were not affected in *C9orf72* expansion carriers regardless of clinical phenotype (Boeve et al 2012, Devenney et al 2014).

Motor features

Motor symptoms were observed in *C9orf72* expansion carriers that consist of bvFTD, FTD-MND and MND cases. Extrapyramidal symptoms with akinetic rigid parkinsonism and a few with tremor were observed (Boeve et al 2012, Hsiung et al 2012, Kaivorinne et al 2013, Mahoney et al 2012b).

One study demonstrated complex repetitive behaviour in *C9orf72* expansion carriers in contrast to simple low-level motor mannerisms are more commonly reported in non-carriers (i.e., hand-rubbing, tapping, humming, or grunting) (Snowden et al 2012). Furthermore, a study demonstrated deep tendon reflexes to be most commonly observed in *C9orf72* expansion carriers (Mahoney et al 2012b).

Neuroimaging features in C9orf72 carriers

Patterns of grey matter atrophy

Grey matter atrophy in *C9orf72* expansion carriers with bvFTD is symmetrical and involves the dorsolateral, medial and orbitofrontal lobes, and also the anterior temporal lobes (Whitwell et al 2012). Differences in the insula, precuneus and cerebellum were also noted (Devenney et al 2014, Khan et al 2012, Mahoney et al 2012b, Sha et al 2012, Simón-Sánchez et al 2012, Whitwell et al 2012). For subcortical structures, the thalamus was affected bilaterally (Mahoney et al 2012b).

Very few have looked at longitudinal disease progression, but one study revealed longitudinal differences bilaterally in the thalamus and in the left globus pallidus, as well as the cerebellum in an 18-month investigation (Mahoney et al 2012a) while another reported progression of atrophy in frontal lobes and ventricular enlargement over 24 months (Boeve et al 2012). However, both studies has a small sample size (n=6 and 8 respectively) (Boeve et al 2012, Mahoney et al 2012b).

Although some studies showed comparable differences between carriers and non-carriers, a fraction of the *C9orf72* carriers were reported with minimal atrophy on neuroimaging, which illustrates their heterogeneity (Boeve et al 2012, Khan et al 2012, Simón-Sánchez et al 2012). Again, variability in these findings may be due to comparison across diverse clinical phenotypes.

The patterns of change in the brain white matter associated with the presence of the *C9orf72* gene expansions remains poorly defined.

Only two studies examined white matter tracts changes in *C9orf72* carriers at a whole-brain level using diffusion tensor imaging (Mahoney et al 2012b, Mahoney et al 2014).

One study investigated white matter as part of a comprehensive study measuring profiles of brain change together with grey matter atrophy and cortical thickness in *C9orf72* carriers. In the group comparison between healthy controls and *C9orf72* carriers with a mixed clinical sample (consists of mostly bvFTD, with the minority being FTD-MND and one nfv-PPA patient), results revealed white matter alterations in both DTI metrics (decrease in FA and increase in RadialD) in the anterior thalamic radiations, uncinate fasciculus, anterior cingulum and anterior corpus callosum bilaterally; and in right posterior corpus callosum, posterior inferior longitudinal fasciculus and superior longitudinal fasciculus. Additional changes which were observed only in RadialD included the left frontal superior longitudinal fasciculus and posterior corpus callosum, and in the right corticospinal tract (Mahoney et al 2012b).